AD_____

Award Number: W81XWH-05-1-0070

TITLE: PECAM-1 and Angiogenesis

PRINCIPAL INVESTIGATOR: Dr. Horace DeLisser

CONTRACTING ORGANIZATION: The University of Pennsylvania
Philadelphia, PA 19104

REPORT DATE: December 2009

TYPE OF REPORT: Final

PREPARED FOR: U.S. Army Medical Research and Materiel Command
Fort Detrick, Maryland 21702-5012

DISTRIBUTION STATEMENT: Approved for public release; distribution unlimited

The views, opinions and/or findings contained in this report are those of the author(s) and should not be construed as an official Department of the Army position, policy or decision unless so designated by other documentation.

REPORT DOCUMENTATION PAGE

Form Approved
OMB No. 0704-0188

1. REPORT DATE *(DD-MM-YYYY)*	2. REPORT TYPE	3. DATES COVERED *(From - To)*
01-12-2009	Final	15 NOV 2004 - 14 NOV 2009

4. TITLE AND SUBTITLE
PECAM-1 and Angiogenesis

5a. CONTRACT NUMBER

5b. GRANT NUMBER
W81XWH-05-1-0070

5c. PROGRAM ELEMENT NUMBER

6. AUTHOR(S)
Dr. Horace DeLisser

E-Mail: delisser@mail.med.upenn.edu

5d. PROJECT NUMBER

5e. TASK NUMBER

5f. WORK UNIT NUMBER

7. PERFORMING ORGANIZATION NAME(S) AND ADDRESS(ES)
The University of Pennsylvania
Philadelphia, PA 19104

8. PERFORMING ORGANIZATION REPORT NUMBER

9. SPONSORING / MONITORING AGENCY NAME(S) AND ADDRESS(ES)
U.S. Army Medical Research and Materiel Command
Fort Detrick, Maryland 21702-5012

10. SPONSOR/MONITOR'S ACRONYM(S)

11. SPONSOR/MONITOR'S REPORT NUMBER(S)

12. DISTRIBUTION / AVAILABILITY STATEMENT
Approved for Public Release; Distribution Unlimited

13. SUPPLEMENTARY NOTES

14. ABSTRACT

It is hypothesized that during in vivo angiogenesis, endothelial PECAM-1-dependent ligand interactions trigger intracellular signaling cascades that facilitate endothelial cell (EC) motility. Three specific aims were proposed to test this hypothesis: (i) Specific Aim #1: Define the role of SHP-2 in mediating PECAM-1-dependent cell motility; (ii) Specific Aim #2: Characterize the PECAM-1-dependent ligand interactions involved in PECAM-1-mediated cell migration; (iii) Specific Aim #3: Determine the role of endothelial PECAM-1 tyrosine phosphorylation and ligand binding during in vivo angiogenesis. In accomplishing these aims we have (i) begun to define a role for PECAM-1 in the formation of filopodia, (ii) made progress toward generating the various constructs and cellular transfectants required for completion of the first two aims; (iii) further defined a role for PECAM-1 in some of the morphological modeling that occurs during angiogenesis; and (iv) done studies of the role of CD44 in in vivo angiogenesis that have complemented our investigations of PECAM-1. These studies are indicative of the progress we have made and may provide new insights into the treatment of angiogenic processes such as tumor growth and wound healing.

15. SUBJECT TERMS
PECAM-1, Angiogenesis, Endothelial Cells, Cell Motility, Filopodia

16. SECURITY CLASSIFICATION OF:			17. LIMITATION OF ABSTRACT	18. NUMBER OF PAGES	19a. NAME OF RESPONSIBLE PERSON
a. REPORT	b. ABSTRACT	c. THIS PAGE			USAMRMC
U	U	U	UU	46	19b. TELEPHONE NUMBER *(include area code)*

Table of Contents

INTRODUCTION

This proposal was based on the hypothesis that during *in vivo* angiogenesis, endothelial PECAM-1-dependent ligand interactions with other molecules in the membrane, or with proteoglycans in the extracellular matrix, trigger PECAM-1 tyrosine phosphorylation and an association of PECAM-1 with SHP-2. This facilitates the recruitment of SHP-2 to the membrane surface, where it mediates the dephosphorylation of focal adhesion proteins, leading to increased turnover of focal adhesions and enhanced endothelial cell motility. To test this hypothesis three Specific Aims were proposed:

Specific Aim #1. Define the role of SHP-2 in mediating PECAM-1-dependent cell motility. Stable cell transfectants expressing PECAM-1 will be transduced with adenoviral vectors encoding one of three SHP-2 dominant negative constructs mutated in the catalytic domain, the C-terminal domain that mediates interactions with scaffold proteins or in both regions. Transduced cells will then be analyzed for (i) the number and distribution of focal adhesions; (ii) the occurrence of critical focal adhesion tyrosine phosphorylation events; and (iii) cell motility using established *in vitro* models of cell migration and tube formation.

Specific Aim #2. Characterize the PECAM-1-dependent ligand interactions involved in PECAM-1-mediated cell migration. Studies will be done of the effects on PECAM-1-dependent migration of altering avb3 surface expression and on the association of $\alpha v\beta 3$ with PECAM-1 during cell migration, while a possible PECAM-1/perlecan interaction and its role in PECAM-1-dependent migration will be investigated by inhibiting the activity of perlecan or its expression by PECAM-1 expressing cells. Parallel studies of the regulation of these interactions by angiogenic factors, as well as their ability to trigger PECAM-1 tyrosine phosphorylation will also be included.

Specific Aim #3. Determine the role of endothelial PECAM-1 tyrosine phosphorylation and ligand binding during *in vivo* angiogenesis. Transgenic mice will be generated on the PECAM-null background that express in an endothelial-restricted manner, (i) wild type PECAM-1; (ii) mutant PECAM-1 in which Y663 and Y686 have been mutated; or (iii) mutant PECAM-1 that is incapable of mediating ligand

binding due to mutations of K151 and R152. *In vivo* angiogenesis will then be studied in these transgenic animals.

BODY

(Manuscripts not included in precious reports are enclosed)

Defining the Role of PECAM-1 in Cell Motility (Specific Aims 1&2)

The role of PECAM-1 in endothelial cell (EC) motility was studied by exploring the activity of cell transfectants expressing human PECAM-1, siRNA treated human ECs and ECs isolated from wild type and PECAM-1-nul mice. These studies confirmed the involvement of PECAM-1 in EC motility and that PECAM-1 stimulates a motile phenotype by promoting the formation of filopodia and by increasing the levels of cdc42, a Rho GTPase involved in the formation of these cellular extensions. These in vitro findings have been correlated with in vivo data in that we have observed decreased EC filopodia during post-natal retinal development (see Cao et al., 2009).

As part of these studies we developed a novel technique that allows for the isolation of pure populations of murine lung EC's, that others will certainly find helpful (see Fehrenbach et al. 2009).

Using cell transfectants expressing human PECAM-1, we studied the effects of co-expressing various constructs of SHP-2, as well as the effects of pharmacologic inhibition of SHP-2 phosphatase activity, on PECAM-1-dependent cell motility. The results of these studies suggest a model for the involvement of SHP-2 in PECAM-1-dependent endothelial cell motility in which SHP-2 binds to phosphorylated PECAM-1, becomes catalytically-active and dephosphorylates PECAM-1, leading to the release of SHP-2 from PECAM-1. The liberated, but now membrane localized SHP-2 subsequently targets paxillin to ultimately activate the ERK/MAPK pathway and downstream events required for cell motility (see Zhu et al., 2010; DeLisser, 2011).

Defining the *In Vivo* Activity of PECAM-1 in Angiogenesis (Specific Aim #3)

Specific Aim #3 was focused on defining the molecular requirements for PECAM-1-dependent function *in vivo* using PECAM-1 transgenic mice. As a part of these studies we focused on completing the characterization of the angiogenic phenotype of PECAM-1-null mice, including investigation of post-natal lung and retinal development (see

DeLisser et al, 2006; Cao et al. 2009). Important and necessary control and comparative studies were done in CD44-null mice. In addition parallel studies were performed using wild type and PECAM-1-null mice which demonstrated that PECAM-1 in the late progression of metastatic tumor foci in lung. This activity is independent of angiogenesis and appears to involve the regulation of endothelial derived factors that regulate the perivascular environment to promote tumor growth (See DeLisser, et al. 2010). Difficulty was encountered in developing the transgenes were to be used to generate transgenic mouse with endothelial-restricted expression of wild type PECAM-1 and efforts are going to develop these mice.

KEY RESEARCH ACCOMPLISHMNETS

- Endothelial CD44 may play a role in mediating the stability of new formed vessels
- PECAM-1 stimulates EC motility by promoting the formation of filopodia
- SHP-2 binds to phosphorylated PECAM-1, becomes catalytically-active and dephosphorylates PECAM-1, leading to the release of SHP-2 from PECAM-1. The liberated, but now membrane localized SHP-2 subsequently targets paxillin to ultimately activate the ERK/MAPK pathway and downstream events required for cell motility.
- The PECAM-1 null mice demonstrate impaired angiogenic responses in a number of model systems.
- PECAM-1 plays a role in tumor metastasis that is independent of its activity in mediating angiogenesis

REPORTABLE OUTCOMES

(1) Manuscripts, abstracts, presentations

- Tzima, E., Irani-Tehrani, M., Kiosses,W.E., Dejana,E., Schultz, D., Englehardt,B., Cao, G., DeLisser, H.M., Schwartz, M.: PECAM-1, VE-cadherin and VEGFR2 Cooperate to Initiate the Endothelial Cell-Specific Response to fluid Shear Stress. *Nature 437:426-431, 2005.*
- DeLisser, H.M., Helmke, BP., Cao, G., Egan, P., Taichman, D., Fehrenbach, M., Zaman, A., Cui, Z., Mohan, G., Baldwin, HS., Davies, PF, Savani, RC.: Loss of PECAM-1 Function Alveolarization. *J. Biol. Clinic 281:8724-8731, 2006*.

- Cao, G., Savani, R.C., Fehrenbach, M., Lyons, C., Zhang, L., Coukos, G., DeLisser, H.M. Involvement of Endothelial CD44 during in Vivo Angiogenesis. *Am. J. Path 169:325-336, 2006.*
- DeLisser, H.M.: Vascular Cell-Cell Adhesion. Laurent GJ and Shapiro SD (Eds.) Encyclopedia of Respiratory Medicine, Elsevier Limited, Oxford UK, pp 29-36, 2006.
- DeLisser, H.M.: The Role of the Extracellular Matrix in Angiogenesis in Lazaar, A. (Ed.) Bronchial Vascular Remodeling in Asthma and COPD. Marcel Dekker, New York, pp 105-125, 2006.
- DeLisser, H.M. Targeting PECAM-1 for Anti-Cancer Therapy. *Can. Boil. Ther.*, 6:121-122, 2007.
- Cao, G., Fehrenbach, M., Williams, J., Finklestein, J., Zhu, J-X DeLisser, H.M. Angiogenesis in PECAM-1-null mice. *Am. J. Path*, 175:903-915, 2009.
- Zhu, J-X, Cao, G., Williams, J., DeLisser, H.M. The Involvement of SHP-2 in PECAM-1-Dependent Cell Motility. *Am J Physiol Cell Physiol.* 299:C854-65, 2010.
- DeLisser H, Liu Y, Desprez PY, Thor A, Briasouli P, Handumrongkul C, Wilfong J, Yount G, Nosrati M, Fong S, Shtivelman E, Fehrenbach M, Cao G, Moore DH, Nyack S, Liggitt D, Kashani-Sabet M, Debs R. Vascular endothelial cell adhesion molecule 1 (PECAM-1) regulates advanced metastatic progression. *Proc Natl Acad Sci U S A*. 107:18616-21, 2010.
- DeLisser HM. Modulators of endothelial cell filopodia: PECAM-1 joins the club. Cell Adh Migr. 2011 Jan 10;5(1).

(2) Licenses applied for and/or issued

- None

(3) Degrees obtained that are supported by this award

- Jeffery Finklestein- Master's Degree in Cell and Molecular Biology

(4) Development of cell lines, tissue or serum repositories

- None

(5) Informatics such as databases and animal models, etc

- None

(6) Funding applied for based on work supported by this award

- VA Meritt Award

(7) Employment or research opportunities applied for and/or received based on experience/training supported by this award

- None

CONCLUSIONS

In accomplishing these aims we have (i) further established a role for PECAM-1 in endothelial cell motility; (ii) defined a role for PECAM-1 in the formation of endothelial filopodia; (iii) confirmed the involvement of SHP-2-PECAM-1 interactions in PECAM-1-dependent cell motility and filopodia formation; (iv) provided data that implicate PECAM-1 in pathological angiogenesis, as well as in post-natal vascular developmental processes, such as those occurring in the eyes and lungs; and (v) developed data that point to an important regulatory role for PECAM-1 in tumor metastasis in the lung (and probably other organs as well).. These studies are indicative of the progress we have made and may provide new insights into the treatment of pathological processes such as tumor growth and spread as well as impaired wound healing.

REFERENCES

NONE

SUPPORTING DATA

NONE

Appendix

PI: Horace M. DeLisser, M.D.

Title: "PECAM-1 and Angiogenesis"

Grant No.: PR0433482

SHP-2 phosphatase activity is required for PECAM-1-dependent cell motility

Jing-Xu Zhu, Gaoyuan Cao, James T. Williams and Horace M. DeLisser

Am J Physiol Cell Physiol 299:C854-C865, 2010. First published 14 July 2010;
doi:10.1152/ajpcell.00436.2009

Am J Physiol Cell Physiol 299: C854–C865, 2010.
First published July 14, 2010; doi:10.1152/ajpcell.00436.2009.

SHP-2 phosphatase activity is required for PECAM-1-dependent cell motility

Jing-Xu Zhu,* Gaoyuan Cao,* James T. Williams, and Horace M. DeLisser

Pulmonary, Allergy and Critical Care Division, Department of Medicine, University of Pennsylvania School of Medicine, Philadelphia, Pennsylvania

Submitted 1 October 2009; accepted in final form 9 July 2010

Zhu J, Cao G, Williams JT, DeLisser HM. SHP-2 phosphatase activity is required for PECAM-1-dependent cell motility. *Am J Physiol Cell Physiol* 299: C854–C865, 2010. First published July 14, 2010; doi:10.1152/ajpcell.00436.2009.—Platelet endothelial cell adhesion molecule-1 (PECAM-1) has been implicated in endothelial cell motility during angiogenesis. Although there is evidence that SHP-2 plays a role in PECAM-1-dependent cell motility, the molecular basis of the activity of SHP-2 in this process has not been defined. To investigate the requirement of SHP-2 in PECAM-1-dependent cell motility, studies were done in which various constructs of SHP-2 were expressed in cell transfectants expressing PECAM-1. We observed that the levels of PECAM-1 tyrosine phosphorylation and SHP-2 association with PECAM-1 were significantly increased in cells expressing a phosphatase-inactive SHP-2 mutant, suggesting that the level of PECAM-1 tyrosine phosphorylation, and thus SHP-2 binding are regulated in part by bound, catalytically active SHP-2. We subsequently found that expression of PECAM-1 stimulated wound-induced migration and the formation of filopodia (a morphological feature of motile cells). These activities were associated with increased mitogen-activated protein kinase (MAPK) activation and the dephosphorylation of paxillin (an event implicated in the activation of MAPK). The phosphatase-inactive SHP-2 mutant, however, suppressed these PECAM-1-dependent phenomena, whereas the activity of PECAM-1 expressing cells was not altered by expression of wild-type SHP-2 or SHP-2 in which the scaffold/adaptor function had been disabled. Pharmacological inhibition of SHP-2 phosphatase activity also suppressed PECAM-1-dependent motility. Furthermore, PECAM-1 expression also stimulates tube formation, but none of the SHP-2 constructs affected this process. These findings therefore suggest a model for the involvement of SHP-2 in PECAM-1-dependent motility in which SHP-2, recruited by its interaction with PECAM-1, targets paxillin to ultimately activate the MAPK pathway and downstream events required for cell motility.

mitogen-activated protein kinase; angiogenesis; leukocyte transendothelial migration

PLATELET ENDOTHELIAL CELL adhesion molecule-1 (PECAM-1) is a transmembrane glycoprotein that is expressed on endothelial cells where it concentrates at intercellular junctions (25, 34). It is also expressed, albeit at lower levels, on platelets and leukocytes. In terms of its endothelial functions, PECAM-1 regulates leukocyte transendothelial migration (50), participates in the molecular sensing of fluid sheer stress (46), and confers resistance to apoptotic or endotoxic stresses (10, 31). PECAM-1 is also involved in angiogenesis (8, 9, 15, 16, 41, 52), where it has been implicated in endothelial cell motility (8, 9, 20, 28, 35). Although initially described as a mediator of cell-cell adhesion, subsequent studies established that PECAM-1 also participates in intracellular signaling (18, 23, 25). This signaling activity is mediated in part by tyrosine residues 663 and 686 of the cytoplasmic domain, each of which falls within a conserved signaling sequence known as the immunoreceptor tyrosine-based inhibitory motif (ITIM) (5, 36). As with other ITIM-containing receptors, phosphorylation of these two tyrosine residues by protein-tyrosine kinases (e.g., Src, Csk, and Fps/Fes family kinases) (7, 27, 30, 47) generates docking sites for the binding and activation of several cytosolic signaling molecules containing Src homology-2 (SH2) domains, including the tyrosine phosphatase SHP-2 (7, 24, 30, 38).

SHP-2 is a ubiquitously expressed 68-kDa nonreceptor protein tyrosine phosphatase composed of two amino-terminal SH2 domains, a catalytic phosphatase domain and COOH-terminal tail containing two tyrosines Y542 and Y580, that form docking sites for SH-2 domain-bearing proteins (11, 14, 45). SHP-2 is activated by the binding of tyrosine-phosphorylated proteins to the NH_2-terminal SH2 domain causing exposure of the active catalytic phosphatase site (2). It has been suggested that the COOH-terminal SH2 domain functions to stabilize associations made by the NH_2-terminal SH2 domain (1). In addition, a number of SH2 domain-containing adapter proteins associate with SHP-2 after receptor activation, including Grb-2 (growth factor receptor-bound protein 2), SHIP-1 [SH2 (Src homology 2)-containing inositol phosphatase-1], and SIT (SHP2-interacting transmembrane adaptor protein) (11, 14), which link surface receptors to intracellular signaling pathways. A large amount of genetic and biochemical data demonstrate that SHP-2 promotes mitogen-activated protein kinase (MAPK) activation in response to diverse agonists. As a result it is a positive component of many growth factors, cytokine and extracellular matrix signaling pathways, and thus plays a role in diverse cellular processes, including proliferation, survival, differentiation, and migration (11, 14). The importance of SHP-2 in vivo is evident by the fact that the loss of expression of functional SHP-2 in developing mice results in death between *days 8.5–10.5* of gestation. These fetuses display multiple defects in mesodermal patterning as well as impaired hematopoietic development in embryonic stem cells (43, 44, 48). In addition, genetic mutations in *PTPN11* that cause hyperactivation of SHP-2 phosphatase activity have been identified in the Noonan syndrome, a human developmental disorder (43, 48), and in various childhood leukemias (29, 44). Activating mutations in SHP-2 have also been detected in sporadic solid tumors (11).

There is evidence that the binding of SHP-2 to PECAM-1 following PECAM-1 tyrosine phosphorylation is involved in the enhancement of cell motility that results from the expression of PECAM-1 (35). The molecular basis of SHP-2's activity in this phenomenon is unknown, particularly, whether the enhanced cell migration mediated by PECAM-1 is due to the activity of SHP-2 as a phosphatase and/or an adaptor/

* J-X. Zhu and G. Cao contributed equally to the manuscript.

Address for reprint requests and other correspondence: H. M. DeLisser, Pulmonary, Allergy and Critical Care Division, SVM-Hill Pavilion, Rm. 410B, 380 South Univ. Ave., Philadelphia, PA 19104-4539 (e-mail: delisser@mail.med.upenn.edu).

scaffolding protein. Using cell transfectants expressing human PECAM-1, we therefore studied the effects of coexpressing various constructs of SHP-2, as well as the effects of pharmacological inhibition of SHP-2 phosphatase activity, on PECAM-1-dependent cell motility. The results of these studies suggest a model for the involvement of SHP-2 in PECAM-1-dependent endothelial cell motility in which SHP-2 binds to phosphorylated PECAM-1, becomes catalytically active, and dephosphorylates PECAM-1, leading to the release of SHP-2 from PECAM-1. The liberated, but now membrane localized, SHP-2 subsequently targets paxillin to ultimately activate the ERK/MAPK pathway and downstream events required for cell motility.

MATERIALS AND METHODS

Reagents and chemicals. All reagents and chemicals were obtained from Sigma (St. Louis, MO) unless otherwise specified. The SHP-2 inhibitor NSC-87877 (13) was obtained from Calbiochem (San Diego, CA). Pfu Ultra High-Fidelity DNA polymerase with reaction buffer was purchased from Stratagene (La Jolla, CA). Restriction enzymes and reaction buffers were purchased from Promega (Madison, WI). Rapid DNA Ligation Kit was purchased from Roche Applied Science (Indianapolis, IN). Kits for DNA plasmid purification and agarose gel extraction were purchased from Qiagen (Valencia, CA). Sequencing and PCR primers were synthesized by Integrated DNA Technologies (Coralville, IA). Competent bacteria and dNTP mix were obtained from Invitrogen (Carlsbad, CA).

Antibodies. The following antibodies targeting human proteins were employed: 4G6, a mouse anti-PECAM-1 antibody (a generous gift from Dr. Steven Albelda, University of Pennsylvania, Philadelphia, PA); 1.3, a mouse anti-PECAM-1 antibody (a generous gift from Dr. Peter Newman, Blood Center of Southeastern Wisconsin, Milwaukee, WI); a rabbit anti-SHP-2 antibody and a mouse anti-phospho-ERK antibody from Cell Signaling Technology (Danvers, MA); a rabbit anti-phosphotyrosine antibody and a mouse anti-paxillin antibody from BD Biosciences, Transduction Laboratories (Lexington, KY); a rabbit anti-ERK antibody from Promega; a rabbit anti-phos-

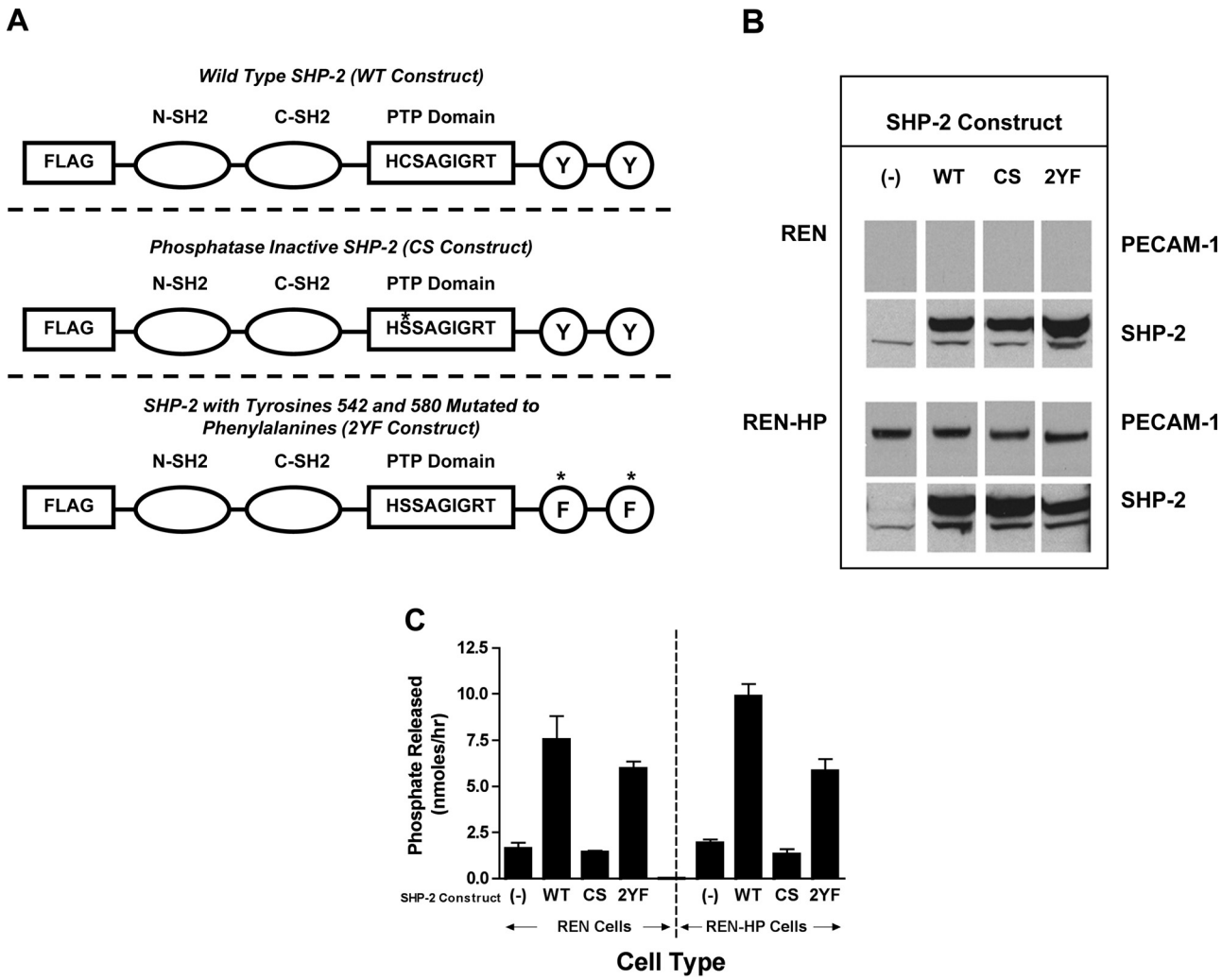

Fig. 1. Expression of Src homology-1 phosphatase (SHP-2) constructs in REN cells and REN cells expressing human platelet endothelial cell adhesion molecule-1 (PECAM-1) (REN-HP). *A*: three constructs that were expressed in REN and REN-HP cells: wild-type SHP-2 (WT), phosphatase-inactive SHP-2 (CS), and SHP-2 with tyrosines 542 and 580 mutated to phenylalanines (2YF). *B*: cell lysates from REN and REN-HP cells expressing the various SHP-2 constructs, demonstrating both the presence of the endogenous SHP-2 (lower molecular weight band) and the transduced SHP-2 in the transfectants expressing a SHP-2 construct. (The data are from the same experiment and the same gel for each antibody and are representative of 3 experiments). *C*: intracellular SHP-2 phosphatase activities of each cell line as determined by the amount of phosphate released by 5 μg of cell lysate (see MATERIALS AND METHODS) ($n = 2$). (The phosphatase data are representative of 2 experiments).

pho-(Tyr-31)-paxillin antibody from Santa Cruz Biotechnology (Santa Cruz, CA); a mouse anti-GAPDH antibody from Chemicon-Millipore (Temecula, CA); and a mouse anti-FLAG antibody from Sigma.

Generation of SHP-2 constructs. The following constructs of SHP-2 with a FLAG-tag were generated: wild-type SHP-2 (WT-SHP-2); phosphatase inactive SHP-2 (cysteine 459 mutated to serine; CS-SHP-2), and SHP-2 in which the scaffold/adaptor function has been disabled (tyrosines 542 and 580 mutated to phenylalanines; 2YF-SHP-2). Briefly, a wild-type SHP-2 construct (Addgene plasmid 8381: pCMV-WT-SHP-2, MA) was subcloned into pcDNA3.1(+) vector with *Hind*III and *EcoR*V to obtain pcDNA-WT-SHP-2 without an hemogglutin antibody (HA) tag. A PCR product of 3xFLAG fragment with restriction digestion sites of *Nhe*I and *Kpn*I was generated from pBICEP-CMV-2 (Sigma). 3xFLAG was subcloned into pcDNA-WT-SHP-2 to generate pcDNA-3xFLAG-WT-SHP-2 (WT-SHP-2). The resulting construct was then subjected to site-directed mutagenesis using the GeneTailor Site-Directed Mutagenesis System (Invitrogen) according to the manufacturer's instructions. Cys459 of SHP-2 was mutated to Ser459 by PCR using the forward primer 5′-CAGGGCCGGTCGTGGTGCACAGCAGTGCTGGAATTGGC-3′ with the reverse primer 5′-GTGCACCACGACCGGCCCTGCATCCATGATGC-3′ to generate pcDNA-3xFLAG-CS-SHP-2 (CS-SHP-2). Point mutations converting Tyr542 and Tyr580 to Phe542 and Phe580 were generated by PCR using the following primer sets: for Y542 to F542, the forward primer 5′-GCAAGAGGAAAGGGCACGAATTTACAAATATTAAGTAT-3′ with the reverse primer 5′TTCGTGCCCTTTCCTCTTGCTTTTCTGCTCTT-3′; for Y580 to F580, the forward primer 5′-GAGAAGACAGTGCTAGAGTCTTTGAAAACGTGGGCCTG-3′ with the reverse primer 5′-GACTCTAGCACTGTCTTCTCTCATTTCTGCAC-3′ to generate pcDNA-3xFLAG-2YF-SHP-2 (2YF-SHP-2). These recombinant wild-type and mutant SHP-2 constructs were then subcloned into

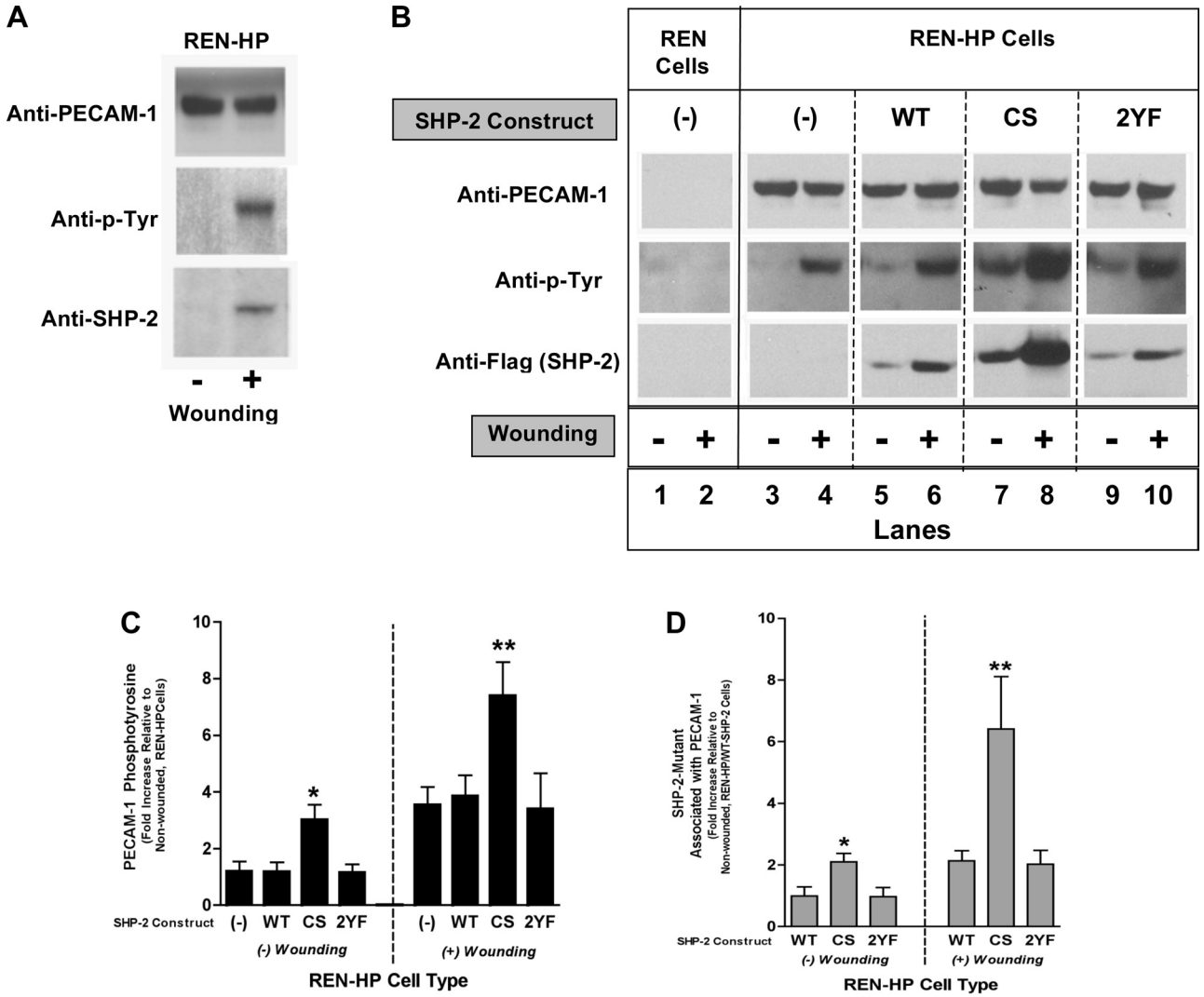

Fig. 2. PECAM-1-SHP-2 association in REN-HP transfectants. Cell lysates from nonwounded or wounded monolayers of REN cells, REN-HP cells, or REN-HP cells expressing WT-SHP-2 (WT), CS-SHP-2 (CS), or 2YF-SHP-2 (2YF) were immunoprecipitated with anti-PECAM-1 and then blotted with anti-PECAM-1, anti-phospho-tyrosine (anti-p-Tyr), anti-SHP-2, or anti-FLAG (to detect SHP-2 constructs). In the REN-HP cells wounding induced PECAM-1 tyrosine phosphorylation that was associated with increased SHP-2/PECAM-1 association (*A*). The same phenomenon was observed for REN-HP cells expressing the various SHP-2 mutants (*B*, *lanes 6*, *8*, *10*). However, the amounts of SHP-2 associated with PECAM-1, both at rest and after wounding, were higher in the cells expressing the CS-SHP-2 construct (*lanes 7* and *8*) compared with the other cell lines. (The data are from the same experiment and the same gel for each antibody. They are representative of 5–6 experiments). Densitometry confirmed that PECAM-1 tyrosine phosphorylation (*C*) (expressed as fold increase compared with nonwounded REN-HP cells) and PECAM-1-SHP-2 association (*D*) (expressed as fold increase compared with nonwounded REN-HP/WT-SHP2 cells) were increased by coexpression of CS-SHP-2. Data were initially normalized to total PECAM-1 and are presented as means ± SE ($n = 5–6$; $^*P < 0.05$, compared with nonwounded REN-HP expressing WT-SHP-2 cells; $^{**}P < 0.05$ compared with wounded REN-HP expressing WT-SHP-2 cells).

pIRESpuro3 expression vector (Clontech Laboratories, Mountain View, CA). The sequences of all constructs were verified by automated DNA sequencing.

Cell culture and transfection. The human mesothelioma cell line REN (40) was cultured in RPMI media supplemented with 10% FBS, penicillin-streptomycin, and 2 mM L-glutamine. REN cell transfectants stably expressing human PECAM-1 (REN-HP) were cultured in the same media with G418 (0.5 mg/ml; GIBCO-BRL, Grand Island, NY) (8, 35). REN or REN-HP cells were transfected with SHP-2 constructs described above using Lipofectamine 2000 (Invitrogen). Stable transfectants were obtained by selection with Puromycin (1 mg/ml) for REN cells and with Puromycin (1 mg/ml) plus G418 (0.5 mg/ml) for REN-HP cells, respectively. Positive clones expressing transfected SHP-2 constructs were confirmed by Western blot analysis.

Intracellular SHP-2 phosphatase activity. The intracellular SHP-2 phosphatase activity of lysates from stably transfected cell lines was determined using DuoSet IC (IntraCellular) Assay Development Systems (R&D Systems, Minneapolis, MN), according to the manufacturer's instructions. Briefly, cell lysates were aliquoted, frozen in liquid nitrogen, and stored at −80°C. Protein concentration was determined using the BCA Protein Assay kit (Thermo Fisher Scientific, Rockford, IL). Fifty microliters of each standard in triplicate were used to construct a standard curve, and the phosphate released over 30 min by 5 μg total protein for each sample was assayed by the manufacturer's protocol. Absorbances were measured on 620 nm with the Beckman Coulter DTX880 Multimode Detector (Beckman Coulter, Fullerton, CA), and the phosphatase activity was calculated with the accompanying software.

In vitro cell proliferation. REN cells and REN cell transfectants were cultured for 24–48 h in 96-well plates (4,000 cells/well), and the number of viable cells were determined using the Promega Cell Titer96 A_{queous} Non-Radioactive Cell Proliferation Assay (Madison WI). This is a colorimetric assay with the absorbances measured at 490 nm.

In vitro wound-induced migration assay. The wounding of confluent cell monolayers was modified from previously published procedures (8, 35). Twenty thousand REN cells and REN cell transfectants were added to 24-well tissue culture plates and allowed to grow to confluence. Linear defects were then made in the monolayer. The wounded culture was washed with PBS and then incubated for 24 h in complete media. With the use of computer-assisted image analysis and the MetaMorph software (Molecular Devices, Sunnyvale, CA), images were obtained immediately after wounding and then 24 h later, and the distance migrated by cells at the wound edge was determined. For each cell type three to five wounds were analyzed.

In vitro tube formation assay. In vitro tube formation was studied using previously described procedures (35). REN cells and REN cell transfectants were plated on ECMatrix gel (a Matrigel equivalent) obtained from Chemicon. Fifty microliters of the solution were added to each well of a 96-well plate and allowed to form a gel at 37°C for 1 h. Twenty thousand cells in 200 μl of complete media were subsequently added to each well and incubated for 8 h at 37°C in 5% CO_2. The wells were washed and the gel and its cells fixed with 3% paraformaldehyde. Total tube length per well was determined by computer-assisted image analysis using the MetaMorph software package.

Immunoprecipitation and immunoblotting. Cultures of confluent cells were serum starved overnight and then incubated for 2 h in medium with or without 0.5 mM sodium orthovanadate at 37°C before scratch wounds were made in the monolayer. For our biochemical analyses, multiple parallel wounds, 1 mm in width were made in the confluent monolayer of cells by drawing a specially fabricated squeegee, with comb-like teeth, across the culture surface of a T-25 flask. We have visually confirmed that with this procedure all of the remaining, attached cells are adjacent to a cell-free zone into which they able are to migrate. One hour after wounding, the cells were washed with ice-cold PBS containing 0.5 mM sodium orthovanadate and and then lysed in TNC (0.01 M Tris-acetate, pH 8.0, 0.5% Nonidet-40, 0.5 mM Ca^{2+}) with 1 mM sodium orthovanadate, 2 mM PMSF, and protease inhibitor cocktail (Sigma) for 20 min on ice. Extracts were clarified for 10 min at 4°C, and the supermatant protein concentrations were determined by the BCA assay kit (Pierce). Equal amounts (100 μg) of protein were incubated with 2 mg of 4G6 anti-PECAM-1 or anti-paxillin antibody with rocking movement overnight at 4°C. Protein A Sepharose beads (GE Healthcore Bio-Sciences, Piscataway, NJ) were added and incubated for an additional 2 h. After binding and collection were completed, the beads were washed three times with DOC wash (50 mM Tris·HCl, pH 7.5, 150 mM NaCl, 1% Triton X-100, 5% deoxycholate, and 0.1% SDS), dissolved in reducing loading buffer to release the immunoprecipitant. Proteins from immunoprecipitation or total cell lysates were resolved by SDS-PAGE (Novex; Invitrogen), followed by transfer onto nitrocellulose membranes using the iBlot Dry Blotting System (Invitrogen), which employs semidry electrotransfer. Membranes were washed in 1× TTBS for 2–3 min, blocked with 2% BSA, and incubated with the primary antibody in 2% BSA for 1 h at room temperature or overnight at 4°C. Unbound antibodies were washed off with TTBS before membranes were incubated with horseradish per-

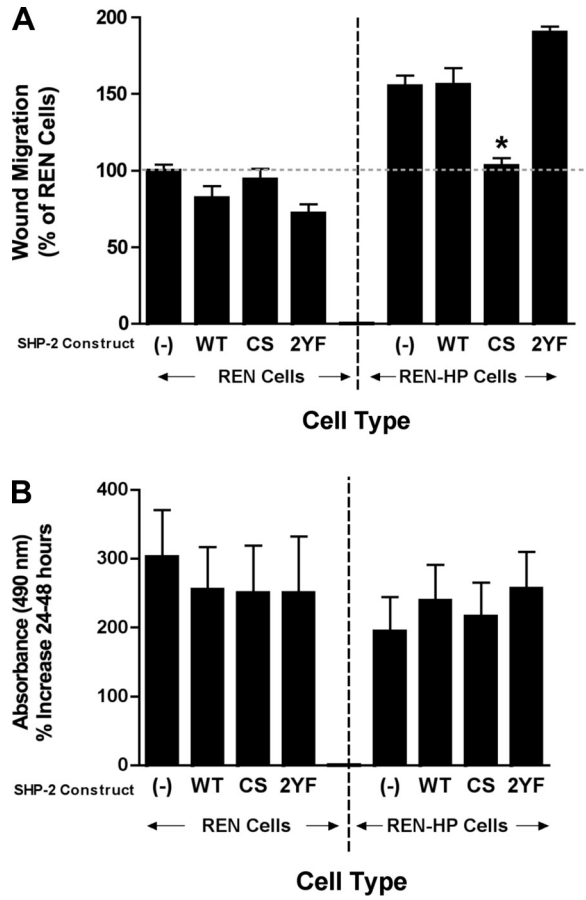

Fig. 3. Effects of the expression of SHP-2 constructs on the migration and proliferation of REN and REN-HP cells. Wound-induced migration (*A*) and cell proliferation (*B*) were studied in REN and REN-HP cells expressing WT, CS, or 2YF constructs. The expression of CS-SHP-2 abrogated the stimulation of cell motility mediated by the expression of PECAM-1, whereas cell proliferation was not affected by the presence of any of the constructs. Data are presented as means ± SE (n = 3–4, for the proliferation studies; n = 6 for the migration studies; $^*P < 0.0001$). The data presented are representative of least 3 experiments.

oxidase-labeled species-specific secondary antibodies for 1 h at room temperature. After the membranes were again washed with PBS, bound antibody signals were detected by ECL substrate and documented on X-ray film. The chemiluminescent signals were quantified by densitometry (ImageQuant; Amersham, Piscataway, NJ).

Assessing the morphology of plated cells. REN cells or REN cell transfectants, resuspended in complete M199 medium, were lightly seeded into uncoated two-well Lab-Tek Chamber slides (Nunc, Thermo Fischer Scientific, Rochester, NY) followed by culturing for 2–3 days. Digital images were then captured. With the use of computer-assisted image analysis, the points on either side of the base of a filopodium, at which the stalk of the filopodium angles with the cell surface, were located and a line was drawn between these two points. A second line was then drawn from the center of the first line through the center of filopodium to its tip, the length of which was taken as the length of the filopodium.

Statistical analyses. Differences among groups were analyzed using one-way ANOVA. Results are presented as means ± SE. When statistically significant differences were found ($P < 0.05$), individual comparisons were made using the Bonferroni-Dunn test.

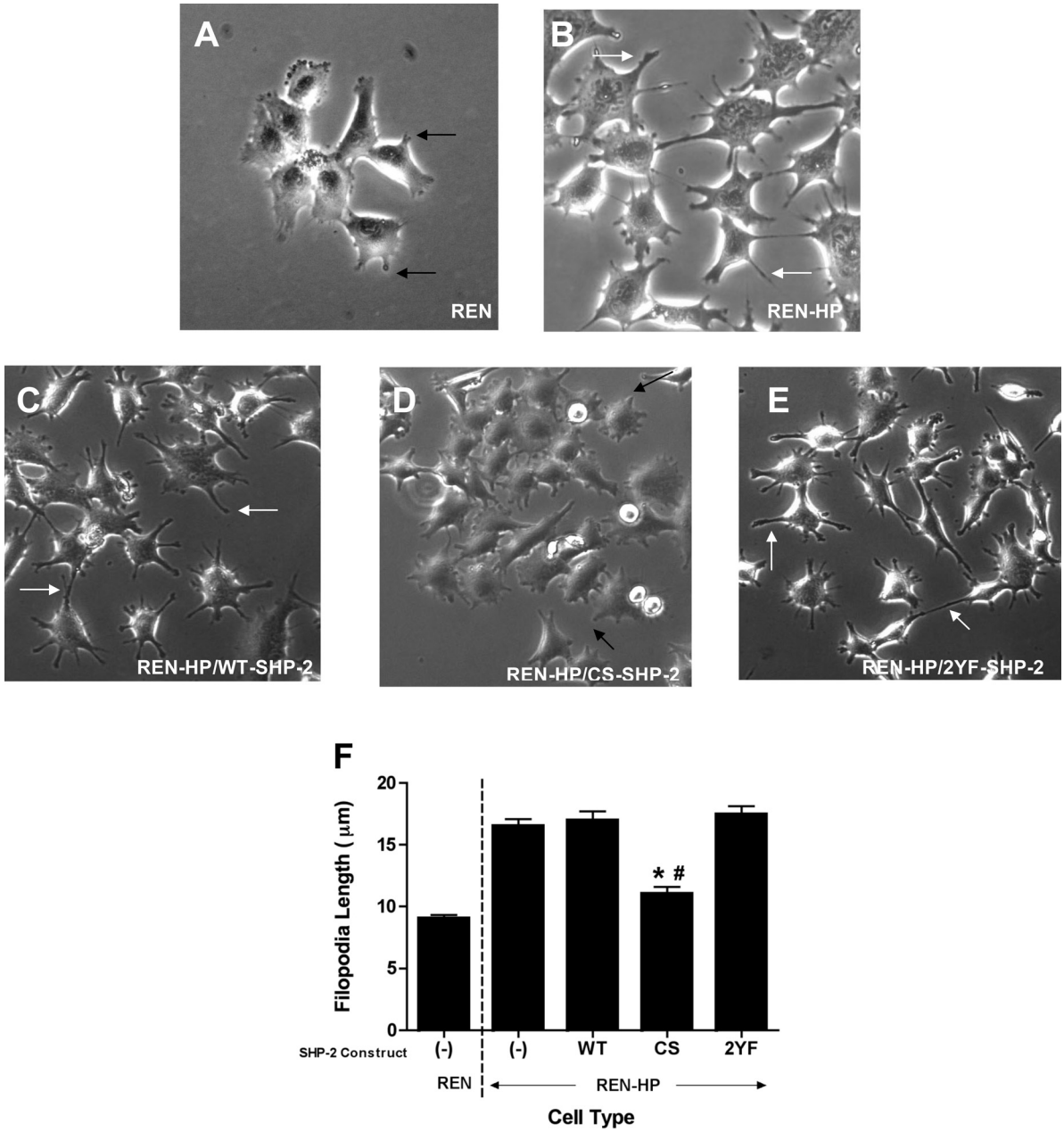

Fig. 4. Effects of the expression of SHP-2 constructs on the formation of filopodia in REN and REN-HP cells. Shown are REN cells (*A*), REN-HP cells expressing no SHP-2 constructs (*B*), and REN-HP cells expressing WT-SHP-2 (*C*), CS-SHP-2 (*D*), or 2YF-SHP-2 (*E*) constructs. Filopodia were longer in the REN-HP cells (*B*, white arrows) compared with those of the REN cells (*A*, black arrows). The morphology of the filopodia on the REN-HP cells expressing WT-SHP-2 (*C*) and 2YF-SHP-2 (*E*) were similar to the REN-HP cells (*B*), whereas the REN-HP/CS-SHP-2 cells (*D*, black arrows) had a morphology that was reminiscent of the nontransfected REN cells (*A*). The mean filopodia length was determined for each cell line (*F*). For the REN-HP/CS-SHP-2 cells, the mean filopodia length was significantly less than that of the REN-HP, REN-HP/WT-SHP-2, and REN-HP/2YF-SHP-2 cells and not significantly different from the nontransfected REN cells. Data are presented as means ± SE ($n = 100$; $*P < 0.0001$, compared with REN-HP cells; $\#P > 0.05$, compared with REN cells). The data presented are representative of 3 experiments.

RESULTS

Expression of SHP-2 constructs in REN cell transfectants. The expression of PECAM-1 in the REN cell mesothelioma line (40) has provided a useful system for modeling the function of endothelial PECAM-1 (8, 19, 26, 33, 35, 42, 49). Admittedly, there are potential limitations to use of REN cells as a model for endothelial cells, given the tumor cell origin of these cells. REN cells, however, do have a number of features that make them an attractive system for modeling the endothelium. First, they form cobblestone cell monolayers reminiscent of endothelial cells. Second, REN cells do not express PECAM-1 yet have several relevant endothelial surface molecules (e.g., αvβ3, ICAM-1, VCAM-1, and VEGFR-1). Third, in both endothelial cells and REN cell transfectants expressing human PECAM-1 (REN-HP): *1*) PECAM-1 concentrates at cell-cell junctions (35); *2*) tube-like structures form on Matrigel (8, 35); *3*) H_2O_2 activates a calcium-permeant, nonselective cation current (26); and *4*) wound-induced cell migration is associated with PECAM-1 tyrosine phosphorylation and SHP-2 association (35). Finally, REN-HP cells and human endothelial cells behave similarly with respect to the internalization and intracellular trafficking of surface-bound anti-PECAM-1 antibodies (19, 33, 49).

To define the requirements of SHP-2 in PECAM-1-dependent cell motility, the following constructs of SHP-2 with a FLAG-tag were expressed in REN or REN-HP cells: wild-type SHP-2 (WT-SHP-2); phosphatase inactive SHP-2 (cysteine 459 mutated to serine; CS-SHP-2); and SHP-2 in which the scaffold/adaptor function has been disabled (tyrosines 542 and 580 mutated to phenylalanines; 2YF-SHP-2) (Fig. 1*A*). These constructs were successfully expressed at comparable levels in REN and REN-HP cells (Fig. 1*B*). As expected, the SHP-2 phosphatase activity was increased in the cells expressing WT-SHP-2 or 2YF-SHP-2 but not CS-SHP-2 (Fig. 1*C*). Furthermore, the expression levels of these constructs were such that they would exceed and displace the endogenous SHP-2. In the cells transfected with the SHP-2 constructs, we observed that the amount of endogenous SHP-2 was somewhat increased over that found in cells without these constructs. This suggests that the processes that degrade or turnover SHP-2 in the cell have a defined capacity and that the SHP-2 mutants, because of their abundance, out compete the endogenous SHP-2 for these processes.

Increased PECAM-1 tyrosine phosphorylation and SHP-2 association in PECAM-1 transfectants expressing phosphatase-inactive SHP-2. The wounding of confluent monolayers of PECAM-1-expressing cells such as HUVEC or REN-HP cells induces the tyrosine phosphorylation of PECAM-1 (on Y663 and Y686) and the subsequent binding of SHP-2 to PECAM-1 (35). PECAM-1 tyrosine phosphorylation was therefore investigated in REN-HP transfectants expressing the SHP-2 constructs (Fig. 2). As noted previously (35), the wounding of REN-HP cells induced PECAM-1 tyrosine phosphorylation and recruitment of the endogenous SHP-2 (Fig. 2*A*). The wounding of REN-HP cells expressing WT-SHP-2 (Fig. 2*B*, *lanes 5* and *6*) or 2YF-SHP-2 (Fig. 2*B*, *lanes 9* and *10*) induced PECAM-1 tyrosine phosphorylation that was comparable to control REN-HP transfectants (Fig. 2*B*, *lanes 3* and *4*) and accompanied by increased SHP-2 binding to PECAM-1. The behavior of the REN-HP cells expressing CS-SHP-2 (Fig. 2*A*, *lanes 7* and *8*), however, differed significantly from the other SHP-2 transfectants in two important respects. First, quiescent (unwounded) REN-HP/CS-SHP-2 cells demonstrated PECAM-1 tyrosine phosphorylation and SHP-2 association that exceeded the levels of resting WT-SHP-2 and 2YF-SHP-2 transfectants (Fig. 2*B*, *lanes 7* compared with *lanes 5* and *9*; and Fig. 2, *C* and *D*). Second, while wounding did in fact stimulate PECAM-1 tyrosine phosphorylation and SHP-2 binding (Fig. 2*B*, *lanes 7* and *8*), the levels of tyrosine phosphorylation and SHP-2 binding associated with wounded REN-HP/CS-SHP-2 cells were two to three times that of the other REN-HP transfectants (Fig. 2*A*, *lane 8* compared with *lanes 6*, and *10*; and Fig. 2, *C* and *D*). These data suggest that the level of PECAM-1 tyrosine phosphorylation, and thus SHP-2 binding, are regulated in part by bound, phosphatase-active SHP-2. This is consistent with a model in which SHP-2

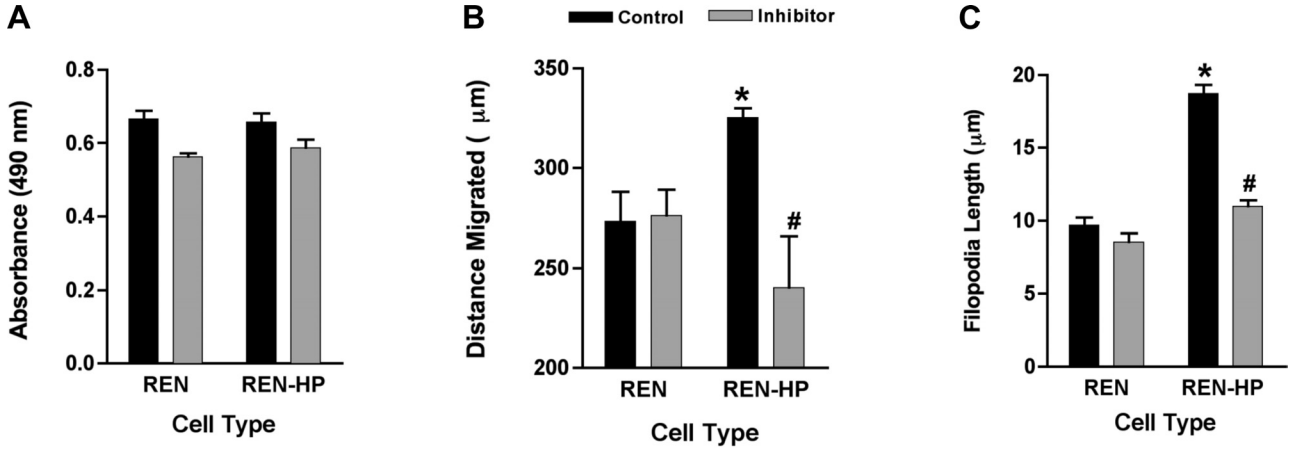

Fig. 5. Effects of NCS-87877 on the proliferation, cell migration, and filopodia formation of REN and REN-HP cells. Proliferation (*A*) ($n = 4$), wound-induced migration (*B*) ($n = 3$), and filopodia formation (*C*) ($n = 100$) were assessed in REN and REN-HP cells cultured in media without or with NSC-87877 (20 μM). Although the inhibitor induced a very modest decrease in proliferation for both cell types (*A*), it specifically suppressed the enhancements in wound migration and filopodia length that were stimulated by the expression of PECAM-1 in REN-HP cells. Data are presented as means ± SE. When compared with control REN cells, $*P < 0.01$, for the proliferation and migration studies and <0.0001 for the filopodia experiments; $\#P > 0.05$, compared with inhibitor-treated REN cells.

binds phosphorylated PECAM-1, becomes catalytically active, and dephosphorylates PECAM-1 leading to the release of SHP-2.

Decreased cell migration, but preserved proliferation, in PECAM-1 transfectants expressing phosphatase-inactive SHP-2. The expression of PECAM-1 in REN cells stimulates an increase in wound-induced cell migration, and SHP-2 has been implicated in this process (35). Wound-induced migration was therefore studied in REN and REN-HP cells expressing the SHP-2 constructs (Fig. 3*A*). The expression of PECAM-1 in REN cells induced a 50% increase in cell motility, which was not augmented further by the presence of WT-SHP-2. This suggests that the endogenous levels of SHP-2 are fully sufficient to mediate this phenomenon. Significantly, the enhanced motility observed in REN-HP cells was completely lost if CS-SHP-2 was simultaneously expressed, whereas the augmented migration was preserved in the 2YF-SHP-2 transfectants. The expression of WT-SHP-2, CS-SHP-2, or 2YF-SHP-2 did not significantly alter the motility of REN cells lacking PECAM-1 (Fig. 3*A*). These motility data are not related to changes in cell proliferation as the expression of PECAM-1 in REN cells does not significantly alter cell proliferation. Furthermore, the presence of WT-SHP-2, CS-SHP-2 or 2YF-SHP-2 did not inhibit the proliferation of REN or REN-HP cells (Fig. 3*B*). Together, these data suggest that PECAM-1-dependent cell migration is mediated by catalytically active SHP-2.

Decreased filopodia formation in PECAM-1 transfectants expressing phosphatase-inactive SHP-2. Filopodia are a feature of actively motile cells, mediating several functions required for cell migration (21, 32). We have previously demonstrated that PECAM-1 increases the rate and/or efficiency of filopodia formation (9). Therefore, this activity may be one of the mechanisms by which PECAM-1 promotes cell motility. Our finding that the expression of CS-SHP-2 abrogated the enhanced motility observed after transfection with PECAM-1 led us to also explore the effects of our SHP-2 constructs upon filopodia formation by REN-HP cells (Fig. 4). REN cell transfectants expressing PECAM-1 are characterized by numerous, long filopodia (Fig. 4*B*). Although REN-HP transfectants expressing WT-SHP-2 or 2YF-SHP-2 were morphologically similar to control REN-HP cells (Fig. 4, *C* and *E*), transfectants

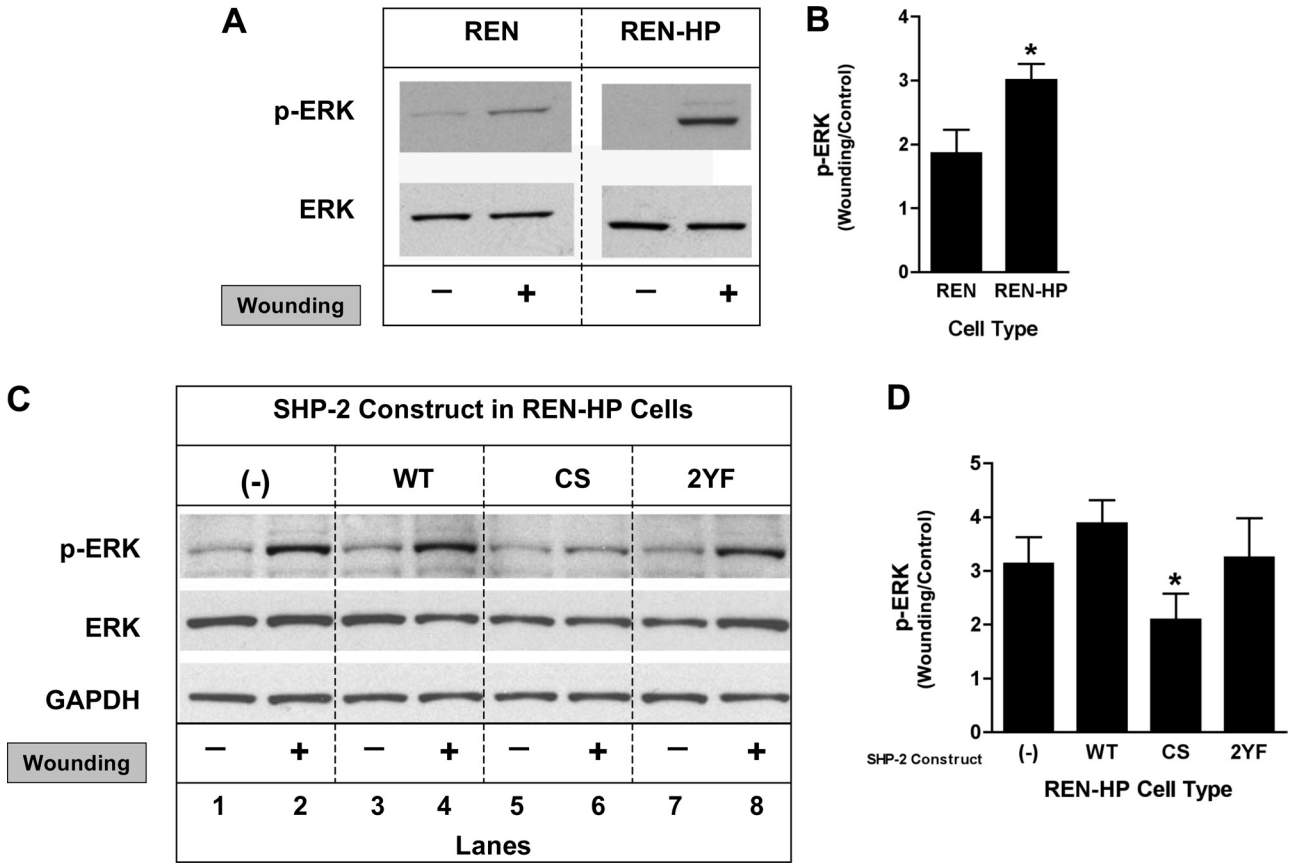

Fig. 6. Effects of the expression of SHP-2 constructs on wound-induced ERK activation in REN and REN-HP cells. Cell lysates from nonwounded or wounded monolayers of REN or REN-HP cells were immunoblotted with anti-phopho-ERK and anti-ERK antibodies. *A*: expression of PECAM-1 in REN cells resulted in increased phospho-ERK levels after wounding compared with nontransfected REN cells. *B*: densitometry confirmed that ERK activation following wounding of REN cells (expressed as the ratio of wounding/control) was increased by the expression of PECAM-1. Data are presented as means ± SE ($n = 4$; $^*P < 0.05$, compared with REN cells). *C*: expression of the CS-SHP-2 (CS) construct in REN-HP cells inhibited ERK activation (*lanes 5* and *6* compared with *lanes 1* and *2*) following wounding, while the presence of WT-SHP-2 (WT) or 2 YF-SHP-2 (2YF) did not suppress PECAM-1-dependent, wound-induced, ERK activation (*lanes 3* and *4*, and *lanes 7* and *8*, compared with *lanes 1* and *2*). *D*: densitometry confirmed that the ERK activation mediated by PECAM-1 (expressed as the ratio of wounding/control) was suppressed by coexpression of CS-SHP-2. Data are presented as means ± SE ($n = 3$; $^*P < 0.05$, compared with REN-HP/WT cells). The densitometry were all initially normalized to total ERK expression. (The data presented in *A* and *C* are from the same experiment and the same gel for each antibody. They are representative of 3–4 experiments).

expressing CS-SHP-2 had filopodia morphology that was reminiscent of the nontransfected REN cells (Fig. 4, *A* and *D*). The mean filopodia length was determined for the various cell lines and was found for the REN-HP cells to be twice that of the nontransfected REN cells (Fig. 4*F*). Although the mean filopodia lengths for the REN-HP/WT-SHP-2 and REN-HP/2YF-SHP-2 cells were comparable to the REN-HP cells, the mean filopodia length for the REN-HP/CS-SHP-2 transfectants was not significantly different from that of the nontransfected REN cells. Filopodia formation in REN cells was not affected by the expression of the SHP-2 constructs (data not shown). These findings parallel what we observed for cell migration (Fig. 3) and implicate PECAM-1/SHP-2 interactions in the formation of filopodia during PECAM-1-dependent cell motility.

Pharmacological inhibition of SHP-2 phosphatase activity inhibits PECAM-1-dependent motility and filopodia formation. The data presented above, based on a molecular approach, provided evidence that PECAM-1-dependent cell motility and filopodia formation are mediated through the phosphatase activity of SHP-2. To confirm these findings with an alternative strategy, we also studied the effects of NSC-87877, a potent and specific inhibitor SHP-2 phosphatase activity, on the behavior of REN and REN-HP cells (13). NSC-87877 (20 μM) induced a very modest and comparable (~10%) inhibition of proliferation in both cell lines (Fig. 5*A*). In contrast, the enhanced cell migration and filopodia formation induced by the presence of PECAM-1 in REN-HP cells were completely abrogated by NSC-87877, without any effects on the motility and filopodia of the control REN cells (Fig. 5, *B* and *C*). A similar pattern of effects was seen with HUVEC treated with this inhibitor (data not shown). These data thus provide pharmacological confirmation of the importance of the SHP-2 phosphatase activity in PECAM-1-dependent cell motility.

Expression of PECAM-1 increases ERK activation, an effect inhibited by expression of phosphatase-inactive SHP-2. MAPK has been shown to play a role in cell motility and in the formation of filopodia (6, 14, 22, 37, 51). The activation of extracellular signal-regulated kinase (ERK) was therefore determined in REN and REN-HP cells (Fig. 6). We found that ERK activation following wounding of confluent cell monolayers was increased in the REN-HP cells compared with the control REN cells (Fig. 6, *A* and *B*). The increase in ERK activation resulting from the presence of PECAM-1 in REN-HP cells was not enhanced further by the expression of WT-SHP-2 but was abrogated by the expression of CS-SHP-2 (Fig. 6, *B* and *C*). PECAM-1-dependent ERK activation was not altered by the presence of 2YF-SHP-2. ERK phosphorylation in REN cells during wound-induced migration was not significantly altered by the expression of these SHP-2 constructs (data not shown). This suggests that catalytically active SHP-2 in the context of PECAM-1-dependent cell motility mediates an activation of the ERK/MAPK pathway.

Expression of PECAM-1 suppresses paxillin tyrosine phosphorylation, an effect reversed by expression of phosphatase-inactive SHP-2. One model for the activation of ERK involves the tyrosine dephosphorylation of paxillin and the subsequent release of Src kinase from paxillin-dependent inhibition (14, 37). We therefore assessed the effects on paxillin tyrosine phosphorylation of expressing the SHP-2 constructs in REN-HP cells (Fig. 7). As has been previously reported (35), we found that the overall level of paxillin tyrosine phosphorylation following wounding was significantly reduced in REN-HP cells compared with control REN cells (Fig. 7*A*, *lane 2* compared with *lane 1*). In REN-HP cells that expressed WT-SHP-2 or 2YF-SHP-2, the levels of paxillin tyrosine phosphorylation were similarly reduced (Fig. 7*A*,

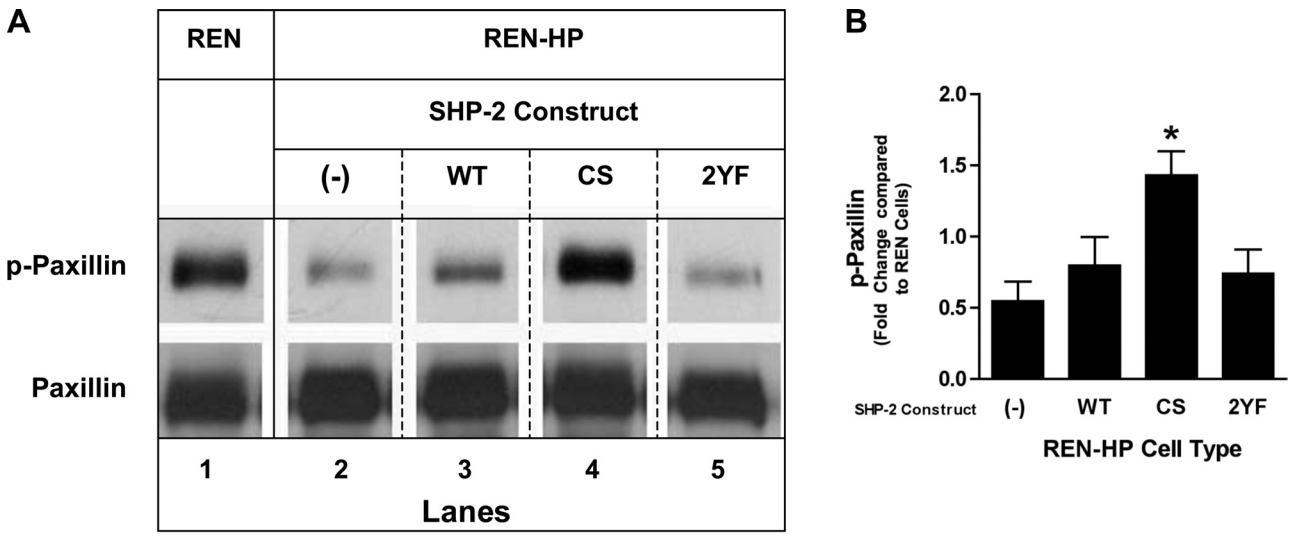

Fig. 7. Effects of the expression of SHP-2 constructs on wound-induced paxillin phosphorylation in REN and REN-HP cells. *A*: cell lysates from wounded monolayers of REN cells, REN-HP cells, and REN-HP cells expressing WT, CS, or 2YF constructs were immunoprecipitated with anti-paxillin antibody and then immunoblotted with anti-phospho-paxillin and anti-paxillin antibodies. In the REN-HP cells, wounding induced paxillin dephosphorylation (*lane 2* compared with *lane 1*) that was reversed by expression of CS-SHP-2 (*lane 4* compared with *lanes 1* and *2*). The presence of WT-SHP-2 or 2YF-SHP-2 did not reverse PECAM-1-dependent, wound-induced, paxillin dephosphorylation (*lanes 3* and *5*, and *1* and *2*). (The data are from the same experiment and the same gel for each antibody. They are representative of 5 experiments). *B*: densitometry confirmed that the dephosphorylation of paxillin mediated by PECAM-1 (expressed as fold change compared with REN cells) was reversed by coexpression of CS-SHP-2. Data are presented as means ± SE ($n = 5$; $^*P < 0.05$, compared with REN-HP cells). Paxillin levels in the nonwounded cells were comparable and were not altered by the expression of any of the SHP-2 constructs (data not shown).

lanes 3 and *5* compared with *lane 2*). In contrast, when CS-SHP-2 was expressed in REN-HP cells, paxillin tyrosine phosphorylation was preserved and even enhanced compared with that of nontransfected REN cells (Fig. 7*A*, *lane 4* compared with *lane 1* and Fig. 7*B*). Phosphopaxillin levels in REN cells during wound-induced migration were not increased by the presence of the CS mutant (data not shown). These data provide evidence of a mechanistic role for SHP-2 in the stimulation of PECAM-1-dependent cell motility through the dephosphorylation of paxillin and the subsequent activation of the ERK/MAPK pathway.

PECAM-1-dependent tube formation is not inhibited by the expression of phosphatase-inactive SHP-2. A number of studies have demonstrated that the presence of PECAM-1 promotes the in vitro formation of cord-like/tubular networks by endothelial cells or cellular transfectants expressing PECAM-1 (8, 35, 52). We therefore studied the ability of PECAM-1 transfectants expressing our SHP-2 mutants to form tubular structures on Matrigel (Fig. 8). We found that cord/tube formation was similar in control REN-HP transfectants and transfectants expressing the SHP-2 constructs (Fig. 8, *E–I*). In particular, although the CS-SHP-2 mutant inhibited PECAM-1-dependent motility (Fig. 3*A*), it did not suppress PECAM-1-dependent cord/tube formation (Fig. 8, *G* and *I*). This suggests that the stimulation of cord-like/tubular networks mediated by the expression of PECAM-1 is not due merely to an enhancement in cell motility and may be less dependent on PECAM-1/SHP-2 interactions.

DISCUSSION

The studies in this paper were done with the overall goal of furthering our understanding of the role of PECAM-1 as a mediator of endothelial cell motility during angiogenesis. The mechanisms by which PECAM-1 enhances cell migration still remain to be determined, although previous studies have indirectly implicated a role for SHP-2 in the ability of PECAM to stimulate endothelial cell motility (35). In these prior investigations, the ability of PECAM-1 to promote cell migration was eliminated by mutations of Y663 and Y686 in the cytoplasmic domain that led to the loss of the molecule's ability to bind to SH2 domain containing proteins such as SHP-2 (35). In this report we specifically demonstrate that overexpression of catalytically inactive SHP-2, but not wild-type SHP-2 or SHP-2 in which the adaptor/scaffold functions have been disabled, eliminates the ability of PECAM-1 to enhance cell migration (Fig. 3). Given that the various SHP-2 constructs were expressed at comparable levels, the effects of the catalytically inactive

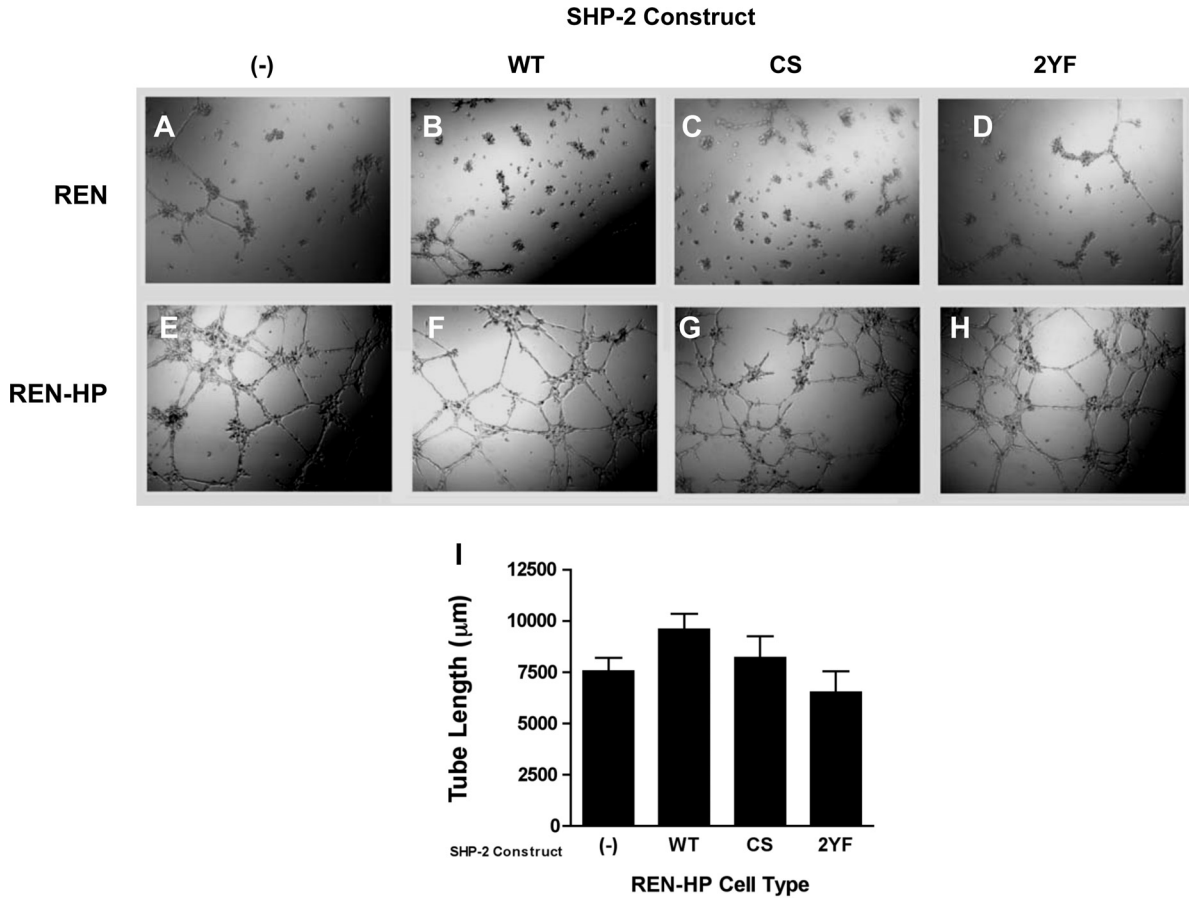

Fig. 8. Cord/tube formation on Matrigel by REN cells and REN-HP cells expressing SHP-2 constructs. Shown are REN cells (*A–D*) and REN-HP cells (*E–H*), expressing no SHP-2 constructs (*A* and *E*), WT-SHP-2 (*B* and *F*), CS-SHP-2 (*C* and *G*), or 2YF-SHP-2 (*D* and *H*) plated on Matrigel. REN cells did not form cord/tube-like networks on Matrigel, whereas all of the REN-HP cell transfectants did form cord/tube-like networks at comparable levels. Cord/tube formation was quantitated using image analysis (*I*). There were no significant differences between the various cell lines ($n = 6$). The data presented are representative of 3 experiments.

SHP-2 are unlikely to be related to "flooding" the cells with excess SHP-2. In addition, the enhanced motility mediated by the presence of PECAM-1 was completely abrogated by a specific pharmacological inhibitor of SHP-2 phosphatase activity (Fig. 5). Consequently, our studies now provide direct evidence for the involvement of SHP-2 in PECAM-1-dependent motility. These data also point to the importance of the phosphatase activity of SHP-2, rather than its adaptor/scaffold functions, in this process.

Although there is still more to be learned, our data offer some clues regarding the activity of SHP-2 as a mediator of PECAM-1-dependent motility. First, in REN-HP cells expressing the phosphatase-inactive SHP-2 mutant, both at rest or following wounding, we found that the levels of PECAM-1 tyrosine phosphorylation and SHP-2 association were significantly increased when compared with control REN-HP cells. In contrast, significant changes were not induced by the expression of the other constructs (Fig. 2). These data are consistent with a dynamic interaction between SHP-2 and PECAM-1 in which the level of PECAM-1 tyrosine phosphorylation, and thus SHP-2 binding, are regulated in part by bound, catalytically active SHP-2.

Second, we found that the stimulation of migration and filopodia formation induced by the expression of PECAM-1 was associated with increased ERK activation that was suppressed by coexpression of catalytically inactive SHP-2 (Fig. 6). There are a number of downstream targets of activated ERK (e.g., MLCK, FAK, and calpain) whose phosphorylation promotes processes required for efficient cell locomotion (12, 14, 22). For certain stimuli, SHP-2 may mediate the activation of ERK (14, 37). Our finding that PECAM-1-dependent cell migration was associated with increased ERK activation, which was inhibited by phosphatase-inactive SHP-2 (Fig. 5), is therefore consistent with previous reports. Furthermore, these data suggest that PECAM-1 in the context of endothelial cell motility, through SHP-2, may play a role in the upstream regulation of ERK.

Finally, our data suggest a mechanism for this PECAM-1-dependent ERK activation. During wound-induced migration we observed that PECAM-1 mediated a significant dephosphorylation of paxillin that was reversed by coexpression of phosphatase-inactive SHP-2 (Fig. 7). This is significant because there is evidence that Csk, by binding to phosphorylated paxillin, mediates inhibitory signals that repress ERK activation (14, 37). In initial studies, we have observed that the amount of Csk associated with paxillin during wound-induced migration was always significantly greater in the cells expressing the CS-SHP-2 mutant compared with the other transfectants (data not shown). Consequently, in the setting of PECAM-1-stimulated cell migration, dephosphorylation of paxillin by SHP-2, which was recruited and potentially activated by PECAM-1, may serve to trigger an ERK/MAPK-dependent signaling cascade by relieving Csk-mediated inhibition.

Our finding that expression of the catalytically inactive SHP-2 construct in REN-HP suppresses PECAM-1-dependent cell motility without inhibiting the capacity of these cells to form cord-like/tubular networks (Fig. 8) suggests that the ability of PECAM-1 to promote in vitro cord/tube formation is independent of its ability to stimulate cell migration. Additionally, in previous studies we have shown that loss of the ability of PECAM-1 to bind to SH2 domain containing proteins inhibits PECAM-1-dependent in vitro tube formation, implicating molecules such as SHP-2 in this process (15). Our data, however, suggest this inhibition is not due to the loss of a PECAM-1/SHP-2 interaction, pointing to the possibility that other PECAM-1-binding, SH2 domain containing proteins, may substitute for or be more important than SHP-2 in mediating the ability of PECAM-1 to stimulate to the formation of tubular/cord-like networks. We would stress

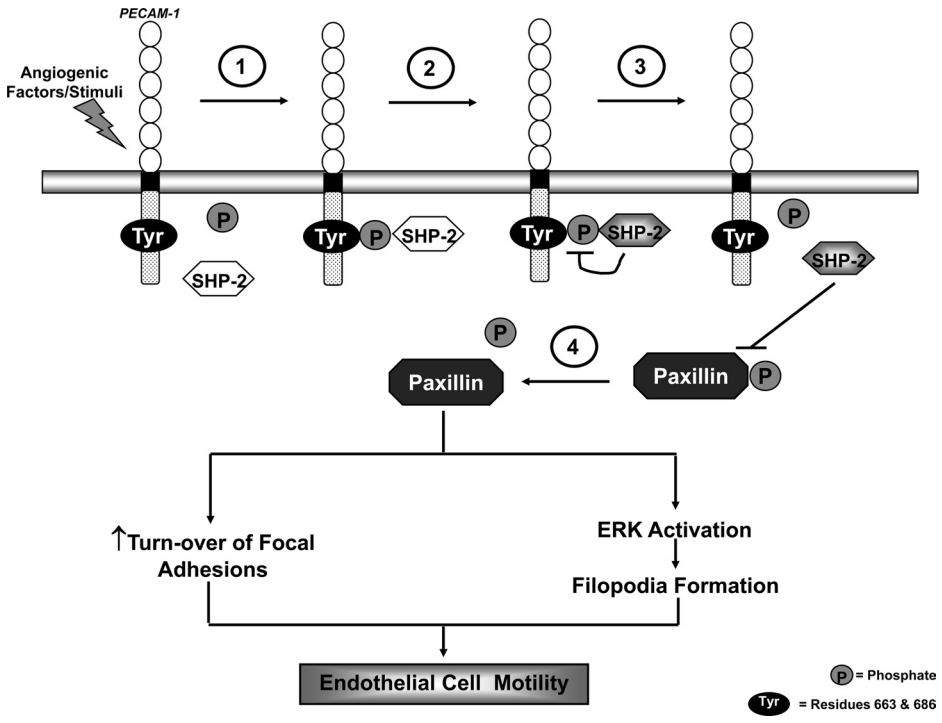

Fig. 9. A proposed model for the involvement of PECAM-1 in endothelial cell motility during angiogenesis. Angiogenic factors and/or conditions stimulate PECAM-1 tyrosine phosphorylation and the binding of SHP-2 to PECAM-1 (*step 1*). This association of SHP-2 with PECAM-1 results in activation of its phosphatase activity (*step 2*). The activated SHP-2 dephosphorylates the PECAM-1 molecule to which it is bound, leading to its release from PECAM-1 (*step 3*). The liberated SHP-2 subsequently targets paxillin, dephosphorylating it (*Step 4*), to trigger events such as the turnover of focal adhesions and ERK-mediated activation of filopodia formation, which ultimately promote endothelial cell motility. (Tyr = residues 663 and 686; *P* = phosphate).

that our data neither preclude some other molecular interaction with PECAM-1 that might contribute to junctional stabilization, nor do they exclude the involvement of PECAM-1 in the maintenance of junctional stability during quiescence.

Although a number of elements remain to be confirmed, we propose a model (Fig. 9) for the involvement of PECAM-1 in endothelial motility during angiogenesis in which angiogenic factors and/or stimuli trigger the tyrosine phosphorylation of PECAM-1 and the subsequent binding of SHP-2 to PECAM-1. This PECAM-1/SHP-2 interaction accomplishes two things: the recruitment of SHP-2 to the membrane and the activation of its phosphatase activity, possibly by conformational changes stimulated by PECAM-1-binding. With its phosphatase activity now "turned on," SHP-2 then dephosphoylates the PECAM-1 molecule to which it is bound, resulting in the release of SHP-2. The liberated SHP-2, now localized at the membrane, promotes the turnover of focal adhesions by dephosphorylating constituent proteins such as paxillin (35). The membrane-localized SHP-2 also mediates dephosphoylation events that activate the ERK pathway, a consequence of which is the enhanced formation of filopodia. The net effects of these events are increased cell motility and a role for PECAM-1 in facilitating these processes through the recruitment and activation of SHP-2.

ACKNOWLEDGMENTS

This work was supported by grants from the Department of Defense (PR043482) and the National Heart, Lung, and Blood Institute (HL-079090).

DISCLOSURES

No conflicts of interest, financial or otherwise, are declared by the author(s).

REFERENCES

1. **Araki T, Nawa H, Neel BG.** Tyrosyl phosphorylation of Shp2 is required for normal ERK activation in response to some, but not all, growth factors. *J Biol Chem* 278: 41677–41684, 2003.
2. **Barford D, Neel BG.** Revealing mechanisms for SH2 domain mediated regulation of the protein tyrosine phosphatase SHP-2. *Structure* 6:249–254, 1998.
3. **Bazzoni G, Dejana E.** Endothelial cell-to-cell junctions: molecular organization and role in vascular homeostasis. *Physiol Rev* 84: 869–901, 2004.
4. **Bentires-Alj M, Paez JG, David FS, Keilhack H, Halmos B, Naoki K, Maris JM, Richardson A, Bardelli A, Sugarbaker DJ, Richards WG, Du J, Girard L, Minna JD, Loh ML, Fisher DE, Velculescu VE, Vogelstein B, Meyerson M, Sellers WR, Neel BG.** Activating mutations of the noonan syndrome-associated SHP2/PTPN11 gene in human solid tumors and adult acute myelogenous leukemia. *Cancer Res* 64:8816–8820, 2004.
5. **Billadeau DD, Leibson PJ.** ITAMs versus ITIMs: striking a balance during cell regulation. *J Clin Invest* 109: 161–168, 2002.
6. **Brahmbhatt AA, Klemke RL.** ERK and RhoA differentially regulate pseudopodia growth and retraction during chemotaxis. *J Biol Chem* 278: 13016–13025, 2003.
7. **Cao MY, Huber M, Beauchemin N, Famiglietti J, Albelda SM, Veillette A.** Regulation of mouse PECAM-1 tyrosine phosphorylation by the Src and Csk families of protein-tyrosine kinases. *J Biol Chem* 273: 15765–15772, 1998.
8. **Cao G, O'Brien CD, Zhou Z, Sanders SM, Greenbaum JN, Makrigiannakis A, DeLisser HM.** The involvement of human PECAM-1 in angiogenesis and in vitro endothelial cell migration. *Am J Physiol Cell Physiol* 282: C1181–C1190, 2002.
9. **Cao G, Fehrenbach M, Williams J, Finklestein J, Zhu JX, DeLisser HM.** Angiogenesis in PECAM-1-null mice. *Am J Pathol* 175: 903–915, 2009.
10. **Carrithers M, Tandon S, Canosa S, Michaud M, Graesser D, Madri JA.** Enhanced susceptibility to endotoxic shock and impaired STAT3 signaling in CD31-deficient mice. *Am J Pathol* 166: 185–196, 2005.
11. **Chan G, Kalaitzidis D, Neel BG.** The tyrosine phosphatase Shp2 (PTPN11) in cancer. *Cancer Metastasis Rev* 27: 179–192, 2008.
12. **Chang L, Karin M.** Mammalian MAP kinase signaling cascades. *Nature* 410: 37–40, 2001.
13. **Chen L, Sung S, Yip LR, Lawrence HR, Ren Y, Guida WC, Sebti SN, Lawrence NJ, Wu J.** Discovery of a novel Shp2 protein tyrosine phosphatase inhibitor. *Mol Pharmacol* 70: 562–570, 2006.
14. **Dance M, Montagner A, Salles JP, Yart A, Raynal P.** The molecular functions of Shp2 in the Ras/Mitogen-activated protein kinase (ERK1/2) pathway. *Cell Signal* 20: 453–459, 2008.
15. **DeLisser HM, Christofidou-Solomidou M, Strieter RM, Burdick MD, Robinson CS, Wexler RS, Kerr JS, Garlanda C, Merwin JR, Madri JA, Albelda SM.** Involvement of endothelial PECAM-1/CD31 in angiogenesis. *Am J Pathol* 151: 671–677, 1997.
16. **Dimaio TA, Wang S, Huang Q, Scheef EA, Sorenson CM, Sheibani N.** Attenuation of retinal vascular development and neovascularization in PECAM-1-deficient mice. *Dev Biol* 315: 72–88, 2008.
17. **Duncan GS, Andrew DP, Takimoto H, Kaufman SA, Yoshida H, Spellberg J, Luis de la Pompa J, Elia A, Wakeham A, Karan-Tamir B, Muller WA, Senaldi G, Zukowski MM, Mak TW.** Genetic evidence for functional redundancy of platelet/endothelial cell adhesion molecule-1 (PECAM-1): CD31-deficient mice reveal PECAM-1-dependent and PECAM-1-independent functions. *J Immunol* 162: 3022–3030, 1999.
18. **Fujiwara K.** Platelet endothelial cell adhesion molecule-1 and mechanotransduction in vascular endothelial cells. *J Intern Med* 259: 373–380, 2006.
19. **Garnacho C, Albelda SM, Muzykantov VR, Muro S.** Differential intra-endothelial delivery of polymer nanocarriers targeted to distinct PECAM-1 epitopes. *J Control Release* 130: 226–33, 2008.
20. **Gratzinger D, Canosa S, Engelhardt B, Madri JA.** Platelet endothelial cell adhesion molecule-1 modulates endothelial cell motility through the small G-protein Rho. *FASEB J* 17: 1458–1469, 2003.
21. **Gupton SL, Gertler FB.** Filopodia: the fingers that do the walking. *Sci STKE* 400: re5, 2007.
22. **Huang C, Jacobson Schaller, MD K.** MAP kinases and cell migration. *J Cell Sci* 117: 4619–4628.
23. **Ilan N, Madri JA.** PECAM1: old friend, new partners. *Curr Opin Cell Biol* 15: 515–524, 2003.
24. **Jackson DE, Ward CM, Wang R, Newman PJ.** The protein-tyrosine phosphatase SHP-2 binds platelet/endothelial cell adhesion molecule-1 (PECAM-1) and forms a distinct signaling complex during platelet aggregation. Evidence for a mechanistic link between PECAM-1- and integrin-mediated cellular signaling. *J Biol Chem* 272: 6986–6993, 1997.
25. **Jackson DE.** The unfolding tale of PECAM-1. *FEBS Lett* 540: 7–14, 2003.
26. **Ji G, O'Brien CD, Feldman M, Manevich Y, Lim P, Sun J, Albelda SM, Kotlikoff MI.** PECAM-1 (CD31) regulates a hydrogen peroxide-activated nonselective cation channel in endothelial cells. *J Cell Biol* 157: 173–84, 2002.
27. **Kogata N, Masuda M, Kamioka Y, Yamagishi A, Endo A, Okada M, Mochizuki N.** Identification of Fer tyrosine kinase localized on microtubules as a platelet endothelial cell adhesion molecule-1 phosphorylating kinase in vascular endothelial cells. *Mol Biol Cell* 14: 3553–3564, 2003.
28. **Kondo S, Scheef EA, Sheibani N, Sorenson CM.** PECAM-1 isoform-specific regulation of kidney endothelial cell migration and capillary morphogenesis. *Am J Physiol Cell Physiol* 292: C2070–C2083, 2007.
29. **Loh ML, Vattikuti S, Schubbert S, Reynolds MG, Carlson E, Lieuw KH, Cheng JW, Lee CM, Stokoe D, Bonifas JM, Curtiss NP, Gotlib J, Meshinchi S, Le Beau MM, Emanuel PD, Shannon KM.** Mutations in PTPN11 implicate the SHP-2 phosphatase in leukemogenesis. *Blood* 103: 2325–2331, 2004.
30. **Lu TT, Barreuther M, Davis S, Madri JA.** Platelet endothelial cell adhesion molecule-1 is phosphorylatable by c-Src, binds Src-Src homology 2 domain, and exhibits immunoreceptor tyrosine-based activation motif-like properties. *J Biol Chem* 272: 14442–14446, 1997.
31. **Maas M, Stapleton M, Bergom C, Mattson DL, Newman DK, Newman PJ.** Endothelial cell PECAM-1 confers protection against endotoxic shock. *Am J Physiol Heart Circ Physiol* 288: H159–H164, 2005.
32. **Mattila PK, Lappalainen P.** Filopodia: molecular architecture and cellular functions. *Nat Rev Mol Cell Biol* 9: 446–454, 2008.
33. **Muzykantov VR, Christofidou-Solomidou M, Balyasnikova I, Harshaw DW, Schultz L, Fisher AB, Albelda SM.** Streptavidin facilitates internalization and pulmonary targeting of an anti-endothelial cell antibody (platelet-endothelial cell adhesion molecule 1): a strategy for vas-

cular immunotargeting of drugs. *Proc Natl Acad Sci USA* 96:2379–2384, 1999.
34. **Newman PJ.** The biology of PECAM-1. *J Clin Invest* 99: 3–8, 1997.
35. **O'Brien C, Cao G, Makringiannakis A, DeLisser HM.** The Role of immunoreceptor tyrosine-based inhibitory motifs of platelet endothelial cell adhesion molecule (PECAM-1) in PECAM-1 dependent cell migration. *Am J Physiol Cell Physiol* 287: C1103–C1113, 2004.
36. **Ravetch JV, Lanier LL.** Immune inhibitory receptors. *Science* 290: 84–89, 2000.
37. **Ren Y, Meng S, Mei L, Zhao ZJ, Jove R, Wu J.** Roles of Gab1 and SHP2 in paxillin tyrosine dephosphorylation and Src activation in response to epidermal growth factor. *J Biol Chem* 279: 8497–8505, 2005.
38. **Sagawa K, Kimura T, Swieter M, Siraganian RP.** The protein-tyrosine phosphatase SHP-2 associates with tyrosine-phosphylated adhesion molecule PECAM-1 (CD31). *J Biol Chem* 272: 31086–31091, 1997.
39. **Saxton TM, Henkemeyer M, Gasca S, Shen R, Rossi DJ, Shalaby F, Feng GS, Pawson T.** Abnormal mesoderm patterning in mouse embryos mutant for the SH2 tyrosine phosphatase Shp-2. *EMBO J* 16: 2352–2364, 1997.
40. **Smythe WR, Hwang HC, Amin KM, Eck SL, Davidson BL, Wilson JM, Kaiser LR, Albelda SM.** Use of recombinant adenovirus to transfer the herpes simplex virus thymidine kinase (HSVtk) gene to thoracic neoplasm: an effective in vitro drug sensitization system. *Cancer Res* 54: 2055–2059, 1994.
41. **Solowiej A, Biswas P, Graesser D, Madri JA.** Lack of platelet endothelial cell adhesion molecule-1 attenuates foreign body inflammation because of decreased angiogenesis. *Am J Pathol* 162: 953–962, 2003.
42. **Sun J, Paddock C, Shubert J, Zhang HB, Amin K, Newman PJ, Albelda SM.** Contributions of the extracellular and cytoplasmic domains of platelet-endothelial cell adhesion molecule-1 (PECAM-1/CD31) in regulating cell-cell localization. *J Cell Sci* 113: 1459–1469, 2000.
43. **Tartaglia M, Mehler EL, Goldberg R, Zampino G, Brunner HG, Kremer H, van der Burgt I, Crosby AH, Ion A, Jeffery S, Kalidas K, Patton MA, Kucherlapati RS, Gelb BD.** Mutations in PTPN11, encoding the protein tyrosine phosphatase SHP-2, cause Noonan syndrome. *Nat Genet* 29: 465–468, 2001.
44. **Tartaglia M, Niemeyer CM, Fragale A, Song X, Buechner J, Jung A, Hählen K, Hasle H, Licht JD, Gelb BD.** Somatic mutations in PTPN11 in juvenile myelomonocytic leukemia, myelodysplastic syndromes and acute myeloid leukemia. *Nat Genet* 34: 148–150, 2003.
45. **Tonks NK.** Protein tyrosine phosphatases: from genes, to function, to disease. *Nat Rev Mol Cell Biol* 7: 833–846, 2006.
46. **Tzima E, Irani-Tehrani M, Kiosses WB, Dejana E, Schultz DA, Engelhardt B, Cao G, DeLisser HM, Schwartz MA.** A mechanosensory complex that mediates the endothelial cell response to fluid shear stress. *Nature* 437: 426–431, 2005.
47. **Udell CM, Samayawardhena LA, Kawakami Y, Kawakami T, Craig AW.** Fer and Fps/Fes participate in a Lyn-dependent pathway from FcepsilonRI to platelet-endothelial cell adhesion molecule 1 to limit mast cell activation. *J Biol Chem* 281: 20949–20957, 2006.
48. **Wang S, Yu WM, Zhang W, McCrae KR, Neel BG, Qu CK.** Noonan syndrome/leukemia-associated gain-of-function mutations in SHP-2 phosphatase (PTPN11) enhance cell migration and angiogenesis. *J Biol Chem* 284: 913–20, 2009.
49. **Wiewrodt R, Thomas AP, Cipelletti L, Christofidou-Solomidou M, Weitz DA, Feinstein SI, Schaffer D, Albelda SM, Koval M, Muzykantov VR.** Size-dependent intracellular immunotargeting of therapeutic cargoes into endothelial cells. *Blood* 99: 912–922, 2002.
50. **Woodfin A, Voisin MB, Nourshargh S.** PECAM-1: a multi-functional molecule in inflammation and vascular biology. *Arterioscler Thromb Vasc Biol* 27: 2514–2523, 2007.
51. **Yang W, Klaman LD, Chen B, Araki T, Harada H, Thomas SM, George EL, Neel BG.** An Shp2/SFK/Ras/Erk signaling pathway controls trophoblast stem cell survival. *Dev Cell* 10: 317–327, 2006.
52. **Zhou Z, Christofidou-Solomidou M, Garlanda C, DeLisser HM.** Antibody against Murine PECAM-1 Inhibits Tumor Angiogenesis in Mice. *Angiogenesis* 3: 181–188, 1999.

The American Journal of Pathology, Vol. 175, No. 2, August 2009

DOI: 10.2353/ajpath.2009.090206

Vascular Biology, Atherosclerosis and Endothelium Biology

Angiogenesis in Platelet Endothelial Cell Adhesion Molecule-1-Null Mice

Gaoyuan Cao, Melane L. Fehrenbach, James T. Williams, Jeffrey M. Finklestein, Jing-Xu Zhu, and Horace M. DeLisser

From the Pulmonary, Allergy and Critical Care Division, Department of Medicine, University of Pennsylvania School of Medicine, Philadelphia, Pennsylvania

Platelet endothelial cell adhesion molecule (PECAM)-1 has been previously implicated in endothelial cell migration; additionally, anti-PECAM-1 antibodies have been shown to inhibit *in vivo* angiogenesis. Studies were therefore performed with PECAM-1-null mice to further define the involvement of PECAM-1 in blood vessel formation. Vascularization of subcutaneous Matrigel implants as well as tumor angiogenesis were both inhibited in PECAM-1-null mice. Reciprocal bone marrow transplants that involved both wild-type and PECAM-1-deficient mice revealed that the impaired angiogenic response resulted from a loss of endothelial, but not leukocyte, PECAM-1. *In vitro* wound migration and single-cell motility by PECAM-1-null endothelial cells were also compromised. In addition, filopodia formation, a feature of motile cells, was inhibited in PECAM-1-null endothelial cells as well as in human endothelial cells treated with either anti-PECAM-1 antibody or PECAM-1 siRNA. Furthermore, the expression of PECAM-1 promoted filopodia formation and increased the protein expression levels of Cdc42, a Rho GTPase that is known to promote the formation of filopodia. In the developing retinal vasculature, numerous, long filamentous filopodia, emanating from endothelial cells at the tips of angiogenic sprouts, were observed in wild-type animals, but to a lesser extent in the PECAM-1-null mice. Together, these data further establish the involvement of endothelial PECAM-1 in angiogenesis and suggest that, *in vivo*, PECAM-1 may stimulate endothelial cell motility by promoting the formation of filopodia. ***(Am J Pathol 2009, 175:903–915; DOI: 10.2353/ajpath.2009.090206)***

Platelet endothelial cell adhesion molecule-1 (PECAM-1) is a 130-kd transmembrane glycoprotein member of the Ig superfamily expressed on endothelial cells (ECs) as well as leukocytes and platelets.[1] Although it was originally recognized as a protein capable of binding interactions with itself and possibly other non-PECAM-1 molecules,[2–6] there is now a significant body of evidence that PECAM-1 also participates in signaling cascades.[7,8] Of note, PECAM-1 has two tyrosine residues (Y663 and Y686) that each fall within a conserved signaling sequence known as the immunoreceptor tyrosine-based inhibitory motif.[9,10] Phosphorylation of these tyrosine residues enables the binding of Src homology (SH)-2 domain containing molecules, including the SHP-2 tyrosine phosphatase.[11–14] Consistent with an involvement in blood vessel formation,[15–17] PECAM-1 has been implicated in the adhesive and signaling events required for endothelial cell migration,[17,18] a process critical to angiogenesis. These studies of human ECs, and cellular transfectants expressing human PECAM-1, have suggested that PECAM-1 may promote endothelial cell motility by recruiting SHP-2 to the cell membrane, which induces the turnover of focal adhesions.[18]

The finding that anti-PECAM-1 antibodies impair vessel formation supports a role for PECAM-1 during *in vivo* angiogenesis.[15–17] Mice deficient in the expression of PECAM-1 are viable, suggesting that vascular development in the absence of PECAM-1 is sufficient to allow for adequate embryogenesis.[19] However, subsequent studies have shown that the loss of PECAM-1 results in decreased neutrophil recruitment in response to interleukin-1[20,21] and in other inflammatory settings,[22,23] enhanced susceptibility to endotoxic shock,[24] increased endothelial sensitivity to apoptotic stress,[25] and impaired alveolarization.[26] To date, however, *in vivo* angiogenesis has been investigated in these animals in only a limited number of reports.[27,28] Studies were therefore performed in PECAM-1-null mice to more fully define the formation of vessels in several animal models, as well as the func-

Supported by Department of Defense grant PR043482 (to H.M.D.) and National Institutes of Health grant HL079090 (to H.M.D).

Accepted for publication April 28, 2009.

Address reprint requests to Horace M. DeLisser, M.D., Pulmonary, Allergy and Critical Care Division, SVM-Hill Pavilion, Room 410B, 380 South University Avenue, Philadelphia, PA 19104-3945. E-mail: delisser@mail.med.upenn.edu.

tional activity of ECs isolated from wild-type and PECAM-null mice.

We found that vascularization of subcutaneous Matrigel implants, as well as tumor angiogenesis, were inhibited in PECAM-1-null mice. Reciprocal bone marrow transplants involving wild-type and PECAM-1-deficient mice revealed that the impaired angiogenic response resulted from a loss of endothelial PECAM-1 and not leukocyte PECAM-1. In subsequent studies of ECs isolated from these animals, we found that *in vitro* cell migration was significantly compromised in the ECs isolated from PECAM-1-deficient mice. Further, a feature of an actively motile cell includes the presence of cellular protrusions known as filopodia,[29,30] which mediate several functions required for cell migration. The formation of filopodia was impaired in PECAM-1-null ECs, and in human umbilical vein endothelial cells (HUVEC) treated with anti-PECAM-1 antibody or in which PECAM-1 expression had been knocked down by siRNA. In addition, expression of PECAM-1 in cellular transfectants promoted filopodia formation. The expression of PECAM-1 increased the protein levels of Cdc42, a Rho GTPase known to promote the formation of filopodia.[31–35] These *in vitro* data were consistent with the finding that reduced numbers of endothelial filopodial extensions were detected in PECAM-1-null mice during postnatal vascularization of the retina in the developing murine eye. Together, these data further establish the involvement of endothelial PECAM-1 in the formation of vessels and suggest that, *in vivo*, PECAM-1 may stimulate endothelial cell motility by promoting the formation of filopodia.

Materials and Methods

Reagents and Chemicals

All reagents and chemicals were obtained from Sigma (St. Louis, MO) unless otherwise specified.

Antibodies

The following antibodies against murine surface receptors were used: mAb 390, rat anti-PECAM-1[15,16]; rat anti-ICAM-1[36]; and rat anti-ICAM-2 (Southern Biotech, Birmingham, AL). The following antibodies were also used: Cdc42 and VE-cadherin (Santa Cruz Biotechnology, Santa Cruz, CA); Rac1 and RhoA (BD Transduction Laboratories, San Jose, CA); and GAPDH (Chemicon/Millipore, Temecula, CA). Cell surface antibody binding was determined by flow cytometry using previously described procedures.[18]

Cell Lines

The H5V murine endothelial line,[37] B16 murine melanoma line (obtained from the ATCC), and ID8-VEGF tumor line[38] were cultured in Dulbecco's modified Eagle's medium containing 10% fetal bovine serum, penicillin/streptomycin, and 2 mmol/L L-glutamine, with insulin also added to the medium for the culturing of the ID8-VEGF cells. Lung ECs were isolated from wild-type and PECAM-1-null mice using published protocols.[39] Mouse ECs and HUVEC (Clonetics, San Diego, CA) were cultured on gelatin in medium 199 containing 12.7% fetal bovine serum, 75 μg/ml endothelial growth factor, 100 μg/ml heparin and 2 mmol/L glutamine. Mouse ECs and HUVEC were used between passages 2 and 6. The human mesothelioma cell line, REN,[18] was cultured in RPMI medium supplemented with 10% fetal bovine serum, penicillin/streptomycin, and 2 mmol/L L-glutamine. REN cell transfectants stably expressing human PECAM-1 (REN-HP) were cultured in the same media with G418 (0.5 g/L; Gibco BRL, Grand Island, NY).

Animals

The Institutional Animal Care and Utilization Committees at both the Wistar Institute and the University of Pennsylvania School of Medicine approved all animal care procedures. PECAM-1-null mice that had been backcrossed for >10 generations onto a C57BL/6 background[22] were the kind gift of Dr. Joseph Madri (Yale University) through Dr. Steven Albelda (University of Pennsylvania). Wild-type mice, also on a C57BL/6 background, were obtained from Taconic (Germantown, NY).

Matrigel Neovascularization Model

Wild-type and PECAM-1-null mice in the C57BL/6 background were injected subcutaneously with 0.3 ml of Matrigel (Chemicon/Millipore) containing 1×10^6 B16 melanoma cells to induce the growth of vessels into the gel. After 5 to 7 days, the animals were sacrificed. The gels were then harvested and either processed for hemoglobin analysis as a measure of the vascularization of the gels or fixed in 10% formalin for paraffin sections and hematoxylin and eosin staining. Tissue adjacent to as well as distant from the gel were also harvested and processed for silver staining as previously described.[40]

Tumor Growth and Angiogenesis

A total of 2×10^6 B16 melanoma or ID8-VEGF ovarian tumor cells in a total volume of 50 μl were injected subcutaneously into the flanks of wild-type and PECAM-1-null mice. After 14 days (B16 melanoma) or 9 weeks (ID8-VEGF ovarian tumor), the mice were sacrificed and the tumors harvested, weighed, and processed for staining. For quantitation of angiogenesis, frozen sections of comparably sized tumors were stained with ICAM-2 antibody to identify murine blood vessels. To assess the tumor angiogenic response, serial sections were obtained from different levels within the tumor separated by ~100 μm. A total of four to eight levels per tumor and four to six 40X fields per level were analyzed. Computer-assisted image analysis (Image-Pro Plus program, Media Cybernetics, Silver Spring, MD) was then used to determine the percentage of tumor occupied by vessels.

Generation of Bone Marrow Chimeric Animals

Bone marrow chimeric mice were generated as previously described.[41] Briefly, to generate recipient animals, 6-week-old wild-type or PECAM-1 null mice were irradiated with 1000 rads from a Cs-137 irradiation source. Within 24 hours after irradiation, donor marrow was obtained from the femur and tibia of non-irradiated mice, and 5×10^6 cells were injected via the tail vein into the irradiated recipient mice. Experiments were subsequently conducted 4 to 6 weeks after transplantation. Flow cytometry analysis of leukocytes, using an anti-mouse PECAM-1 antibody, confirmed the phenotype of each chimeric mouse.

Immunohistochemical Staining

Immunohistochemistry was performed using a commercially available kit according to the manufacturer's instructions (ABC Immunodetection kit, Vector Laboratories, Burlingame, CA). Briefly, 6-μm-thick sections were prepared by cryostat, transferred to glass slides, and fixed in ice-cold acetone and rinsed in phosphate-buffered saline (PBS). The sections were then treated with 0.5% H_2O_2 in PBS for 30 minutes, and then blocked with 0.5% bovine serum albumin for 30 minutes. The primary antibody was applied for 1 hour, washed, and then incubated with biotinylated secondary antibody for 60 minutes. The reaction was developed with an avidin-biotin complex reaction and the sections lightly counterstained with hematoxylin.

In Vitro *Cell Proliferation*

ECs were cultured for 24 hours in 96-well plates (4000 cells/well) and the number of viable cells determined using the Promega CellTiter 96 AQ_{ueous} non-radioactive cell proliferation assay (Madison WI).

In Vitro *Cell Death Detection*

For the studies of apoptosis, confluent cells were exposed for 5 hours to serum-free medium or complete medium with or without antibody. Apoptosis was then assessed using the APOPercentage apoptosis assay (Biocolor Ltd, Belfast, N. Ireland).

In Vitro *Wound-Induced Migration Assay*

Endothelial cell wounding was performed as previously described.[18] Twenty thousand murine ECs (primary or H5V cells) were added to 24-well tissue culture plates and allowed to grow to confluence. Linear (primary ECs) or circular (H5V cells) defects were then scratched into the monolayer. The wounded culture was washed with PBS and then incubated for 24 hours in medium (with 1% serum) with antibodies (100 μg/ml) included for studies with H5V cells. Images were obtained immediately after wounding and then again 24 hours later. The distance migrated by cells at the wound edge (primary ECs) or change in wound area (H5V cells) were determined using computer-assisted image analysis. For each condition, three to five wounds were analyzed. The data are presented as distance migrated (primary ECs) or as change in wound area expressed as a percentage of control (H5V cells).

In Vitro *Matrigel Invasion/Migration Assay*

Matrigel-coated Transwell inserts (Costar; 8-μm pore filter) were prepared by twice adding 100 μl of Matrigel (250 μg/ml) to the Transwell and allowing the Matrigel to dry at 37°C in a non-humidified oven for 24 hours. Murine ECs were labeled overnight with [^{3}H]thymidine and resuspended to a concentration of 200,000 cells/ml in low serum media (5% serum), with antibodies (100 μg/ml) included for studies with H5V cells. The resulting cell suspensions (500 μl) were then placed in Transwell filter inserts, which in turn were placed in 12-well plates containing 20% serum media and incubated for 8 (H5V cells) or 18 (primary EC) hours at 37°C in 5% CO_2. The cells migrated through the Matrigel, passed through the pores of the filter, and adhered on the lower surface of the filter. After incubation the wells were removed, washed, and the top surface of the filter wiped with a cotton swab. The filters were then carefully cut out, placed in scintillation fluid, and counted in a β-counter. The data are presented as percent cells migrated (primary ECs) or as cells migrated expressed as a percentage of control (H5V).

Assessing the Morphology of Plated Cells

Mouse ECs, HUVEC, or REN cells resuspended in complete medium were seeded into four-well Lab-Tek chamber slides (Nunc, Thermo Fischer Scientific, Rochester, NY), that were uncoated (REN cells) or coated with 1% gelatin (ECs). Subsequently, the cells were allowed to spread for predetermined times at 37°C, fixed with 2% paraformaldehyde for 5 minutes and then stained with 0.1% toluidine blue. Images were then captured and analyzed by computer-assisted image analysis.

siRNA-Mediated Knockdown of Protein Expression

siRNA oligos specific for PECAM-1 were obtained from Applied Biosystems/Ambion (Austin, TX). To knock down protein expression, cells were grown to 80% confluence in 12-well dishes and then transduced at 37°C 5% CO_2 for 6 hours with 0.1 μmol/L siRNA according to the manufacturer's (Santa Cruz) instructions.

Visualization and Quantification of Retinal Vasculature

The vasculature of the developing mouse retina was processed and visualized using published procedures.[42] Briefly, mouse eyes were fixed in 4% paraformaldehyde

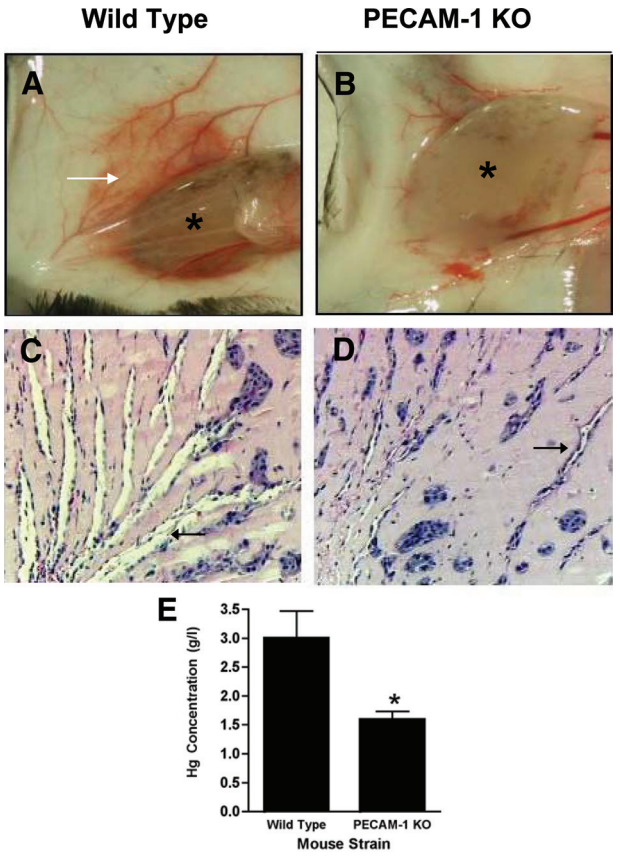

Figure 1. Neovascularization of Matrigel implants in wild-type and PECAM-1-null mice. Shown are images of subcutaneous Matrigel implants (**asterisks**) containing B16 melanoma cells as a source of angiogenic factors harvested after 5 days from wild-type (**A**) and PECAM-1-null (PECAM KO) (**B**) animals. A "blush" of vessel proliferation (**white arrow**) was evident around the implants from the wild-type animal that was not present in the PECAM-1-null mice. H&E staining demonstrated the presence of many more vessels (**black arrows**) invading the gels in the wild-type (**C**) mice compared with the gels from the PECAM-1-deficient mice (**D**). The vascularization of the gels, as assessed by hemoglobin concentration (**E**), was significantly reduced in PECAM-1-null mice compared with wild-type mice. Data are presented as means ± SE ($n = 10$, $^*P < 0.01$).

in PBS at 4°C overnight and then washed with PBS. Retinas were dissected, permeabilized in PBS with 1% bovine serum albumin and 0.5% Triton X-100 at 4°C overnight, rinsed in PBS, washed twice in PBlec (PBS, pH 6.8, 1% Triton-X100, 0.1 mmol/L $CaCl_2$, 0.1 mmol/L $MgCl_2$, 0.1 mmol/L $MnCl_2$), and incubated in biotinylated isolectin B4 (*Bandeiraea simplicifolia*, Sigma-Aldrich), 20 μg/ml in PBlec at 4°C overnight. After five washes in PBS, samples were incubated with fluorescein avidin D (Vector Laboratories, Burlingame, CA) diluted 1:100 in PBS, 0.5% bovine serum albumin, and 0.25% Triton X-100 at 4°C for 6 hours. After washing and a brief postfixation in paraformaldehyde, the retinas were flat-mounted using Vectashield Hard Set (H-1400, Vector Laboratories) and then analyzed using fluorescence microscopy (Olympus IX70) and the Metamorph imaging system (Molecular Devices, Downingtown, PA).

Western Blotting

Total cell lysates were loaded in equal protein amounts (10 μg) determined by BCA (Pierce, Rockford, IL). Proteins were resolved by sodium dodecyl sulfate-polyacrylamide gel electrophoresis (Novex; Invitrogen) followed by transfer onto nitrocellulose membranes using the iBlot dry blotting system (Invitrogen), which employs semidry electrotransfer. Membranes were washed in 1X TTBS for 2 to 3 minutes, blocked with 5% blotting grade blocker solution from Bio-Rad Laboratories (Hercules, CA), and incubated with the primary antibody in 2% bovine serum albumin for 1 hour at room temperature. Unbound antibodies were washed off with TTBS before membranes were incubated with horseradish peroxidase-labeled species-specific secondary antibodies for 1 hour at room temperature. After again washing the membranes with PBS, bound antibody signals were detected by enhanced chemiluminescence substrate and documented on X-ray film. The chemiluminescent signals were quantified by densitometry (ImageQuant, Amersham, Piscataway, NJ) and normalized to the housekeeping protein GAPDH.

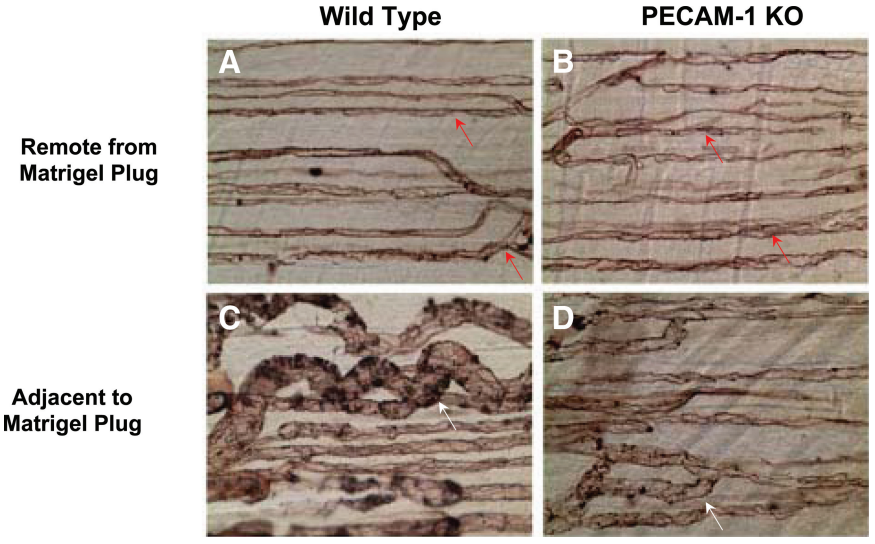

Figure 2. Morphology of vessels remote from and adjacent to Matrigel implants in wild-type and PECAM-1-null mice. Skin tissue was harvested from wild-type (**A** and **C**) and PECAM-1-null (PECAM-1 KO) mice (**B** and **D**) from areas remote from (**A** and **B**) and adjacent to (**C** and **D**) the Matrigel implants and the vasculature visualized by silver staining. In areas remote from the Matrigel plugs the morphology and pattern of the vasculature were similar in wild-type and PECAM-1null mice (**A** and **B**, **red arrows**), while the vessels adjacent to and invading the gels in PECAM-1-null mice were less dilated and tortuous than the comparable vessels in wild-type animals (**C** and **D**, **white arrows**).

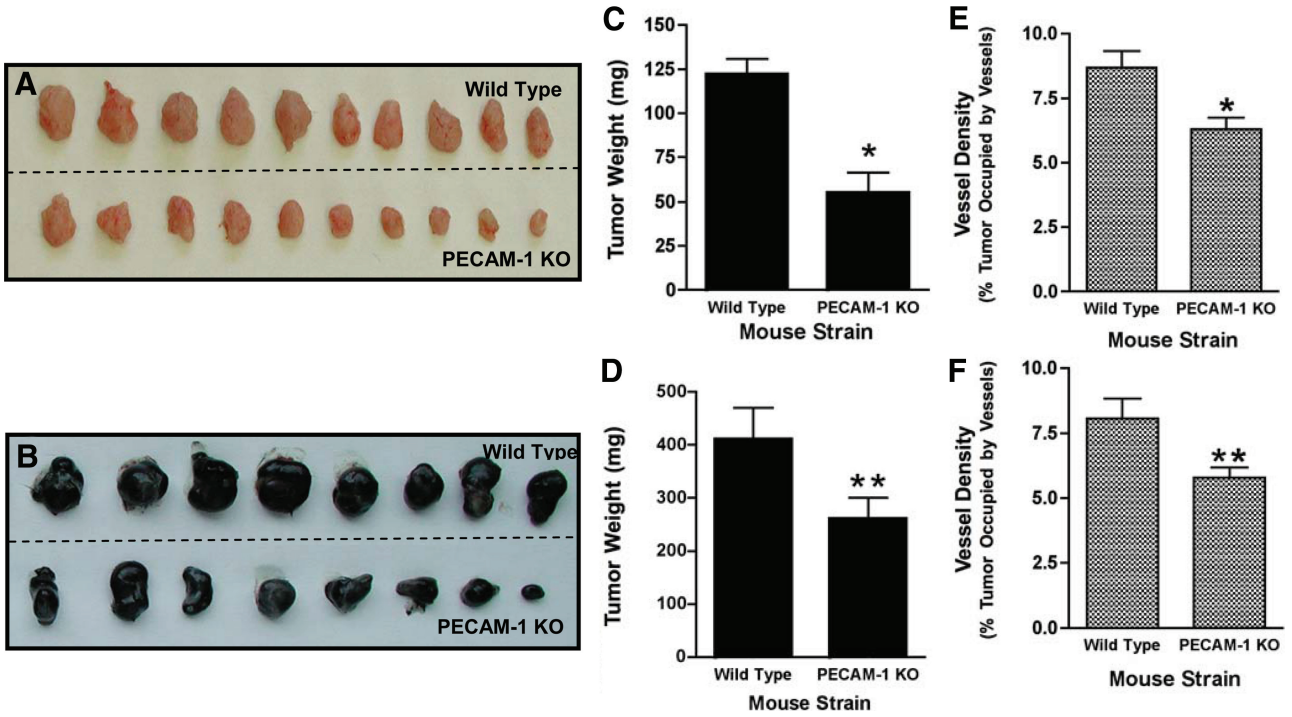

Figure 3. Tumor growth and angiogenesis in wild-type and PECAM-1-null mice. The growth of the ID8-VEGF ovarian tumor line (**A** and **C**) and a B16 melanoma line (**B** and **D**), as accessed by tumor weight, was significantly inhibited in the PECAM-1-null (PECAM-1 KO) mice (ID8, $n = 10$, $^{*}P < 0.002$; B16, $n = 22$, $^{**}P = 0.05$). The vessel densities in tumors of comparable sizes, as assessed by percentage of the tumor occupied by vessels (**E** and **F**), were significantly reduced in the PECAM-1-null mice (ID8, $n = 10$, $^{*}P < 0.02$; B16, $n = 8$, $^{**}P < 0.008$). Data are presented as means ± SE.

Statistical Analyses

Differences among groups were analyzed using one-way analysis of variance. Results are presented as means ± SE. When statistically significant differences were found ($P < 0.05$), individual comparisons were made using the Bonferroni/Dunn test.

Results

Reduced Vascularization of Matrigel Implants in PECAM-1-Null Mice

To confirm the results of previous antibody studies implicating PECAM-1 in vessel formation, *in vivo* murine angiogenesis was studied in mice deficient in the expression of PECAM-1.[19] Initial studies were done with a model in which vessels develop over 5 to 7 days around and within subcutaneously implanted Matrigel plugs containing B16 tumor cells as a source of angiogenic growth factors (Figure 1). After 5 days, a "blush" of vessel proliferation was seen surrounding plugs in the wild-type animals that was not evident in the PECAM-1-null mice (Figure 1, A and B). Further histological analysis of extracted implants demonstrated that the vascularization of implants from PECAM-1-null animals was strikingly less than that observed for the wild-type mice (Figure 1, C and D). Consistent with this, vascularization of the plugs, as assessed by hemoglobin concentration, was significantly reduced (50%) in the PECAM-1 knockout mice compared with wild-type animals (Figure 1E). Silver staining of vessels in the skin was also done to assess the morphology of vessels invading the Matrigel plugs (Figure 2). Vessels remote from the Matrigel plugs in both animal strains were similar in appearance and size (Figure 2, A and B). In contrast, the vessels adjacent to the Matrigel implants were much more dilated and tortuous in the wild-type mice, compared with those of the PECAM-1-deficient animals (Figure 2, C and D). This suggests that the absence of PECAM-1 may disrupt and alter *in vivo* angiogenesis.

Reduced Tumor Growth and Angiogenesis in PECAM-1-Null Mice

To extend the findings of the Matrigel studies, the subcutaneous growth and associated tumor angiogenesis of an ovarian tumor line overexpressing VEGF (ID8) and the B16 melanoma line were investigated in PECAM-1-null mice (Figure 3). When compared with the growth observed in wild-type mice, it was noted that the growth of both of these tumors was significantly reduced (40 to 50%) in the PECAM-1-deficient animals (Figure 3, A–D). The vessel density of comparably sized tumors obtained from wild-type and mutant mice was subsequently determined using ICAM-2 staining to identify murine vessels (Figure 3, E and F). Using computer-assisted image analysis, the vessel density was found to be significantly reduced for both tumors grown in the PECAM-1-null mice. This suggests that the inhibition of tumor growth in the PECAM-1-null mice resulted from a reduced angiogenic response.

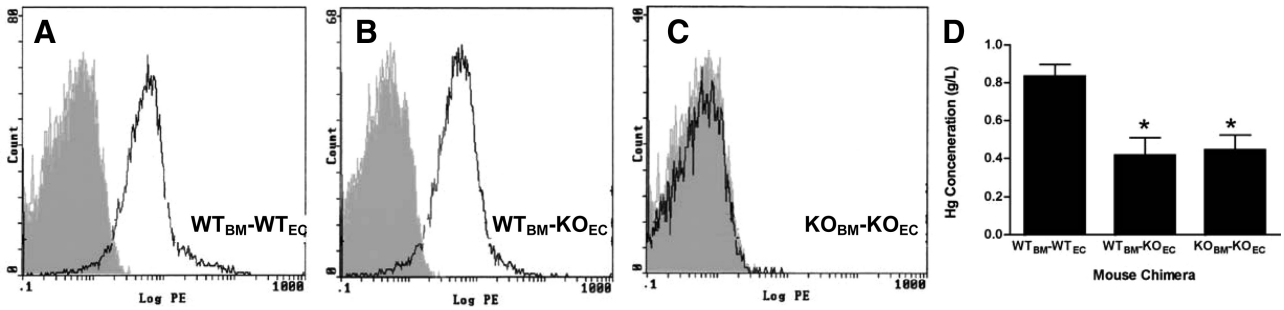

Figure 4. Neovascularization of Matrigel implants in bone marrow chimeric mice. Vascularization of subcutaneous Matrigel implants was studied in the following chimeric (donor-recipient) mice: wild-type into wild-type (WT_{BM}-WT_{EC}), wild-type into PECAM-1-null (WT_{BM}-KO_{EC}), PECAM-1-null into PECAM-1-null (KO_{BM}-KO_{EC}). Flow cytometry analysis confirmed the successful engraftment of the mice (**A--C**). The angiogenic responses (assessed by hemoglobin concentration) WT_{BM}-KO_{EC} KO_{BM}-KO_{EC} were very similar but were significantly reduced compared with the WT_{BM}-WT_{EC} (**D**). Data are presented as means ± SE ($n = 8$, $^*P < 0.05$).

Murine Angiogenesis Involves Endothelial PECAM-1

Recruited leukocytes, tissue macrophages, and circulating bone marrow-derived progenitor endothelial cells have been identified as cellular participants during *in vivo* angiogenesis and thus, as PECAM-1 expressing cells, they may also contribute to the participation of PECAM-1 in this process.[43–48] To identify the possible involvement of PECAM-1 expressed on leukocytes, macrophages, and/or circulating endothelial progenitor cells in vessel formation, bone marrow chimeric animals were generated to selectively propagate bone marrow-derived wild-type vascular cells against a background of PECAM-1-deficient endothelium. This approach was used successfully to distinguish the importance of endothelial versus platelet PECAM-1 in hemostasis.[41] Experiments were done in which the following chimeric (donor-recipient) mice were generated: wild-type into wild-type (WT_{BM}-WT_{EC}; wild-type control), wild-type into PECAM-1 knockout (WT_{BM}-KO_{EC}) and PECAM-1 knockout into PECAM-1 knockout (KO_{BM}-KO_{EC}; knockout control). Flow cytometry analysis confirmed that the blood leukocytes from the WT_{BM}-WT_{EC} and WT_{BM}-KO_{EC} mice expressed PECAM-1, while the leukocytes from the KO_{BM}-KO_{EC} animals were devoid of PECAM-1 (Figure 4, A–C). The vascularization of subcutaneously implanted Matrigel plugs was subsequently studied (Figure 4D). The angiogenic responses in the WT_{BM}-KO_{EC} and KO_{BM}-KO_{EC} mice were very similar but were significantly reduced compared with the WT_{BM}-WT_{EC} mice. The levels of inhibition in the WT_{BM}-KO_{EC} and KO_{BM}-KO_{EC} chimeric animals (50%) were comparable with what was observed with the PECAM-1-null mice (Figure 1). The failure of wild-type, PECAM-1-positive leukocytes and/or bone marrow-derived endothelial progenitor cells to restore the wild-type phenotype in the knockout animals is consistent with the endothelial involvement of PECAM-1 during *in vivo* angiogenesis.

Reduced Cell Migration by PECAM-1-Null ECs

The studies in the bone marrow chimeric animals indicate that the loss of endothelial PECAM-1 function inhibits *in vivo* angiogenesis. To further investigate this, the activity of endothelial cells isolated from wild-type and PECAM-1-null animals was studied. Cell proliferation and levels of apoptosis (in the absence of stress) in wild-type and PECAM-1-deficient ECs were comparable (Figure 5, A and B). However, it was found that wound-induced migration, as well as the migration of single cells through matrix-coated filters, were significantly less in PECAM-1-null ECs compared with wild-type ECs (Figure 5, C and D). These findings are consistent with previous studies, which have demonstrated that expression of PECAM-1 in cellular transfectants increases cell motility[17,18] and suggest that inhibition of vessel formation observed in PECAM-1-null mice is due in part to impairment in PECAM-1-dependent cell motility. Also consistent with these data is the finding that (acute) inhibition of murine PECAM-1 function with an anti-PECAM-1 antibody inhibits the cell migration of a murine endothelial cell line (Figure 5, E and F).

Loss of PECAM-1 Inhibits the Formation of Filopodia by ECs, while Filopodia Formation Is Stimulated by the Expression of PECAM-1

The phenotype of a motile cell is characterized morphologically by the presence of cellular protrusions such as filopodia and lamellipodia.[29,30] Given the involvement of PECAM-1 in the motility of ECs, we analyzed the initial morphology of wild-type and PECAM-1-deficient murine ECs plated on gelatin as they transitioned over 2 to 3 hours from adherent rounded cells to flattened spread cells to polarized cells with various cellular protrusions. Within 40 minutes after plating, the majority of wild-type ECs (nearly 70%) displayed various filopodial extensions, while most (>90%) of the PECAM-1-null cells still demonstrated a rounded or flattened morphology (Figure 6, A–C). The absence of PECAM-1, however, did not prevent the eventual formation of filopodia, as after 90 minutes, the null cells did begin to form filopodia (data not shown). We also observed that the morphology of HUVEC in which PECAM-1 expression had been suppressed by ~90%, using siRNA treatment, was notable for few cells with long cellular extensions, compared with

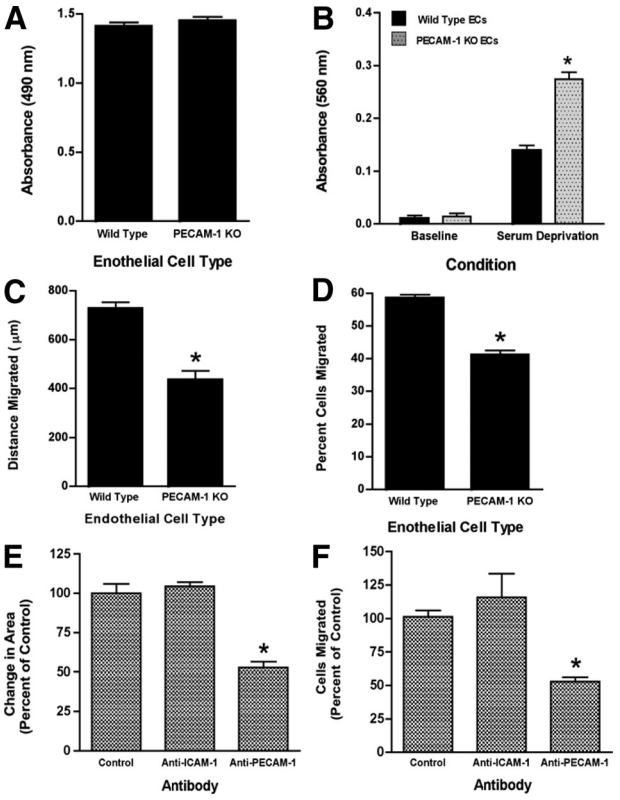

Figure 5. *In vitro* function of murine ECs isolated from wild-type and PECAM-1-null mice. **A:** The proliferation of wild-type and PECAM1-null (PECAM-1 KO) ECs cultured for 24 hours in the presence of serum was assessed using a colorimetric assay and measurement of the reaction mixture at 490 nm. The proliferative responses of the two cell types were comparable ($n = 4$). **B:** Apoptosis was assessed after 5 hours in the presence or absence of serum. PECAM-1 KO ECs were more susceptible to apoptosis induced by serum deprivation ($n = 15$, $^*P < 0.001$, compared with wild-type ECs). **C:** Linear defects were made in confluent cell monolayers and closure of the wounds after 24 hours was assessed by computer-assisted image analysis. Wound-induced migration was decreased in the PECAM-1-null ECs ($n = 8$, $^*P < 0.001$). **D:** The percentage of cells migrating through Matrigel-coated Transwell filters was reduced in the PECAM-1-deficient ECs ($n = 4$, $^*P < 0.001$). **E** and **F:** Anti-mouse PECAM-1 antibody inhibited the closure of circular wounds in confluent monolayers of H5V murine ECs ($n = 4$, $^*P < 0.0002$, compared with control) as well as the migration of these cells through Matrigel-coated filters ($n = 3$–4, $^*P < 0.05$, compared with control). Data are presented as means ± SE.

the cells that were treated with control siRNA (Figure 7, A–D). To confirm these findings from murine and human ECs, we investigated the effect of expressing human PECAM-1 in the REN cell human mesothelioma line (which does not express PECAM-1).[18] The expression of human PECAM-1 in REN cells resulted in filopodia that were significantly longer than those that formed in the control cells. The mean filopodial length was 27.4 μm for REN-HP cells compared with 15.1 for the REN cells ($n = 60$, $P < 0.0001$; data are presented as SE). Thus while nearly 80% of the filopodia in the control cells were less than 20 μm in length, the majority (67%) of filopodia in the REN cell transfectants were longer than 20 μm, with more than 16% extending beyond 40 μm (Figure 8, A–C). Taken together these data indicate that PECAM-1 increases the rate and/or promotes the efficiency of filopodia formation in ECs.

Anti-PECAM-1 Antibodies Inhibit Filopodia Formation by HUVEC

PECAM-1 has been reported to participate in binding interactions both with itself (homophilic adhesion) and with several non-PECAM-1 molecules (heterophilic adhesion), including heparan-containing proteoglycans.[2–6] To determine whether PECAM-1-dependent ligand interactions might play a role in the ability of PECAM-1 to promote endothelial filopodia formation, we studied the effects of two functionally distinct antibodies: mAb 37, which blocks heterophilic binding; and mAb 62, which blocks both homophilic and heterophilic bindings.[49] We found that the initial formation of filopodia by HUVEC was suppressed by both antibodies but not by control IgG (Table 1). Given the functional properties of the antibodies (mAb 37 only blocks heterophilic binding) and the fact that these studies were done with non-confluent cells, these data suggest that endothelial cell filopodia formation may be mediated by PECAM-1-dependent heterophilic binding to matrix proteins.

Expression of PECAM-1 Increases Cdc42 Levels

Rho GTPases, including Rho, Rac, and Cdc42, act as molecular switches that regulate signal transduction pathways by cycling between a GDP-bound inactive form and a GTP-bound active form.[31–35] Although they influence a wide range of biochemical processes, their best-defined activity is in the regulation of actin dynamics: Rho A causes the formation of stress fibers; Rac1 results in the formation of lamellipodia and membrane ruffling; and Cdc42 leads to the formation of filopodia.[31–35] Given the finding that the expression of PECAM-1 promotes filopodia formation, we sought to determine the expression level of Cdc42 in cells expressing PECAM-1. We observed that the loss of PECAM-1 in murine ECs was associated with decreased Cdc42 protein expression (Figure 9, A and B), while the presence of PECAM-1 in REN cells up-regulated the expression of Cdc42 (Figure 9, C and D). In contrast, the expression of RhoA and Rac1 appeared to be independent of changes in the levels of PECAM-1.

Decreased Endothelial Tip Cell Filopodia in PECAM-1-Null Mice during Vascularization of the Developing Retina

The development of the retinal vasculature of mice is completed after birth and provides an excellent model for studying postnatal physiological angiogenesis.[50,51] It involves the initial formation of a superficial vascular plexus (week 1) across the surface of the retina that subsequently sprout vessels that penetrate into the retina to give rise to the deep retinal vascular plexuses (weeks 2–4). The developing superficial vascular plexus, as it advances from the central retinal artery across the retinal surface, provides an in vivo system for studying ECs

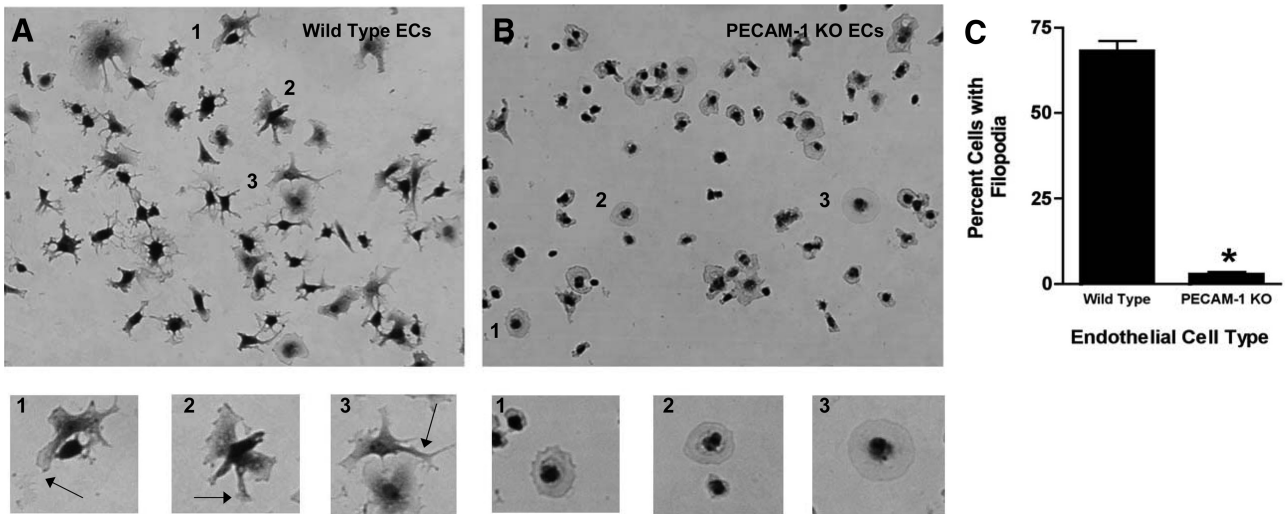

Figure 6. Filopodia formation by wild-type and PECAM-1-null ECs. Shown are wild-type (**A**) and PECAM-1-null (PECAM-1 KO) ECs (**B**) 40 minutes after plating on gelatin. At this time point, the wild-type ECs have quickly transitioned to a morphology in which the majority of cells have filopodia (**A1-3**, **arrows**). In contrast, the PECAM-1 KO ECs at 40 minutes have attached and spread, but few display filopodia (**B1–3**). The formation of filopodia was assessed by determining the percentage of cells with filopodial extensions (**C**) and was found to be significantly reduced in the PECAM-1-null ECs. Data are presented as means ± SE (n = 4, $^*P < 0.0001$).

located at the tips of angiogenic sprouts and the filopodia emanating from these tip cells. We therefore analyzed the retinal vasculature from 5-day-old wild-type and PECAM-1-null mice that were stained with fluorescein isothiocyanate-labeled isolectin-B. The density of the developing retinal vasculature of the PECAM-1-null mice was significantly less than that of the wild-type animals (Figure 10, A and B). For PECAM-1-null mice the number of retinal vessel branch points/mm^2 and closed capillary loops/mm^2 were decreased, while the mean retinal area (μm^2) enclosed within a closed capillary loop was increased, data that are all consistent with a less dense vascular plexus (Table 2). Further, in the retina of wild-type mice, numerous angiogenic sprouts are observed at the advancing edge of the vascular plexus, with multiple long filamentous filopodia extending from the ECs at the tips of each sprout (Figure 10, C and E). In contrast, the angiogenic sprouts of the retinal vasculature from the PECAM-1-deficient mice tended to appear more blunt ended and the filopodial extensions emanating from the sprouts

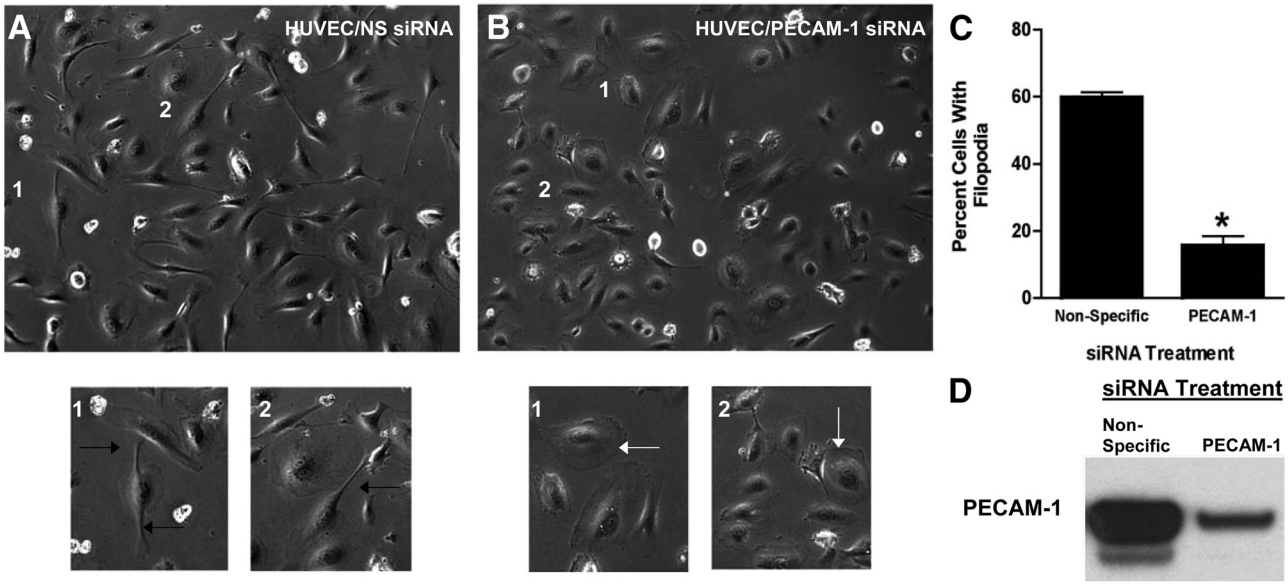

Figure 7. Filopodia formation by HUVEC treated with PECAM-1 siRNA. HUVEC plated on gelatin were transduced with nonspecific (**A**) or PECAM-1 (**B**) siRNA and then viewed after 72 hours (at the point of maximal PECAM-1 suppression). Cells with filopodia were numerous in the HUVEC treated with control siRNA (**A1** and **2**, **black arrows**), while most of the HUVEC exposed to PECAM-1 siRNA lacked filopodial extensions (**B1** and **2**, **white arrows**). The formation of filopodia was assessed by determining the percentage of cells with filopodial extensions (**C**) and was found to be very significantly reduced in the cells treated with PECAM-1 siRNA (n = 5, $^*P < 0.0001$). Data are presented as means ± SE. Western blot analysis is displayed from cell lysates of HUVEC treated with nonspecific or PECAM-1 siRNA (**D**). PECAM-1 expression after PECAM-1 siRNA treatment was reduced to 12% of the expression in nonspecific siRNA controls as assessed by densitometry. Staining for β-actin demonstrated equal loading (data not shown).

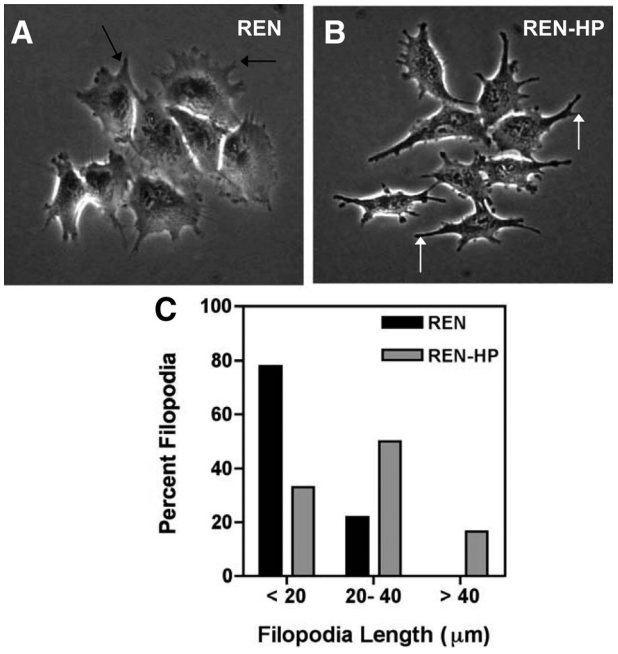

Figure 8. Filopodia formation by REN cells and REN cells expressing human PECAM-1. Shown are REN cells (**A**) and REN-HP cells (**B**). Filopodia were short and rudimentary in the REN cells (**A**, **black arrows**), but were increased in length in cells (**B**, **white arrows**). The frequency distribution of the lengths of the filopodia (< 20 μm, 20–40 μm, and >400 μm) was plotted (**C**) and revealed that unlike the REN cells, the majority of filopodia emanating from the REN-HP cells were greater than 20 μm and frequently extended beyond 40 μm (n = 60).

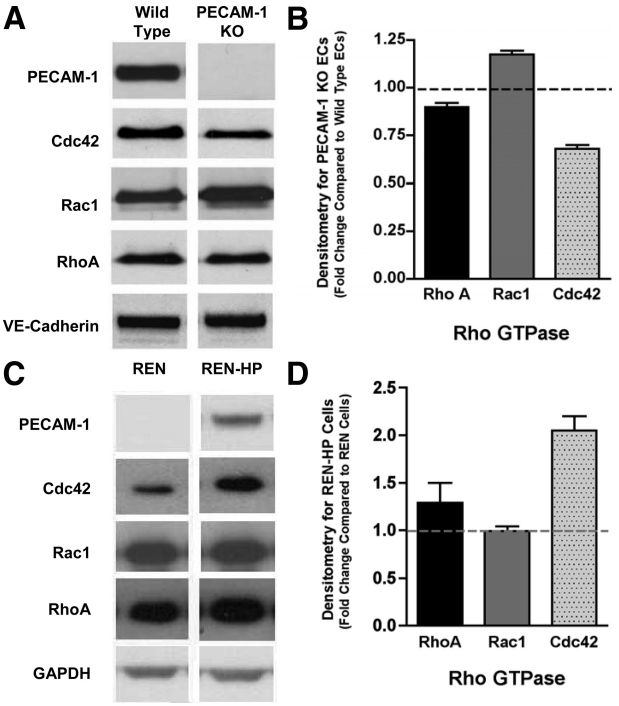

Figure 9. PECAM-1 expression and Cdc42 levels. Cell lysates from wild-type and PECAM-1-null (PECAM-1 KO) ECs (**A** and **B**), and from REN cells and REN-HP cells (**C** and **D**) were immunoblotted with antibodies against PECAM-1, Cdc42, Rac1, RhoA, VE-cadherin, and GAPDH. The loss of PECAM-1 in murine ECs decreased Cdc42 protein expression (**A**), while the presence of PECAM-1 in REN-HP cells increased the expression of Cdc42 (**C**). Densitometric analysis was performed (**B** and **D**). The data were normalized to GAPDH and expressed for the PECAM-1 KO ECs as fold change compared with wild-type ECs (n = 2) and for the REN-HP cells as fold change compared with REN cells (n = 3). Data are presented as means ± SE.

were fewer in number and shorter in length (Figure 10, D and F). These data provide further (*in vivo*) evidence of the involvement of PECAM-1 in the formation of endothelial cell filopodia.

Discussion

In this report, studies were done with PECAM-1-null mice to further define the involvement of PECAM-1 during *in vivo* angiogenesis. We found that vascularization of subcutaneous Matrigel implants, as well as tumor angiogenesis, were inhibited in PECAM-1-null mice. Reciprocal bone marrow transplants involving wild-type and PECAM-1-deficient mice revealed that the impaired angiogenic response resulted from a loss of endothelial and not leukocyte PECAM-1. In subsequent studies of ECs isolated from these animals, we found that *in vitro* wound and single cell migration were significantly compromised in the ECs isolated from PECAM-1-deficient mice. The formation of filopodia was also impaired in PECAM-1-null ECs and in HUVEC treated with anti-PECAM-1 antibody or in which PECAM-1 expression had been suppressed by siRNA. In addition, expression of PECAM-1 in cellular transfectants promoted filopodia formation. Consistent with these data, were the findings that the protein levels of Cdc42, a Rho GTPase known to promote the formation of filopodia, were increased by the expression of PECAM-1. In the developing retinal vasculature, the ECs at the tips of angiogenic sprouts in wild-type animals displayed long filamentous filopodia, while filopodial extensions emanating from the endothelial tip cells in the PECAM-1-null animals were fewer in number and shorter in length. Together, these data further establish the involvement of endothelial PECAM-1 in the formation of vessels and suggest that *in vivo*, PECAM-1 may stimulate endothelial cell motility by promoting the formation of filopodia.

Table 1. Effect of Anti-PECAM-1 Antibody on the Formation of Filopodia by HUVEC

Antibody treatment	IgG	mAb 37	mAb 62
Percent cells with filopodia	44 ± 5	13.6 ± 4*	16 ± 6*

HUVEC were plated on gelatin in the presence of IgG, mAb 37, or mAb 62 (100 μg/ml), and the percentage of cells with filopodia was determined after 1 hour. Compared with IgG, both antibodies decreased the percentage of cells with filopodia (n = 5–7, *P < 0.01). Data are presented as means ± SE.

*P < 0.01.

A role for PECAM-1 during *in vivo* angiogenesis was initially established by studies demonstrating that anti-PECAM-1 antibody treatment inhibited corneal neovascularization induced by angiogenic implants,[15] vascularization of subcutaneous Matrigel plugs,[15] and tumor angiogenesis.[15–17] The availability of PECAM-1-null mice[19] has provided the opportunity to further explore the activity of PECAM-1 during *in vivo* angiogenesis. These PECAM-1-deficient mice are viable, suggesting that vascular development in the absence of PECAM-1 is suffi-

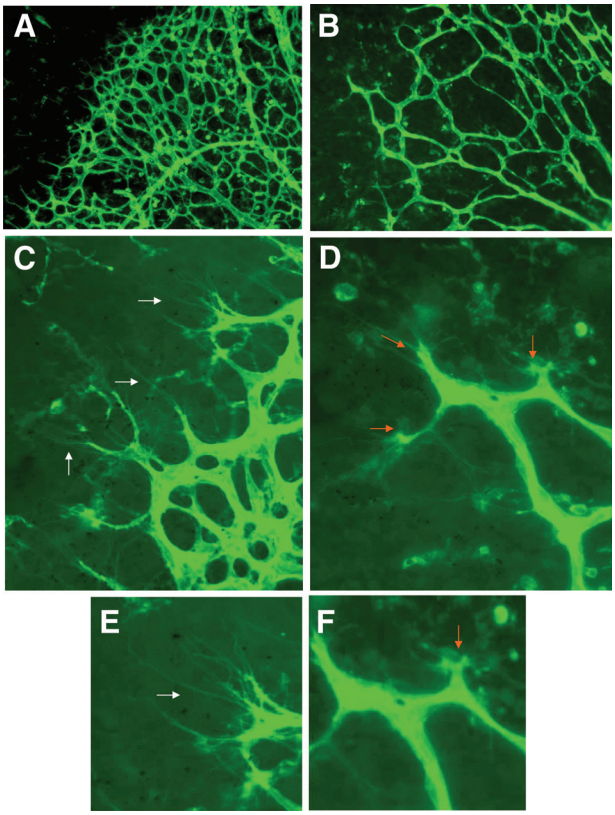

Figure 10. Postnatal retinal vascularization. Shown is the leading edge of the developing retinal vasculature, stained by fluorescein isothiocyanate-labeled isolectin-B in wild-type (**A**, **C**, **E**), and PECAM-1-null mice (**B**, **D**, **F**). The density and complexity of the vascular plexus were greater in the wild-type (**A**) compared with the PECAM-1-deficient mice (**B**) (see Table 2). Long filamentous filopodia extending from the endothelial tip cells of the angiogenic sprouts were observed in the wild-type mice (**C** and **E**, **white arrows**), while the angiogenic sprouts of the retinal vasculature from the PECAM-1-null mice (**D** and **F**, **red arrows**) were more blunt ended and displayed few of the filamentous filopodial projections.

cient to allow for adequate embryogenesis. As a result, only a limited number of studies to date have investigated the formation of blood vessels in PECAM-1-null mice. We found that the vascularization of subcutaneous Matrigel implants (Figure 1) and two subcutaneous tumors (Figure 3) were reduced in PECAM-1-deficient mice. These findings are consistent with that of Solowiej and associates who noted an impaired angiogenic response in a model of foreign body-induced chronic inflammation.[27] Together, these data point to a role for PECAM-1 in pathological angiogenesis. Of note, while the vessels invading the Matrigel implants in the wild-type animals were large and tortuous, the invading vessels in the PECAM-1-deficient mice were smaller in caliber and less irregular (Figure 2). These PECAM-1-null vessels were also less leaky (data not shown). This suggests that the loss of PECAM-1, independent of any impairment in endothelial motility (see below), leads to a "normalization" of blood vessels. It has been proposed that antiangiogenic agents may enhance the tumoricidal actions of cytotoxic drugs by "normalizing" the tumor vasculature in a way that allows for sustained drug delivery.[52] This raises the possibility that PECAM-1 antagonists may serve as effective adjuvant cancer agents (see below).

Table 2. Quantitation of the Vascularization of the Developing Postnatal Mouse Retina

Mouse strain	Number of branch points/mm^2	Number of capillary loops/mm^2	Mean retinal area enclosed within a capillary loop (μm^2)
Wild-type	349 ± 31	373 ± 22	2133 ± 76
PECAM-1-null	221 ± 11*	235 ± 13*	3686 ± 186*

The number of retinal vessel branch points/mm^2 (n = 6–8) and closed capillary loops/mm^2 (n = 6–8), as well as the mean retinal area (μm^2) enclosed within a closed capillary loop (n = 9–12), were determined for wild-type and PECAM-1-null mice (*$P < 0.0001$).

We also noted that the initial postnatal vascularization of the murine retina was impaired in the PECAM-1-null mice (Figure 10). These data confirm the findings of DiMaio et al who have also studied postnatal retinal vasculature development in PECAM-1-deficient mice.[28] The vascular pattern and density, however, were similar in wild-type and PECAM-1-null adult mice (data not shown), suggesting that the loss of PECAM-1 delays but does not prevent the eventual normal development of the retinal vasculature. These findings are similar to what was observed for murine postnatal lung development, where lung alveolarization was delayed in the PECAM-1-deficient mice (due to presumed impairments in angiogenesis) but had substantially recovered by the time the mice reached adulthood.[26] These data further implicate PECAM-1 in postnatal vascular developmental processes such as those that might be occurring in the eyes and lungs. However, in a model of dermal wound healing we have found that the rate of wound closure and the extent of wound angiogenesis were similar in wild-type and PECAM-1-null-mice or in mice treated with control IgG or anti-PECAM-1 antibody (data not shown). These data are consistent with the finding that anti-human PECAM-1 antibody treatment did not inhibit wound angiogenesis in human skins grafted onto SCID mice.[53] This suggests that the involvement of PECAM-1 in blood vessel formation may depend on the tissue context and angiogenic stimulus.

PECAM-1 is expressed not only on ECs but also on bone marrow-derived cells such as recruited leukocytes, tissue macrophages, and circulating endothelial progenitor cells, which also participate in angiogenesis.[43–48] The absence of PECAM-1 on these bone marrow-derived cells, in addition to the loss of PECAM-1 on ECs, could contribute to the altered angiogenic phenotype of the PECAM-1-deficient mice. The inability of wild-type PECAM-1-expressing leukocytes and/or bone marrow-derived endothelial progenitor cells to restore the wild-type phenotype in the PECAM-1-null animals (WT_{BM}-KO_{EC}) provides strong evidence for the endothelial involvement of PECAM-1 during *in vivo* angiogenesis (Figure 4).

We have previously reported that anti-human PECAM-1 antibody inhibits the cell migration of HUVEC,[17] while expression of human PECAM-1 in non-PECAM-1-expressing cell lines promotes cell motility.[17,18] Our finding that the loss or antibody antagonism of murine PECAM-1 inhibits the motility of murine ECs (Figure 5) is therefore consistent with the results of these earlier stud-

ies of human PECAM-1. The data presented here are also in agreement with studies of murine kidney ECs, which demonstrated that the absence of PECAM-1 caused these cells to be less migratory.[54]

The mechanism of PECAM-1's involvement in endothelial motility has been the subject of previous investigations.[18] These studies have suggested that the angiogenic activation of ECs results in PECAM-1 tyrosine phosphorylation and the binding of the SHP-2 phosphatase to PECAM-1. This interaction results in the recruitment of SHP-2 to the cell membrane, where it mediates the dephosphorylation of focal adhesion proteins such as paxillin and vinculin. These dephosphorylation events in turn stimulate the disassembly and turnover of focal adhesions and thus promote endothelial cell motility. The data presented in this report suggest that PECAM-1 may enhance endothelial motility by also promoting the formation of filopodia, a feature of actively motile cells.[29,30] As noted above, we found that the loss of PECAM-1 in murine ECs or HUVEC inhibited the initial formation of filopodial protrusions, while the expression of PECAM-1 in a non-PECAM-1 cell line stimulated filopodia formation (Figures 6–8). Our data are consistent with the finding that PECAM-1-null platelets were impaired in their capacity to extend filopodia.[55] However, an earlier report by Gratizinger and associates found that re-expression of human PECAM-1 in a transformed, PECAM-1-null, mouse endothelial cell line suppressed the formation of filopodia.[56] The reasons for the differences between our study and this earlier report are unclear, but may reflect differences in the cell lines that were used.

Further evidence for the involvement of PECAM-1 in the formation of filopodia comes from the fact that ECs at the tips of the developing retinal vasculature in the PECAM-1-deficient mice were notable for a paucity of long filopodial projections (Figure 10). With respect to this observation, we would note that Dimaio et al in their study of retinal vascular development did not detect a significant difference between wild-type and PECAM-1-null mice in the number of endothelial tip cell filopodia in the developing retina.[28] The reasons for this difference between our study and theirs are not clear, but may be due in part to different methods used to stain the vasculature.

Filopodia probe and sense for chemicals in the pericellular environment, act as hubs for signal transduction, and mediate attachment to the extracellular matrix, processes that are all integral to directed cell migration.[29,30] It is therefore not surprising that a molecule such PECAM-1 that stimulates the formation of filopodia also promotes EC motility. We have also observed that PECAM-1 not only promotes filopodia formation but concentrates at the tips of filopodial protrusions (data not shown), a finding that has been reported for other cell adhesion and surface molecules such as VEGF receptor, cadherins, and integrins.[42,57] The specific mechanisms by which PECAM-1 enhances the formation of filopodia remain to be determined but are the subject of ongoing investigation. We have, however, found that two anti-PECAM-1 antibodies that block PECAM-1-dependent heterophilic binding also inhibit filopodia formation by subconfluent HUVEC (Table 1). This suggests that PECAM-1-dependent heterophilic ligand interactions[2,6] with constituents of the extracellular matrix may be involved in the stimulation of filopodia formation by PECAM-1, although the existence of these interactions has been questioned.[4] Small GTPases of the Rho superfamily (RhoA, Rac1, and Cdc42) have been linked to actin cytoskeletal remodeling and morphological changes involved in cell motility, with Cdc42 implicated in the formation of filopodia.[31–35] Our data indicating that the protein levels of Cdc42 are increased in cells expressing PECAM-1 (Figure 9) are therefore consistent with a role for PECAM-1 in the formation of filopodia. The mechanisms by which PECAM-1 regulates Cdc42 expression are currently being investigated.

The findings of this study (Figure 3), as well as that of previous reports using antibody inhibition of PECAM-1,[16,17] raise the possibility of PECAM-1 as a potential target for cancer therapy.[58] Not only does the loss or inhibition of PECAM-1 function block tumor growth and angiogenesis, it also may act to normalize pathological vessels (Figure 2), an activity that facilitates the efficacy of antitumor agents.[52] Anti-PECAM-1 therapy is likely to be well tolerated, since the absence of PECAM-1 does not result in a lethal vascular phenotype,[19] deleterious effects have not been noted in animals treated with anti-PECAM-1 antibodies,[15–17] and the absence of PECAM-1 function does not appear to prevent or inhibit dermal wound healing (see above). However, given its potential role in protecting against endotoxic and apoptotic stresses[24,25] and as a mediator of leukocyte recruitment,[20–23] human clinical trials will be required to establish the ultimate safety of therapy targeted against PECAM-1. In this regard, further studies with the goal of specifically defining the role of PECAM-1 as a facilitator of endothelial cell motility will be very important.

References

1. Newman PJ: The biology of PECAM-1. J Clin Invest 1997, 99:3–8
2. DeLisser HM, Yan HC, Newman PJ, Muller WA, Buck CA, and Albelda SM: Platelet/endothelial cell adhesion molecule-1 (CD31)-mediated cellular aggregation involves cell surface glycosaminoglycans. J Biol Chem 1993, 268:16037–16046
3. Sun J, Williams J, Yan HC, Amin KM, Albelda SM, DeLisser HM: Platelet endothelial cell adhesion molecule-1 (PECAM-1) homophilic adhesion is mediated by immunoglobulin-like domains 1 and 2 and depends on the cytoplasmic domain and the level of surface expression. J Biol Chem 1996, 271:18561–18570
4. Sun Q, Paddock C, Visentin GP, Zukowski MM, Muller WA, Newman PJ: Cell surface glycosaminoglycans do not serve as ligands for PECAM-1. J Biol Chem 1998, 273:11483–11490
5. Deaglio S, Morra M, Mallone R, Ausiello CM, Prager E, Garbarino G, Dianzani U, Stockinger H, and Malavasi F: Human CD38 (ADP-ribosyl cyclase) is a counter-receptor of CD31, an Ig superfamily member. J Immunol 1998, 160:395–402
6. Coombe DR, Stevenson SM, Kinnear BF, Gandhi NS, Mancera RL, Osmond RI, Kett WC: Platelet endothelial cell adhesion molecule 1 (PECAM-1) and its interactions with glycosaminoglycans: 2. Biochemical analyses Biochemistry 2008, 47:4863–4875
7. Newman PJ, Newman, DK: Arterioscler. Thromb Vasc Biol 2003, 23:953–964
8. Ilan N, Madri: JA: Curr Opin Cell Biol 2003, 15:515–524
9. Ravetch JV, Lanier LL: Immune inhibitory receptors. Science 2000, 290:84–89
10. Billadeau DD, Leibson PJ: ITAMs versus ITIMs: striking a balance during cell regulation. J Clin Invest 2002, 109:161–168

11. Jackson DE, Ward CM, Wang R, Newman PJ: The protein-tyrosine phosphatase SHP-2 binds platelet/endothelial cell adhesion molecule-1 (PECAM-1) and forms a distinct signaling complex during platelet aggregation. Evidence for a mechanistic link between PECAM-1- and integrin-mediated cellular signaling J Biol Chem 1997, 272:6986–6993
12. Lu TT, Barreuther M, Davis S, Madri JA: Platelet endothelial cell adhesion molecule-1 is phosphorylatable by c-Src, binds Src-Src homology 2 domain, and exhibits immunoreceptor tyrosine-based activation motif-like properties. J Biol Chem 1997, 272:14442–14446
13. Cao MY, Huber M, Beauchemin N, Famiglietti J, Albelda SM, Veillette A: Regulation of mouse PECAM-1 tyrosine phosphorylation by the Src and Csk families of protein-tyrosine kinases. J Biol Chem 1998, 273:15765–15772
14. Sagawa K, Kimura T, Swieter M, Siraganian RP: The protein-tyrosine phosphatase SHP-2 associates with tyrosine-phosphylated adhesion molecule PECAM-1 (CD31). J Biol Chem 1997, 272:31086–31091
15. DeLisser HM, Christofidou-Solomidou M, Strieter RM, Burdick MD, Robinson CS, Wexler RS, Kerr JS, Garlanda C, Merwin JR, Madri JA, Albelda SM: Involvement of endothelial PECAM-1/CD31 in angiogenesis. Am J Pathol 1997, 151:671–677
16. Zhou Z, Christofidou-Solomidou M, Garlanda C, and DeLisser HM: Antibody against murine PECAM-1 inhibits tumor angiogenesis in mice. Angiogenesis 1999, 3:181–188
17. Cao G, O'Brien CD, Zhou Z, Sanders SM, Greenbaum JN, Makrigiannakis A, DeLisser HM: Involvement of human PECAM-1 in angiogenesis and in vitro endothelial cell migration. Am J Physiol Cell Physiol 2002, 282:C1181–C1190
18. O'Brien CD, Cao G, Makrigiannakis A, DeLisser HM: Role of immunoreceptor tyrosine-based inhibitory motifs of PECAM-1-dependent cell migration. Am J Physiol Cell Physiol 2004, 287:C1103–C1113
19. Duncan GS, Andrew DP, Takimoto H, Kaufman SA, Yoshida H, Spellberg J, Luis de la Pompa J, Elia A, Wakeham A, Karan-Tamir B, Muller WA, Senaldi G, Zukowski MM, Mak TW: Genetic evidence for functional redundancy of platelet/endothelial cell adhesion molecule-1 (PECAM-1): CD31-deficient mice reveal PECAM-1-dependent and PECAM-1-independent functions. J Immunol 1999, 162:3022–3030
20. Thompson RD, Noble KE, Larb KY, Dewar A, Duncan GS, Mak TW, Nourshargh S: Platelet-endothelial cell adhesion molecule-1 (PECAM-1)-deficient mice demonstrate a transient and cytokine-specific role for PECAM-1 in leukocyte migration through the perivascular basement membrane. Blood 2001, 97:1854–1860
21. Woodfin A, Reichel CA, Khandoga A, Corada M, Voisin MB, Scheiermann C, Haskard DO, Dejana E, Krombach F, Nourshargh S: JAM-A mediates neutrophil transmigration in a stimulus-specific manner in vivo: evidence for sequential roles for JAM-A and PECAM-1 in neutrophil transmigration. Blood 2007, 110:1848–1856
22. Albelda SM, Lau KC, Chien P, Huang ZY, Arguiris E, Bohen A, Sun J, Billet JA, Christofidou-Solomidou M, Indik ZK, Schreiber AD: Role for platelet-endothelial cell adhesion molecule-1 in macrophage Fcgamma receptor function. Am J Respir Cell Mol Biol 2004, 31:246–255
23. Schenkel AR, Chew TW, Muller WA: Platelet endothelial cell adhesion molecule deficiency or blockade significantly reduces leukocyte emigration in a majority of mouse strains. J Immunol 2004, 173:6403–6408
24. Carrithers M, Tandon S, Canosa S, Michaud M, Graesser D, Madri JA: Enhanced susceptibility to endotoxic shock and impaired STAT3 signaling in CD31-deficient mice. Am J Pathol 2005, 166:185–196
25. Maas M, Stapleton M, Bergom C, Mattson DL, Newman DK, Newman PJ: Endothelial cell PECAM-1 confers protection against endotoxic shock. Am J Physiol Heart Circ Physiol 2005, 288:H159–H164
26. DeLisser HM, Helmke BP, Cao G, Egan PM, Taichman D, Fehrenbach M, Zaman A, Cui Z, Mohan GS, Baldwin HS, Davies PF, Savani RC: Loss of PECAM-1 function impairs alveolarization. J Biol Chem 2006, 281:8724–8731
27. Solowiej A, Biswas P, Graesser D, Madri JA: Lack of platelet endothelial cell adhesion molecule-1 attenuates foreign body inflammation because of decreased angiogenesis. Am J Pathol 2003, 162:953–962
28. Dimaio TA, Wang S, Huang Q, Scheef EA, Sorenson CM, Sheibani N: Attenuation of retinal vascular development and neovascularization in PECAM-1-deficient mice. Dev Biol 2008, 315:72–88
29. Mattila PK, Lappalainen P: Filopodia: molecular architecture and cellular functions. Nat Rev Mol Cell Biol 2008, 9:446–454
30. Gupton SL, Gertler FB: Filopodia: the fingers that do the walking. Sci STKE 2007, 400:re5
31. Schmitz AA, Govek EE, Böttner B, Van Aelst L: Rho GTPases: signaling, migration, and invasion. Exp Cell Res 2000, 261:1–12
32. Raftopoulou M, Hall A: Cell migration: rho GTPases lead the way. Dev Biol 2004, 265:23–32
33. Wennerberg K, Der CJ: Rho-family GTPases: it's not only Rac and Rho (and I like it). J Cell Sci 2004, 117:1301–1312
34. Cerione RA: Cdc42: new roads to travel. Trends Cell Biol 2004, 14:127–132
35. Sinha S, Yang W: Cellular signaling for activation of Rho GTPase Cdc42. Cell Signal 2008, 20:1927–1934
36. Doerschuk CM, Quinlan WM, Doyle NA, Bullard DC, Vestweber D, Jones ML, Takei F, Ward PA, Beaudet AL: The role of P-selectin and ICAM-1 in acute lung injury as determined using blocking antibodies and mutant mice. J Immunol 1996, 157:4609–4614
37. Garlanda C, Parravicini C, Sironi M, De Rossi M, Wainstok de Calmanovici R, Carozzi F, Bussolino F, Colotta F, Mantovani A, Vecchi A: Progressive growth in immunodeficient mice and host cell recruitment by mouse endothelial cells transformed by polyoma middle-sized T antigen: implications for the pathogenesis of opportunistic vascular tumors. Proc Natl Acad Sci USA 1994, 91:7291–7295
38. Zhang L, Yang N, Garcia JR, Mohamed A, Benencia F, Rubin SC, Allman D, Coukos G: Generation of a syngeneic mouse model to study the effects of vascular endothelial growth factor in ovarian carcinoma. Am J Pathol 2002, 161:2295–2309
39. Fehrenbach ML, Cao G, Williams JT, Finklestein JM, Zhu J-X, Delisser HM. Isolation of murine lung endothelial cells. Am J Physiol Lung Cell Mol Physiol 2009, 296:L1096–1103
40. McDonald DM: Endothelial gaps and permeability of venules in rat tracheas exposed to inflammatory stimuli. Am J Physiol Lung Cell Mol Physiol 1994, 266:L61–L83
41. Mahooti S, Graesser D, Patil S, Newman P, Duncan G, Mak T, Madri JA: PECAM-1 (CD31) expression modulates bleeding time in vivo. Am J Pathol 2000, 157:75–81
42. Gerhardt H, Golding M, Fruttiger M, Ruhrberg C, Lundkvist A, Abramsson A, Jeltsch M, Mitchell C, Alitalo K, Shima D, Betsholtz C: VEGF guides angiogenic sprouting utilizing endothelial tip cell filopodia. J Cell Biol 2003, 161:1163–1177
43. Schruefer R, Lutze N, Schymeinsky J, Walzog B: Human neutrophils promote angiogenesis by a paracrine feedforward mechanism involving endothelial interleukin-8. Am J Physiol Heart Circ Physiol 2005, 288:H1186–1192
44. Chavakis T, Cines DB, Rhee JS, Liang OD, Schubert U, Hammes HP, Higazi AA, Nawroth PP, Preissner KT, Bdeir K: Regulation of neovascularization by human neutrophil peptides (alpha-defensins): a link between inflammation and angiogenesis. FASEB J 2004, 18:1306–1308
45. Asahara T, Murohara T, Sullivan A, Silver M, van der Zee R, Li T, Witzenbichler B, Schatteman G, Isner JM: Isolation of putative progenitor endothelial cells for angiogenesis. Science 1997, 275: 964–967
46. Crowther M, Brown NJ, Bishop ET, Lewis CE: Microenvironmental influence on macrophage regulation of angiogenesis in wounds and malignant tumors. J Leukoc Biol 2001, 70:478–490
47. Coukos G, Benencia F, Buckanovich RJ, Conejo-Garcia JR: The role of dendritic cell precursors in tumour vasculogenesis. Br J Cancer 2005, 92:1182–1187
48. Conejo-Garcia JR, Buckanovich RJ, Benencia F, Courreges MC, Rubin SC, Carroll RG, Coukos G: Vascular leukocytes contribute to tumor vascularization. Blood 2005, 105:679–681
49. Nakada MT, Amin K, Christofidou-Solomidou M, O'Brien CD, Sun J, Gurubhagavatula I, Heavner GA, Taylor AH, Paddock C, Sun QH, Zehnder JL, Newman PJ, Albelda SM, DeLisser HM: Antibodies against the first Ig-like domain of human platelet endothelial cell adhesion molecule-1 (PECAM-1) that inhibit PECAM-1-dependent homophilic adhesion block in vivo neutrophil recruitment. J Immunol 2000, 164:452–462
50. Dorrell MI, Friedlander M: Mechanisms of endothelial cell guidance and vascular patterning in the developing mouse retina. Prog Retin Eye Res 2006, 25:277–295
51. Fruttiger M: Development of the retinal vasculature. Angiogenesis 2007, 10:77–88

52. Jain RK: Normalization of tumor vasculature: an emerging concept in antiangiogenic therapy. Science 2005, 307:58–62
53. Matsumura T, Wolff K, Petzelbauer P: Endothelial cell tube formation depends on cadherin 5 and CD31 interactions with filamentous actin. J Immunol 1997, 158:3408–3416
54. Kondo S, Scheef EA, Sheibani N, Sorenson CM: PECAM-1 isoform-specific regulation of kidney endothelial cell migration and capillary morphogenesis. Am J Physiol Cell Physiol 2007, 292:C2070–C2083
55. Wee JL, Jackson DE: The Ig-ITIM superfamily member PECAM-1 regulates the "outside-in" signaling properties of integrin alpha(IIb)beta3 in platelets. Blood 2005, 106:3816–3823
56. Gratzinger D, Canosa S, Engelhardt B, Madri JA: Platelet endothelial cell adhesion molecule-1 modulates endothelial cell motility through the small G-protein Rho. FASEB J 2003, 17:1458–1469
57. Tanoue T, Takeichi M: Mammalian Fat1 cadherin regulates actin dynamics and cell-cell contact. J Cell Biol 2004, 165:517–528
58. DeLisser HM: Targeting PECAM-1 for anti-cancer therapy. Cancer Biol Ther 2007, 6:121–122

Cell Adhesion & Migration 5:1, 1-5; January/February 2011; © 2011 Landes Bioscience

Modulators of endothelial cell filopodia

PECAM-1 joins the club

Horace M. DeLisser

Pulmonary, Allergy and Critical Care Division; Department of Medicine; University of Pennsylvania School of Medicine, Philadelphia, PA USA

Filopodia are an important feature of actively motile cells, probing the pericellular environment for chemotactic factors and other molecular cues that enable and direct the movement of the cell. They also act as points of attachment to the extracellular matrix for the cell, generating tension that may act to pull the cell forward and/or stabilize the cell as it moves. Endothelial cell motility is a critical aspect of angiogenesis, but only a limited number of molecules have been identified as specific regulators of endothelial cell filopodia. Recent reports, however, provide evidence for the involvement of PECAM-1, an endothelial cell adhesion and signaling molecule, in the formation of endothelial cell filopodia. This Commentary & View will focus on these studies and their suggestion that at least two PECAM-1-regulated pathways are involved in the processes that enable filopodial protrusions by endothelial cells. Developing a more complete understanding of the role of PECAM-1 in mediating various endothelial cell activities, such as the extension of filopodia, will be essential for exploiting the therapeutic potential of targeting PECAM-1.

Key words: AUTHOR: Please provide 5–7 key words

Submitted: 07/14/10

Accepted: 09/10/10

Previously published online: www.landesbioscience.com/journals/celladhesion/article/13575

Correspondence to: Horace M. DeLisser; Email: delisser@mail.med.upenn.edu

The regulated polymerization of actin filaments result in two morphologically distinct protrusive structures, lamellipodia and filopodia, at the leading edge of motile cells.[1] The lamellipodia are thin (thickness, 0.1–0.2 μm) fan-like projections composed of a branched network of actin.[2,3] In contrast, filopodia are slender, finger-like extensions (diameter, 0.1–0.3 μm), often emanating from lamellipodia, made up of tight bundles of actin filaments.[4,5] With respect to directed cell migration, filopodia are particularly important, probing and sensing the pericellular environment for chemotactic and other molecular cues in the extracellular matrix (ECM) that guide the direction and movement of the cell. They also act as points of attachment to the ECM for the cell, generating tension that may act to pull the cell forward and/or stabilize the cell as it moves. Given these roles, it is not surprising that filopodia contain diverse receptors for ECM proteins and an array of signaling molecules.

The formation of new vessels typically involves the initial outward proliferation and migration of endothelial cells (ECs) from a pre-existing vasculature.[6,7] The tips of these angiogenic sprouts are made up of highly polarized ECs, characterized by the presence of numerous, long, filopodia, that probe the environment, directing the cell toward angiogenic factors.[8] Surprisingly, our understanding of the processes that regulate the formation of these cellular protrusions in ECs is still incomplete. Of note, only a limited number of molecules have been identified as specifically involved in the formation of endothelial filopodia. These include VEGF receptors and the neuroplins.[9,10] Recent reports, however, from our group provide evidence of a role for PECAM-1 as a regulator of filopodia formation in ECs.[11,12]

PECAM-1 is a vascular-associated molecule of the Ig superfamily expressed on leukocytes and platelets as well as ECs, where it is enriched at intercellular junctions.[13-16] PECAM-1 consists of a 574 amino acid extracellular region organized

into six cystine linked Ig-like domains, a 19 amino acid transmembrane domain, and a 118 amino acid cytoplasmic tail.[17] It was initially identified as an adhesion molecule capable of binding interactions with itself or with a number of non-PECAM-1 molecules, including heparin containing proteoglycans.[18-22] However, subsequent studies led to the recognition that PECAM-1 also participates in intracellular signaling.[13-16] Although it does not have any intrinsic catalytic activity, the cytoplasmic domain of PECAM-1 contains two tyrosine residues (Y663 and Y686) that each fall within a conserved signaling sequence known as the immunoreceptor tyrosine-based inhibitory motif (ITIM).[23] Phosphorylation of these two tyrosine residues in PECAM-1 creates docking sites for the binding and activation of several cytosolic signaling molecules containing src homology-2 (SH2) domains. Included among the SH2-containing molecules that associate with PECAM-1 are the protein tyrosine phosphatases, SHP-1 and SHP-2,[24-31] the inosital phosphatase, SHIP[31] and phospholipase C-γ.[31] PECAM-1 may also associate with phosphoinositide 3-kinase[32] and β- or γ-catenin.[33,34] The ability of PECAM-1 to bind to these various cytosolic molecules enables it to potentially modulate the activity of a number of intracellular signaling pathways.

With respect to its endothelial cell functions, PECAM-1 regulates leukocyte transendothelial migration,[35] protects against endotoxic and apoptotic or stresses,[36,37] and contributes to the molecular sensing of fluid sheer stress.[16,38] PECAM-1 is also involved in angiogenesis. The initial evidence for this came from studies demonstrating that anti-PECAM-1 antibodies inhibit corneal neovascularization induced by angiogenic implants,[39] vascularization of subcutaneous Matrigel plugs[39] and tumor angiogenesis.[40,41] Subsequent studies in PECAM-1-null mice[42] have helped to confirm and further refine our understanding of the involvement of PECAM-1 in blood vessel formation. PECAM-1-deficient mice are viable, suggesting that vascular development is sufficiently preserved in the absence of PECAM-1 to permit adequate embryogenesis. However, the angiogenic response in a model of foreign body-induced chronic inflammation[43] and the vascularization of subcutaneous Matrigel implants and subcutaneous tumors are inhibited in PECAM-1-null mice.[11] In addition, post-natal lung development (a process dependent on angiogenesis) and the initial post-natal vascularization of the murine retina are impaired in PECAM-1-deficient mice.[11,44] Significantly, the vascular pattern and density in the eyes and lungs are similar in wild type and PECAM-1-null adult mice (unpublished observations), suggesting that the loss of PECAM-1 delays, but does not prevent the eventual development of the retinal or pulmonary vasculature. Together, these data implicate PECAM-1 in pathological angiogenesis, as well as in post-natal vascular developmental processes, such as those occurring in the eyes and lungs.

One of the mechanisms of PECAM-1's involvement in blood vessel formation appears to be an ability to stimulate endothelial cell motility.[11,41,45-47] Support for this conclusion comes from studies which have shown that anti-PECAM-1 antibodies inhibit the migration of murine and human ECs;[11,41] endothelial cells from PECAM-1-deficient mice are less motile compared to their wild type counterparts;[11,46] and the expression of PECAM-1 in non-PECAM-1 expressing cells enhances cell motility.[12,41,45-47] This activity in stimulating cell motility appears to involve the dephosphorylation of paxillin by the SHP-2 phosphatase.[12,47]

Its involvement in angiogenesis and endothelial cell motility led to an exploration of whether PECAM-1 might also play a role in the formation of endothelial cell filopodia.[11] Under various conditions it was observed that filopodia were more numerous and/or longer in length in: (i) wild type versus PECAM-1-null murine ECs; (ii) control HUVEC compared to HUVEC treated with PECAM-1 siRNA and (iii) cell transfectants expressing human PECAM-1 versus non-transfected controls. The significance of these in vitro data was confirmed by the finding that the length and number of filopodial extensions from ECs at the leading edge of the developing retinal vascular plexus were suppressed in PECAM-1-null mice.[11] The concentration of PECAM-1 in the tips of endothelial filopodia (**Fig. 1**, unpublished observation) is similar to what has been reported for VEGFR-2 (reviewed in ref. 9), and is consistent with a role for PECAM-1 in the formation of these cellular protrusions. PECAM-1 thus represents a new addition to a relative short list of molecules that have been identified as specific regulators of endothelial filopodia formation.

These data may help in part to explain the vascular phenotype of the PECAM-1-null mice.[42] If PECAM-1 is understood as increasing both the length and number of endothelial filopodia, then its presence enables the endothelial cell to more quickly and/or more efficiently assess the pericellular matrix environment for chemotactic or other pro-migratory factors. In this way, rather than being essential for cell migration, PECAM-1 facilitates the process by promoting the efficiency of endothelial cell motility. This might account for why the loss of PECAM-1 does not compromise the formation of the vasculature in the embryo and delays, but does not arrest, post-natal vascular development in the eyes and lungs.

Although the specific mechanisms by which PECAM-1 promotes the formation of filopodia remain to be determined, and are the subject of ongoing studies, both published and unpublished data are suggestive of some possible processes. First, PECAM-1 antibodies that block heterophilic (non-PECAM-1) ligand binding interactions inhibit flipopdia formation by subconfluent HUVEC.[11] This suggests that in the context of an angiogenic, motile endothelial cell, PECAM-1 heterophilic binding interactions with matrix proteins (e.g., proteoglycans) may transduce signals that activate the formation of the bundled, parallel arrays of actin that provide structural support for the filopodia.

Second, the expression of PECAM-1 in cellular transfectants stimulates the formation of filopodial extensions and wound-induced migration, processes that are both associated with increased ERK activation.[12] These phenomena are inhibited by mutations of Y663 and Y686 in the cytoplasmic domain that lead to a loss of the ability of PECAM-1 to bind SHP-2.[47] They are also suppressed by molecular or pharmacological inhibition of the

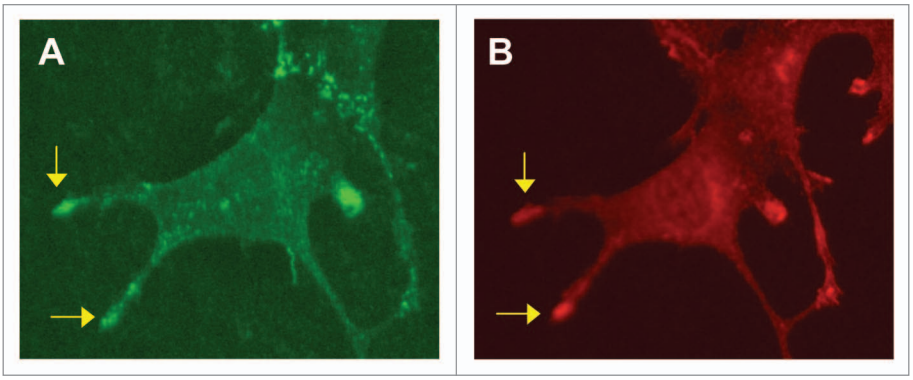

Figure 1. Concentration of PECAM-1 in endothelial filopodia. Shown is an endothelial cell that was immunofluorescently stained for PECAM-1 (A) and VEGFR-2 (B). PECAM-1 and VEGFR-2 are noted to concentrate in the tips of selected filopodia (arrows).

catalytic activity of the SHP-2 phosphatase.[2] Both cell motility and filopodia are downstream consequences of ERK activation.[48,49] Further, SHP-2 dephosphorylation of paxillin, with the subsequent activation of src kinase, is one mechanism for the activation of ERK.[50,51] Our data therefore suggest that the stimulation of filopodia formation mediated by PECAM-1 involves SHP-2-mediated activation of ERK.

Lastly, the presence of PECAM-1 increases the expression of Cdc42 in murine ECs and in PECAM-1-expressing transfectants.[11] This is not surprising given the abundance of data linking this Rho-GTPAse to the formation of filopodia.[51-54] It is important to note, however, that PECAM-1 is expressed at persistently high levels on ECs[17] and thus acute increases in PECAM-1 levels are unlikely to directly mediate an increase in Cdc42 expression during angiogenesis. This therefore suggests that if PECAM-1 regulates Cdc42 expression during angiogenesis, this activity involves changes in the activational state PECAM-1 and/or its interaction with other molecules involved in the regulation of Cdc42. In addition, although disturbance of the PECAM-1-SHP-2 interaction suppresses PECAM-1-dependent filopodia formation, this does not alter the expression of Cdc42 (unpublished data). Together, these data suggest that (i) the influence of PECAM-1 on Rho GTPases in filopodia formation is likely to involve or impact more than just changes in the expression levels of Cdc42 and (ii) filopodia formation mediated by PECAM-1 includes pathways that are dependent as well as independent of SHP-2-regulated ERK activation.

The data generated to date are admittedly descriptive in a number of respects, and the mechanisms of PECAM-1's activity as a regulator of endothelial filopodia are still being defined. Studies, however, of PECAM-1-transfectants suggest a dynamic interaction between PECAM-1 and SHP-2 in which the level of PECAM-1 tyrosine phosphorylation, and thus SHP-2 binding, are regulated by bound, catalytically-active SHP-2.[12] Based on these data, along with what was noted above, we suggest the following working model for the involvement of PECAM-1 in the formation of filopodia (**Fig. 2**). In the setting of post-natal developmental angiogenesis, or during certain forms of pathological angiogenesis, PECAM-1 on angiogenic and/or motile endothelial cells is tyrosine phosphorylated. These phosphorylation events occur either in response to angiogenic growth factor stimulation or are a result of the binding of PECAM-1 to matrix proteins elaborated in the angiogenic context. PECAM-1 phosphorylation subsequently induces the binding of SHP-2 to PECAM-1 and thus its recruitment to the cell membrane. We propose that this binding interaction with PECAM-1 activates the phosphatase activity of SHP-2, with the activated SHP-2 dephosphorylating the PECAM-1 molecule to which it is bound. This leads to the release of SHP-2 from PECAM-1. The liberated, but now membrane localized SHP-2 in turn targets paxillin, dephosphorylating it, to activate Src and eventually ERK-dependent signaling. One of the many consequences of ERK activation that might be relevant to PECAM-1-dependent filopodia formation could be the activation of myosin light chain kinase and the subsequent phosphorylation of the light chains of actin-associated myosins.[49] Additionally, in processes that do not appear to directly involve SHP-2-mediated ERK signaling, and which are poorly understood, PECAM-1 is involved in the regulation of Cdc42 expression. Studies are underway to evaluate the validity of this model.

The involvement of PECAM-1 in pathological angiogenesis has raised the possibility of PECAM-1 as a future target for anti-cancer therapy.[55] The appeal of PECAM-1 is further enhanced by the fact that loss of PECAM-1 does not cause a debilitating vascular phenotype[42] and significant vascular-related side effects have not been observed in mice treated with anti-PECAM-1 antibodies.[39-41] This suggests that anti-PECAM-1 therapy is likely to be well tolerated. However, the involvement of PECAM-1 in the trafficking of white cells[35] and in providing resistance to endotoxic and apoptotic stresses[36,37] means that consideration must still be given to the potential for immunosuppression and/or increased sensitivity to vascular insults during anti-PECAM-1 therapy. Consequently, developing a full understanding of the role of PECAM-1 in mediating endothelial cell functions will be essential for exploiting the therapeutic potential of targeting PECAM-1.

Acknowledgements

This work was supported by grants from the Department of Defense (PR043482)

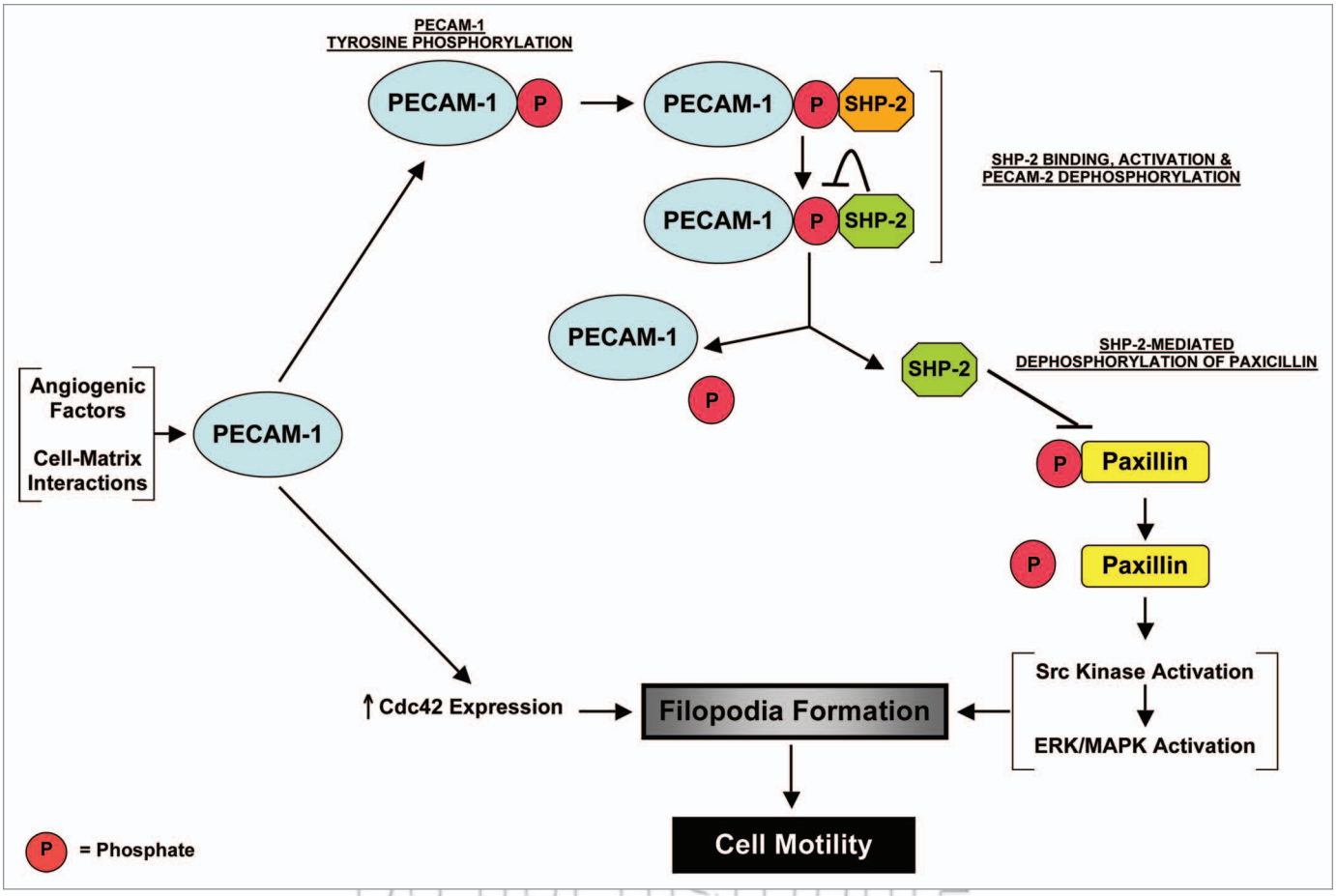

Figure 2. A proposed model for the involvement of PECAM-1 in the formation of endothelial cell filopodia during angiogenesis. During pathological or certain forms of developmental angiogenesis, angiogenic factors and/or cell-matrix interactions stimulate PECAM-1 tyrosine phosphorylation. These phosphorylation events lead to the binding of SHP-2 to PECAM-1 and the activation of SHP-2's phosphatase activity. The activated SHP-2 dephosphorylates the PECAM-1 molecule to which it is bound, leading to its release from PECAM-1. The liberated SHP-2 subsequently targets paxillin, dephosphorylating it, to trigger ERK-mediated activation of filopodia formation. Also, in processes that are still undefined, PECAM-1 may be involved in the regulation of Cdc42 during angiogenesis.

and the National Institutes of Health (HL079090).

References

1. Nambiar R, McConnell RE, Tyska MJ. Myosin motor function: the ins and outs of actin-based membrane protrusions. Cell Mol Life Sci 2010; 67:1239-54.
2. Pollard TD, Borisy GG. Cellular motility driven by assembly and disassembly of actin filaments. Cell 2003; 112:453-65.
3. Small JV, Auinger S, Nemethova M, Koestler S, Goldie KN, Hoenger A, et al. Unravelling the structure of the lamellipodium. J Microsc 2008; 231:479-85.
4. Faix J, Rottner K. The making of filopodia. Curr Opin Cell Biol 2006; 18:18-25.
5. Mattila PK, Lappalainen P. Filopodia: molecular architecture and cellular functions. Nat Rev Mol Cell Biol 2008; 9:446-54.
6. Ferrara N, Kerbel RS. Angiogenesis as a therapeutic target. Nature 2005; 438:967-74.
7. Adams RH, Alitalo K. Molecular regulation of angiogenesis and lymphangiogenesis. Nat Rev Mol Cell Biol 2007; 8:464-78.
8. De Smet F, Segura I, De Bock K, Hohensinner PJ, Carmeliet P. Mechanisms of vessel branching: filopodia on endothelial tip cells lead the way. Arterioscler Thromb Vasc Biol 2009; 29:639-49.
9. Gerhardt H, Golding M, Fruttiger M, Ruhrberg C, Lundkvist A, Abramsson A, et al. VEGF guides angiogenic sprouting utilizing endothelial tip cell filopodia. J Cell Biol 2003; 161:1163-77.
10. Gerhardt H, Ruhrberg C, Abramsson A, Fujisawa H, Shima D, Betsholtz C. Neuropilin-1 is required for endothelial tip cell guidance in the developing central nervous system. Dev Dyn 2004; 231:503-9.
11. Cao G, Fehrenbach M, Williams J, Finklestein J, Zhu JX, DeLisser HM. Angiogenesis in PECAM-1-null mice. Am J Path 2009; 175:903-15.
12. Zhu JX, Cao G, Fehrenbach M, Williams J, DeLisser HM. SHP-2 phosphatase activity is required for PECAM-1-dependent cell motility. Am J Physiol Cell Physiol 2010; In press.
13. Ilan N, Madri JA. PECAM-1: old friend, new partners. Curr Opin Cell Biol 2003; 15:515-24.
14. Jackson DE. The unfolding tale of PECAM-1. FEBS Lett 2003; 540:7-14.
15. Newman PJ, Newman DK. Signal transduction pathways mediated by PECAM-1: new roles for an old molecule in platelet and vascular cell biology. Arterioscler Thromb Vasc Biol 2003; 23:953-64.
16. Fujiwara K. Platelet endothelial cell adhesion molecule-1 and mechanotransduction in vascular endothelial cells. J Intern Med 2006; 259:373-80.
17. Newman PJ, Berndt MC, Gorski J, White GC, II, Lyman S, Paddock C, et al. PECAM-1(CD31) cloning and relation to adhesion molecules of the immunoglobulin gene superfamily. Science 1990; 247:1219-22.
18. Prager E, Sunder-Plassman R, Hansmann C, Koch C, Holter W, Knapp W, et al. Interaction of CD31 with a heterophilic counterreceptor involved in downregulation of human T cell responses. J Exp Med 1996; 184:41-50.
19. DeLisser HM, Yan HC, Newman PJ, Muller WA, Buck CA, Albelda SM. Platelet/endothelial cell adhesion molecule-1 (CD31)-mediated cellular aggregation involves cell surface glycosaminoglycans. J Biol Chem 1993; 268:16037-46.
20. Sun J, Williams J, Yan HC, Amin KM, Albelda SM, DeLisser HM. Platelet endothelial cell adhesion molecule-1 (PECAM-1) homophilic adhesion is mediated by immunoglobulin-like domains 1 and 2 and depends on the cytoplasmic domain and the level of surface expression. J Biol Chem 1996 271:18561-70.
21. Coombe DR, Stevenson SM, Kinnear BF, Gandhi NS, Mancera RL, Osmond RI, et al. Platelet endothelial cell adhesion molecule 1 (PECAM-1) and its interactions with glycosaminoglycans: 2. Biochemical analyses. Biochemistry 2008; 47:4863-75.

22. Sachs UJ, Andrei-Selmer CL, Maniar A, Weiss T, Paddock C, Orlova VV, et al. The neutrophil-specific antigen CD177 is a counter-receptor for platelet endothelial cell adhesion molecule-1 (CD31). J Biol Chem 2007; 282:23603-12.
23. Billadeau DD, Leibson PJ. ITAMs versus ITIMs: striking a balance during cell regulation. J Clin Invest 2002; 109:161-8.
24. Jackson DE, Kupcho KR, Newman PJ. Characterization of phosphotyrosine binding motifs in the cytoplasmic domain of platelet/endothelial cell adhesion molecule-1 (PECAM-1) that are required for the cellular association and activation of the protein-tyrosine phosphatase, SHP-2. J Biol Chem 1997; 272:24868-75.
25. Cao MY, Huber M, Beauchemin N, Famiglietti J, Albelda SM, Veillette A. Regulation of mouse PECAM-1 tyrosine phosphorylation by the Src and Csk families of protein-tyrosine kinases. J Biol Chem 1998; 273:15765-72.
26. Sagawa K, Kimura T, Swieter M, Siraganian RP. The protein-tyrosine phosphatase SHP-2 associates with tyrosine-phosphylated adhesion molecule PECAM-1 (CD31). J Biol Chem 1997; 272:31086-91.
27. Masuda M, Osawa M, Shigematsu H, Harada N, Fujiwara K. Platelet endothelial cell adhesion molecule-1 is a major SH-PTP2 binding protein in vascular endothelial cells. FEBS Lett 1997; 408:331-6.
28. Jackson DE, Ward CM, Wang R, Newman PJ. The protein-tyrosine phosphatase SHP-2 binds platelet/endothelial cell adhesion molecule-1 (PECAM-1) and forms a distinct signaling complex during platelet aggregation. J Biol Chem 1997; 272:6986-93.
29. Hua CT, Gamble JR, Vadas MA, Jackson DE. Recruitment and activation of SHP-1 protein-tyrosine phosphatase by human platelet endothelial cell adhesion molecule-1 (PECAM-1). J Biol Chem 1998; 273:28332-40.
30. Edmead CE, Crosby DA, Southcott M, Poole AW. Thrombin-induced association of SHP-2 with multiple tyrosine-phosphorylated proteins in human platelets. FEBS Lett 1999; 459:27-32.
31. Pumphrey NJ, Taylor V, Freeman S, Douglas MR, Bradfield PF, Young SP, et al. Differential association of cytoplasmic signalling molecules SHP-1, SHP-2, SHIP and phospholipase C-γ1 with PECAM-1/CD31. FEBS Lett 1999; 450:77-83.
32. Pellegatta F, Chierchia SL, Zocchi MR. Functional association of platelet endothelial cell adhesion molecule-1 and phosphoinositide 3-kinase in human neutrophils. J Biol Chem 1998; 273:27768-77.
33. Ilan N, Mahooti S, Rimm DL, Madri JA. PECAM-1 (CD31) functions as a reservoir for and a modulator of tyrosine-phosphorylated β-catenin. J Cell Sci 1999; 112:3005-14.
34. Ilan N, Cheung L, Pinter E, Madri JA. Platelet-endothelial cell adhesion molecule-1 (CD31), a scaffolding molecule for selected catenin family members whose binding is mediated by different tyrosine and serine/threonine phosphorylation. J Biol Chem 2000; 275:21435-43.
35. Woodfin A, Voisin MB, Nourshargh S. PECAM-1: a multi-functional molecule in inflammation and vascular biology. Arterioscler Thromb Vasc Biol 2007; 27:2514-23.
36. Carrithers M, Tandon S, Canosa S, Michaud M, Graesser D, Madri JA. Enhanced susceptibility to endotoxic shock and impaired STAT3 signaling in CD31-deficient mice. Am J Pathol 2005; 166:185-96.
37. Maas M, Stapleton M, Bergom C, Mattson DL, Newman DK, Newman PJ. Endothelial cell PECAM-1 confers protection against endotoxic shock. Am J Physiol Heart Circ Physiol 2005; 288:159-64.
38. Tzima E, Irani-Tehrani M, Kiosses WB, Dejana E, Schultz DA, Engelhardt B, et al. A mechanosensory complex that mediates the endothelial cell response to fluid shear stress. Nature 2005; 437:426-31.
39. DeLisser HM, Christofidou-Solomidou M, Strieter RM, Burdick MD, Robinson CS, Wexler RS, et al. Involvement of endothelial PECAM-1/CD31 in angiogenesis. Am J Pathol 1997; 151:671-7.
40. Cao G, O'Brien CD, Zhou Z, Sanders SM, Greenbaum JN, Makrigiannakis A, et al. The involvement of human PECAM-1 in angiogenesis and in vitro endothelial cell migration. Am J Physiol Cell Physiol 2002; 282:1181-90.
41. Zhou Z, Christofidou-Solomidou M, Garlanda C, DeLisser HM. Antibody against murine PECAM-1 inhibits tumor angiogenesis in mice. Angiogenesis 1999; 3:181-8.
42. Duncan GS, Andrew DP, Takimoto H, Kaufman SA, Yoshida H, Spellberg J, et al. Genetic evidence for functional redundancy of Platelet/Endothelial cell adhesion molecule-1 (PECAM-1): CD31-deficient mice reveal PECAM-1-dependent and PECAM-1-independent functions. J Immunol 1999; 162:3022-30.
43. Solowiej A, Biswas P, Graesser D, Madri JA. Lack of platelet endothelial cell adhesion molecule-1 attenuates foreign body inflammation because of decreased angiogenesis. Am J Pathol 2003; 162:953-62.
44. DeLisser HM, Helmke BP, Cao G, Egan PM, Taichman D, Fehrenbach M, et al. Loss of PECAM-1 function impairs alveolarization. J Biol Chem 2006; 281:8724-31.
45. Gratzinger D, Canosa S, Engelhardt B, Madri JA. Platelet endothelial cell adhesion molecule-1 modulates endothelial cell motility through the small G-protein Rho. FASEB J 2003; 17:1458-69.
46. Kondo S, Scheef EA, Sheibani N, Sorenson CM. PECAM-1 isoform-specific regulation of kidney endothelial cell migration and capillary morphogenesis. Am J Physiol Cell Physiol 2007; 292:2070-83.
47. O'Brien C, Cao G, Makringiannakis A, DeLisser HM. The Role of Immunoreceptor Tyrosine-Based Inhibitory Motifs of Platelet Endothelial Cell Adhesion Molecule (PECAM-1) in PECAM-1 Dependent Cell Migration. Am J Physiol Cell Physiol 2004; 287:1103-13.
48. Brahmbhatt AA, Klemke RL. ERK and RhoA differentially regulate pseudopodia growth and retraction during chemotaxis. J Biol Chem 2003; 278:13016-25.
49. Huang C, Jacobson K, Schaller MD. MAP kinases and cell migration. J Cell Sci 2004; 117:4619-28.
50. Ren Y, Meng S, Mei L, Zhao ZJ, Jove R, Wu J. Roles of Gab1 and SHP2 in paxillin tyrosine dephosphorylation and Src activation in response to epidermal growth factor. J Biol Chem 2005; 279:8497-505.
51. Dance M, Montagner A, Salles JP, Yart A, Raynal P. The molecular functions of Shp2 in the Ras/Mitogen-activated protein kinase (ERK1/2) pathway. Cell Signal 2008; 20:453-9.
52. Raftopoulou M, Hall A. Cell migration: Rho GTPases lead the way. Dev Biol 2004; 265:23-32.
53. Cerione RA. Cdc42: new roads to travel. Trends Cell Biol 2004; 14:127-32.
54. Yang L, Wang L, Zheng Y. Gene targeting of Cdc42 and Cdc42GAP affirms the critical involvement of Cdc42 in filopodia induction, directed migration and proliferation in primary mouse embryonic fibroblasts. Mol Biol Cell 2006; 17:4675-85.
55. DeLisser HM. Targeting PECAM-1 for anti-cancer therapy. Canc Biol Ther 2007; 6:121-2.

Vascular endothelial platelet endothelial cell adhesion molecule 1 (PECAM-1) regulates advanced metastatic progression

Horace DeLisser[a,1], Yong Liu[b,1], Pierre-Yves Desprez[b], Ann Thor[c], Paraskevei Briasouli[b], Chakrapong Handumrongkul[b], Jonathon Wilfong[b], Garret Yount[b], Mehdi Nosrati[d,2], Sylvia Fong[b,3], Emma Shtivelman[b,3], Melane Fehrenbach[a], Gaoyuan Cao[a], Dan H. Moore[b], Shruti Nyack[b], Denny Liggitt[e], Mohammed Kashani-Sabet[d,2], and Robert Debs[b,4]

[a]Department of Medicine, University of Pennsylvania Medical Center, Philadelphia, PA 19104; [b]California Pacific Medical Center Research Institute, San Francisco, CA, 94107; [c]Department of Pathology, University of Colorado, Denver School of Medicine, Aurora, CO 80045; [d]Auerback Melanoma Research Laboratory, University of California San Francisco Cancer Center, University of California, San Francisco, CA 94143; and [e]Department of Comparative Medicine, University of Washington School of Medicine, Seattle, WA 98195

Edited* by James E. Cleaver, University of California, San Francisco, CA, and approved August 17, 2010 (received for review April 7, 2010)

Most patients who die from cancer succumb to treatment-refractory advanced metastatic progression. Although the early stages of tumor metastasis result in the formation of clinically silent micrometastatic foci, its later stages primarily reflect the progressive, organ-destructive growth of already advanced metastases. Early-stage metastasis is regulated by multiple factors within tumor cells as well as by the tumor microenvironment (TME). In contrast, the molecular determinants that control advanced metastatic progression remain essentially uncharacterized, precluding the development of therapies targeted against it. Here we show that the TME, functioning in part through platelet endothelial cell adhesion molecule 1 (PECAM-1), drives advanced metastatic progression and is essential for progression through its preterminal end stage. PECAM-1–KO and chimeric mice revealed that its metastasis-promoting effects are mediated specifically through vascular endothelial cell (VEC) PECAM-1. Anti–PECAM-1 mAb therapy suppresses both end-stage metastatic progression and tumor-induced cachexia in tumor-bearing mice. It reduces proliferation, but not angiogenesis or apoptosis, within advanced tumor metastases. Because its antimetastatic effects are mediated by binding to VEC rather than to tumor cells, anti–PECAM-1 mAb appears to act independently of tumor type. A modified 3D coculture assay showed that anti–PECAM-1 mAb inhibits the proliferation of PECAM-1–negative tumor cells by altering the concentrations of secreted factors. Our studies indicate that a complex interplay between elements of the TME and advanced tumor metastases directs end-stage metastatic progression. They also suggest that some therapeutic interventions may target late-stage metastases specifically. mAb-based targeting of PECAM-1 represents a TME-targeted therapeutic approach that suppresses the end stages of metastatic progression, until now a refractory clinical entity.

metastasis | endothelium | tumor microenvironment

Tumor metastasis requires that a number of sequential steps, including tumor cell invasion, intravasation, homing, extravasation, tumor neoangiogenesis, and proliferation, each be completed successfully (1–4). Thus, tumor metastasis comprises semidiscrete stages, in part driven by distinct cellular events. The tumor microenvironment (TME), both via direct interactions with tumor cells and through paracrine-based signaling, plays an important role in controlling the early stages of metastatic spread (2–4). In contrast, factors that drive the progression of tumor metastases to a life-threatening, preterminal stage are poorly understood. As in earlier stages, they likely involve molecular signaling between malignant cells and their macro- and microenvironments (1, 5, 6).

Advanced metastatic progression causes death in most patients who die from cancer. However, in preclinical models, novel interventions generally are tested directly against locally injected tumors or against early-stage, micrometastatic spread. In contrast, models specifically examining the effects of interventions against the late stages of metastatic progression (the lethal, organ-destructive growth of already advanced metastases) are rarely studied. Antitumor interventions administered during the advanced stages of metastatic progression typically are both ineffective and poorly tolerated. Indeed, key events that define the early stages of metastatic spread may differ from those driving advanced metastatic progression. We hypothesized that testing novel interventions against the early stages of metastatic spread may fail to identify critical factors that selectively regulate the progressive growth of already advanced tumor metastases. Therefore, our studies focused on models assessing the progression of already well-established tumor metastases rather than on models assessing the early stages of metastatic spread.

Platelet endothelial cell adhesion molecule 1 (PECAM-1) is a 130-kDa cell surface protein of the Ig-like superfamily, with six Ig-like domains in the extracellular domain. It is expressed on certain WBC, platelets, and vascular endothelial cells (VEC) and interacts homophilically with itself or heterophilically with putative ligands to tranduce downstream inhibitory signals via its cytoplasmic domain (7, 8). PECAM-1 is involved in a number of processes relevant to growth and the spread of primary tumors, including angiogenesis, vascular permeability, and leukocyte trafficking out of the circulation (9, 10). In addition, earlier studies have shown that systemic delivery of an anti–PECAM-1 ribozyme suppresses the progression of already established tumor metastases (11). We assessed the potential role of PECAM-1 in regulating late-stage metastatic progression. Here, we provide evidence that VEC PECAM-1 regulates proliferation in advanced tumor metastases, independent of its activity as a mediator of angiogenesis. Importantly, anti–PECAM-1 mAb demonstrates potent antimetastatic effects specifically against the lethal preterminal stage of metastatic progression.

Results

Anti–PECAM-1 mAb Inhibits Late-Stage but Not Early-Stage Metastatic Tumor Progression in the Lung. Several aggressively metastatic tumor cell lines, including murine B16-F10 melanoma, 4T1

Author contributions: H.D., P.-Y.D., A.T., P.B., G.Y., D.L., M.K.-S., and R.D. designed research; H.D., Y.L., P.-Y.D., A.T., P.B., C.H., J.W., G.Y., M.N., S.F., E.S., M.F., G.C., D.L., M.K.-S., and R.D. performed research; H.D. contributed new reagents/analytic tools; H.D., Y.L., P.-Y.D., A.T., P.B., C.H., J.W., G.Y., M.N., S.F., E.S., M.F., G.C., D.H.M., S.N., D.L., M.K.-S., and R.D. analyzed data; and H.D., P.-Y.D., A.T., G.Y., S.F., E.S., D.H.M., D.L., M.K.-S., and R.D. wrote the paper.

Conflict of interest statement: H.D., D.L., M.K.-S., and R.D. have financial ownership of Genomic Systems, LLC, an entity that provided partial funding for this work.

*This Direct Submission article had a prearranged editor.

Freely available online through the PNAS open access option.

[1]H.D. and Y.L. contributed equally to this work.

[2]Present address: California Pacific Medical Center Research Institute, San Francisco, CA 94107.

[3]Present address: Bionovo Inc., Emeryville, CA 94608.

[4]To whom correspondence should be addressed. E-mail: debs@cpmcri.org.

This article contains supporting information online at www.pnas.org/lookup/suppl/doi:10.1073/pnas.1004654107/-/DCSupplemental.

mammary carcinoma, and LOX human melanoma, were evaluated. In particular, i.v. injected B16-F10 cells yield highly reproducible numbers of tumor metastases in the lung as well as in extrapulmonary organs, including the ovaries (12). From days 0–7 following i.v. injection (early-stage metastasis), most B16-F10 lung metastases remain small clusters containing <10 cells each. In contrast, by days 12–14 (late-stage metastasis), >35% of metastases are already >3 mm in diameter (5). We used mAb 390, a bioactive anti-murine PECAM-1 mAb (13), which specifically binds to an epitope within a 14-aa sequence of the second Ig-like domain of mouse PECAM-1. mAb390 binds to murine VEC but does not bind to murine or human tumors (13). Furthermore, it does not directly inhibit tumor cell proliferation, alter tumor cell adhesion to VEC or to platelets, or affect the transendothelial migration of tumor cells (Fig. S1 *A–E*). To target early- versus late-stage metastasis selectively, five i.v. doses of mAb 390 or isotype-control mAb were administered either 0–7 or 7–15 d after B16-F10 cell injection. Anti–PECAM-1 mAb significantly ($P < 0.0001$) decreased late-stage but did not affect early-stage tumor metastases (Fig. 1 *A* and *B*). The late-stage–specific anti-metastatic effects produced by mAb 390 are consistent with its inability to inhibit either tumor cell–platelet or tumor–endothelial cell interactions (Fig. S1 *C–E*), processes involved in the initial establishment of distant metastatic tumor foci. Systemic anti–PECAM-1 mAb also significantly reduced the late-stage metastatic progression of two other aggressively metastatic tumor lines, murine 4T1 mammary carcinoma ($P < 0.0001$) (Fig. 1*C*) and human LOX melanoma xenograft tumors ($P < 0.005$) (Fig. 1*D*), demonstrating that anti–PECAM-1 mAb therapy can suppress the late-stage metastatic progression of solid tumor types of different tissue origin. Anti–PECAM-1 mAb 390 has been shown to inhibit PECAM-1–dependent activities specifically and functions in a manner similar to a number of other anti–PECAM-1 antibodies (which bind to epitopes distinct from mAb 390), in a number of in vitro and in vivo assays (8, 14–16).

Enhanced Effectiveness of Anti–PECAM-1 mAb Against Preterminal Metastatic Disease. We next tested anti–PECAM-1 mAb 390 specifically against the preterminal stage of metastatic progression. We assessed the effects of administering one additional preterminal dose (a sixth mAb dose) to mice already severely ill from extensive B16-F10 tumor metastases. This preterminal anti–PECAM-1 mAb dose significantly reduced the percentage of lung occupied by tumor metastases [control group: 34.3 ± 4.2%, standard five-dose mAb 390 group: 19.6 ± 4.2% ($P < 0.05$ versus control); extended six-dose group: 9.0 ± 3.3% ($P < 0.0001$ versus control; $P < 0.05$ versus five-dose group)] (Fig. 2 *A* and *B*). It also reduced ($P < 0.001$) ovarian metastases (Fig. 2*C*), indicating that anti–PECAM-1 mAb therapy is systemically active. The preterminal (sixth mAb) dose also increased total body weight, determined at the time of sacrifice ($P < 0.0005$), when compared with either mice not receiving the preterminal anti-PECAM-1-mAb dose or control groups (Fig. 2*D*). Concurrently, lung tumor weights were significantly reduced in the group receiving the preterminal dose, showing that the preterminal dose better preserved normal body weight. These results indicate that targeting PECAM-1 reduces tumor-induced cachexia. Similarly, a preterminal dose of anti–PECAM-1 mAb 390 also significantly increased antimetastatic efficacy against highly advanced 4T1 metastases (Fig. 2*E*).

Anti–PECAM-1 Antibody Inhibits Tumor Cell Proliferation but Not Apoptosis or Angiogenesis. To identify pathway(s) through which anti–PECAM-1 mAb suppresses preterminal metastatic progression, its effects on tumor proliferative, apoptotic, and angiogenic rates were measured (Table 1). Tumor angiogenic rates were assessed by immunoreactivity to anti-von Willibrand factor (17) and to CD34 (to assess immature angiogenic endothelium) (18–20). Angiogenic and apoptotic (17) rates were comparable. However, the preterminal anti–PECAM-1 mAb dose reduced tumor cell proliferation (21) in highly advanced B16-F10 ($P < 0.005$) tumor metastases. Thus, although anti–PECAM-1 mAb 390 reduces angiogenesis within primary s.c. tumors (13), it specifically suppresses proliferation but has no affect on angiogenesis within advanced tumor metastases. As Fig. 2*A* illustrates, tumor metastases increase in size rapidly during the very late stages of metastatic progression, indicating that these tumor cells are proliferating rapidly. A single additional dose of anti–PECAM-1 mAb administered when metastases are both highly advanced and rapidly proliferating effectively suppressed proliferation. Suppression of proliferation within advanced metastases by the preterminal anti–PECAM-1 mAb dose at least in part explains its marked reduction of advanced metastatic burden.

Decreased Lung Metastases in PECAM-1–KO Mice. Because B16-F10 tumor cells are syngeneic with PECAM-1–KO mice (22), the effects of PECAM-1 on the metastatic progression of B16-F10 also can be studied in KO versus WT mice. Therefore, the development of lung metastases following tail vein injection of B16-F10 cells into WT versus PECAM-1–KO mice was assessed (22). Visible lung metastases were not detected in either WT or KO mice 7 d after tumor cell injection (Fig. 3*A*). However, from days 10–16 after tumor cell injection, the number of metastatic lung tumors (Figs. 3 *A* and *B* and 4 *A* and *C*), as well as lung weight (Fig. 4*E*), was markedly reduced in KO versus WT mice. Even more striking suppression was observed in the size of tumor nodules. Suppression of metastatic tumors also was

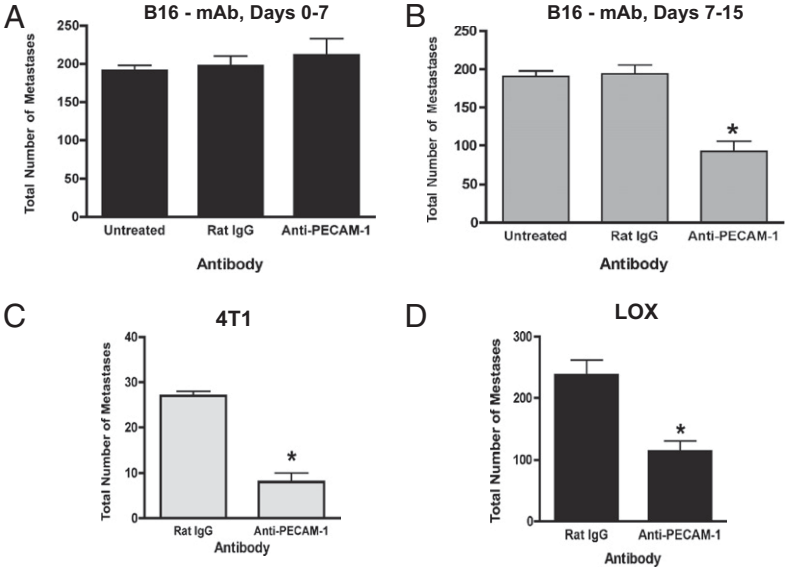

Fig. 1. Anti–PECAM-1 mAb specifically suppresses late-stage but not early-stage metastatic progression. (*A* and *B*) Groups of C57BL/6 mice received 25,000 B16-F10 cells i.v. (day 0). (*A*) In groups receiving early-stage treatment, each mouse received one i.v. injection of 200 μg of anti–PECAM-1 mAb or isotype-control mAb on day 0 and subsequently received one mAb dose every other day through day 7 (five mAb doses). (*B*) In groups receiving late-stage treatment, each mouse received one i.v. injection of 200 μg anti–PECAM-1 or isotype control mAb on day 7 and subsequently received one dose every other day through day 15 (five mAb doses). All mice were euthanized when multiple control mice became moribund. (*C*) BALB/c mice received 25,000 4T1 cells i.v. (*D*) BALB/c nude mice received 1×10^6 LOX cells i.v. Mice received five anti–PECAM-1 or control mAb doses from days 7–15 as above. When multiple control mice became moribund, all mice were euthanized and analyzed. Values represent the mean number of lung metastases ± SEM per mouse ($n = 10$). Potential statistical significance of differences for *A–D* was assessed using pairwise two-sided Student's *t* tests. *$P < 0.05$.

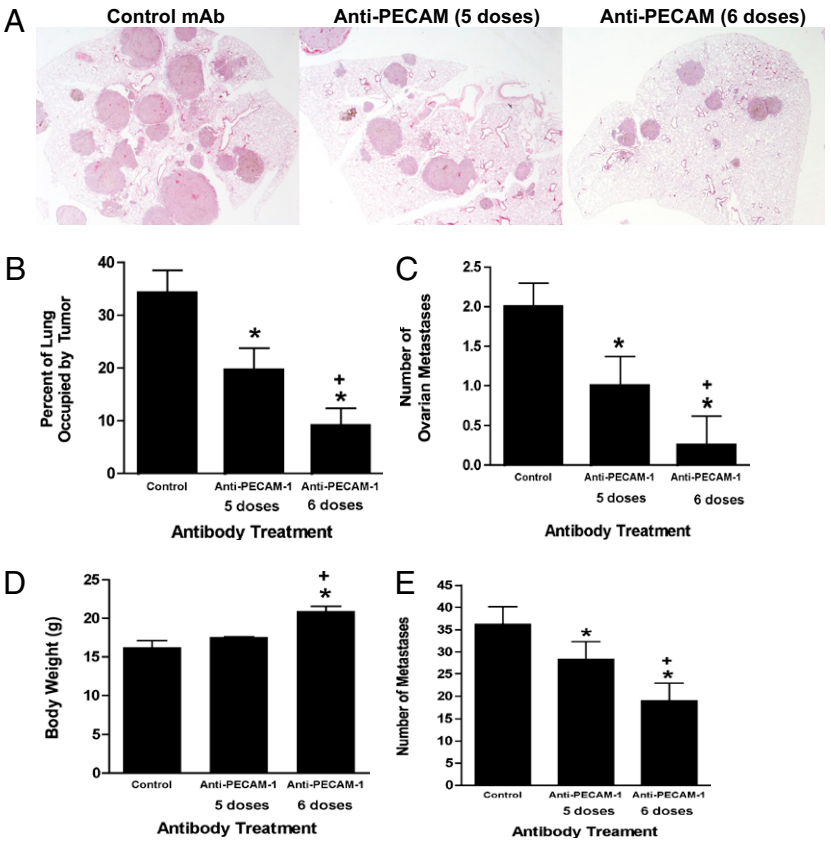

Fig. 2. Preterminal administration of anti–PECAM-1 mAb is highly effective against end-stage metastatic progression. C57BL/6 mice received B16-F10 cells and then five doses (last dose on day 15) or six doses (last dose on day 18) of anti–PECAM-1 or isotype control mAb. All mice were euthanized when multiple control mice became moribund. (*A*) Representative lung sections from mice treated with control mAb and mice treated with five or six doses of anti–PECAM-1 mAb. Metastases stain grayish-red. (*B*) Percent lung area occupied by B16-F10 melanoma. There were significant differences among the three treatments ($P = 0.001$ by Kruskal–Wallis rank test). Also, all pairwise comparisons were significantly different: five doses vs. none, $P = 0.02$; six doses vs. none, $P = 0.002$; and five doses vs. six doses, $P = 0.02$; all pairwise tests were by Mann–Whitney rank test. (*C*) Mean number of B16-F10 ovarian metastases. (*D*) Mean body weight of animals. There were significant differences among the three treatments ($P = 0.002$ by Kruskal–Wallis rank test). Also, six doses vs. none ($P = 0.003$) and five doses vs. six doses ($P = 0.004$) were significantly different. All pairwise tests were by Mann–Whitney rank test. (*E*) BALB/c mice received 25,000 4T1 cells i.v. and then received five doses (last dose on day 15) or six doses (last dose on day 18) of anti–PECAM-1 or isotype control mAb. All mice were euthanized when multiple control mice became moribund. Values represent mean ± SEM ($n = 10$). In *C* and *E*, potential statistical significance of differences was assessed using pairwise two-sided Student's *t* tests. $^{*}P < 0.05$ vs. control; $^{+}P < 0.05$ vs. five doses.

demonstrated in the lungs of KO animals by H&E staining of lungs harvested 15 d after tumor cell injection (Fig. 3*B*). Because anti–PECAM-1 mAb was effective against late- but not against early-stage metastases (Fig. 1 *A* and *B*), we then assessed more precisely whether early-stage metastatic progression was affected in PECAM-1–KO mice. To determine whether the early stages of metastatic spread are controlled differently in PECAM-1–KO versus WT mice, H&E staining was performed on lung tissue obtained at a much earlier time point, 4 d after i.v. injection of B16-F10 tumor cells. Subclinical lesions (<10 cells) detected in the walls of the alveoli at day 4 (Fig. 3*D*) were similar in number and size in WT and PECAM-1–KO mice (Table S1). Unlike the marked differences between WT and KO mice in the number and size of large, macroscopic B16-F10 metastases (Fig. 3 *A* and *B*), numbers of micrometastatic foci were comparable in WT and KO mice (Table S1). Therefore, advanced metastatic progression, but not the early stages of metastatic spread, is suppressed in both PECAM-1–KO mice and WT mice receiving anti–PECAM-1 mAb. Taken together, these data indicate that PECAM-1 plays an important role in regulating the progression of established metastases from subclinical metastatic lesions to macroscopic, life-threatening tumor metastases. However, PECAM-1 appears uninvolved in controlling the initial establishment of metastatic tumor foci or in mediating the passage of primary tumor cells across the vascular endothelium (Fig. S1 *C–E*), events critical to spread from the primary tumor itself.

Reconstitution of PECAM-1–Null Mice with Bone Marrow from WT Mice Does Not Restore the WT Phenotype. Anti–PECAM-1 mAb 390 does not bind to tumor cells either in culture (Fig. S1*A*) or in tumor-bearing mice (13) whose late-stage metastases it suppressed. Furthermore, it does not directly inhibit tumor cell proliferation in vitro (Fig. S1*B*). To determine whether PECAM-1 expressed on VEC and/or bone marrow-derived WBC mediates its prometastatic effects, chimeric mice were generated by reconstituting WT mice with KO marrow (PECAM-1–positive VEC/PECAM-1–negative platelets WBC, designated WT_{EC}-KO_{BM}) or by reconstituting KO mice with WT marrow (PECAM-1–negative endothelium/PECAM-1–positive platelets WBC, designated KO_{EC}-WT_{BM}) (23). Reconstitution of WT animals with KO marrow did not suppress the development of metastases, and reconstitution of KO mice with marrow from WT mice did not restore the WT, prometastatic phenotype (Fig. 4 *A–E*). These data indicate that the antimetastatic

Table 1. Extended anti–PECAM-1 mAb therapy significantly reduces tumor mitotic rates, but not tumor angiogenic or tumor apoptotic rates in mice bearing advanced tumor metastases

B16-F10 tumors	Tumor angiogenesis	Tumor apoptosis*	Tumor mitosis†
Anti–PECAM-1 mAb-treated			
	10.6 ± 1.7‡	9.0 ± 3.4	14.4 ± 1.6¶
	209.7 ± 44.0§		
Control mAb-treated			
	11.3 ± 2.6‡	10.8 ± 4.0	21.5 ± 1.7
	191.7 ± 45.9§		

Mice bearing metastatic B16-F10 or 4T1 tumors were treated with six doses of either anti–PECAM-1 or control mAb and were euthanized as described in Fig. 1. Tumor-bearing lungs were removed and processed, and tumor angiogenic, mitotic, and apoptotic rates were measured as described in *Materials and Methods*. The lack of difference in tumor angiogenic rates between groups was confirmed by assessing immunoreactivity to CD34. Potential statistical significance of differences was assessed using an unpaired two-tailed Student *t* test ($P < 0.05$ vs. control).

*Tumor apoptotic rates were measured as described in *Materials and Methods*.

†Tumor mitosis counts were measured by immunoreactivity to Ki67 (19).

‡Tumor angiogenic rates measured by immunoreactivity to factor VIII-VWF (17).

¶Potential statistical significance of differences was assessed using a pairwise two-sided Student's *t* test. $P < 0.005$ versus control; values are ± SD.

§Tumor angiogenic rates measured by immunoreactivity to CD34 (18).

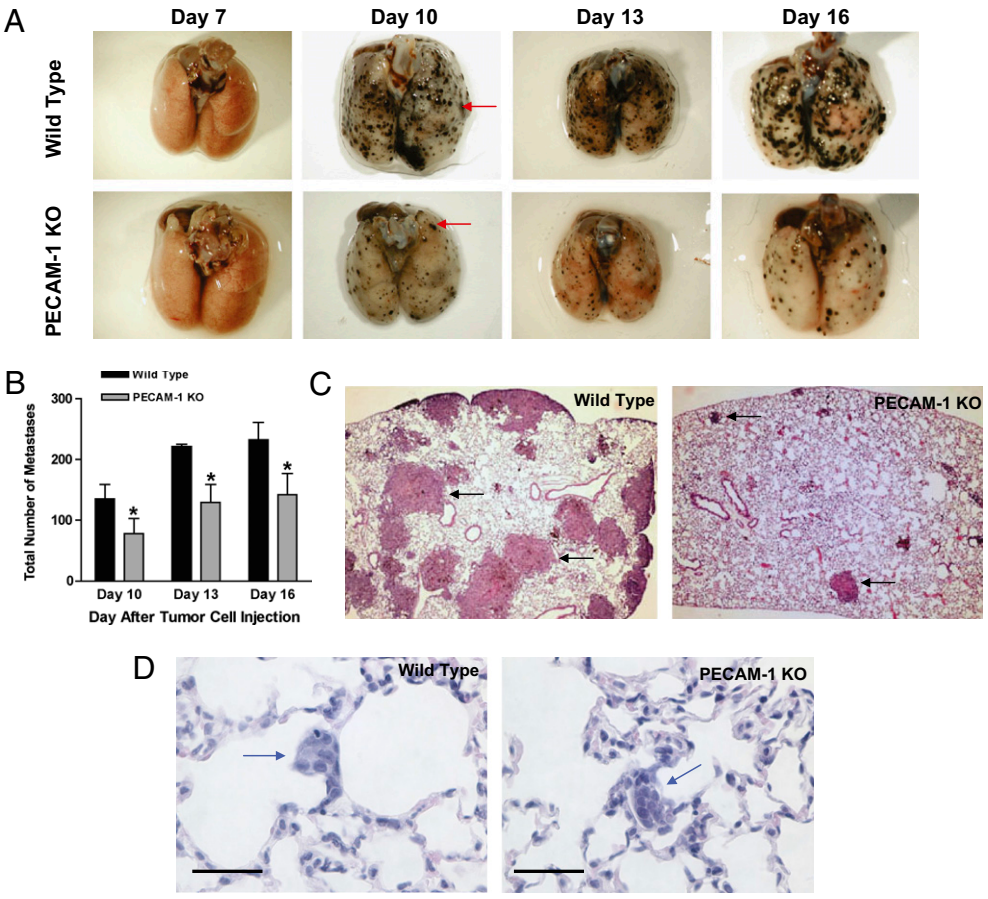

Fig. 3. Late-stage, but not early-stage, metastatic progression of B16-F10 melanoma tumors is suppressed in PECAM-1–KO mice versus WT. (*A*) Representative lungs obtained from WT and PECAM-1–KO animals 7, 10, 13, and 16 d after i.v. injection with B16-F10 melanoma cells. Tumor nodules are not observed on the surface of the lung 7 d after tumor injection, but are readily visible in both WT and PECAM-1–KO mice by day 10 (red arrows). At all time points assessed after day 7, progression of the size and number of tumor metastases was significantly suppressed in PECAM-1–KO mice. (*B*) Mean number of tumor nodules visible on the surface of the right lung in WT and PECAM-1–KO mice on days 10, 13, and 16. At least 40 nodules were analyzed from three mice for each strain. Values are mean ± SEM ($n = 2$ or 3; $P < 0.001$; pairwise two-sided Student's t test). A marked suppression in the mean area of these nodules was observed in PECAM-1–KO mice (day 16: WT 1.14 vs. PECAM-1–KO 0.26 mm^2; $^*P < 0.05$ vs. WT). (*C*) H&E-stained lung tissues demonstrating large macroscopic nodules (black arrows) were greatly increased in number and size in the WT versus PECAM-1–KO mice, 15 d after tumor cell injection. (*D*) Small, subclinical lesions (<10 cells) detected in the walls of the alveoli (blue arrows) in lungs harvested 4 d following tumor cell injection. Unlike the marked differences in the number and size of large, macroscopic B16-F10 metastases in WT and PECAM-1–KO mice (*A* and *B*), the number and size of micrometastatic foci were comparable in WT and PECAM-1–KO mice (Table S1). (Scale bar: 50 μm.)

effects observed in PECAM-1–KO mice, and likely those produced by anti–PECAM-1 mAb 390, are mediated by blocking VEC PECAM-1.

PECAM-1–Dependent Paracrine Factors Regulate Tumor Proliferation. We developed a variant of a 3D coculture system as a model for tumor cell–VEC interactions within the tumor microenvironment. Tumor cells are added to capillary-like structures (CLS) of VEC already formed on a basement-membrane substrate. VEC do not divide once plated on Matrigel (24). Although these CLS typically regress within 24–36 h (24), adding tumor cells maintained CLS integrity for ≥5 d. Anti–PECAM-1 mAb, unlike control mAb, suppressed B16-F10 or 4T1 proliferation by 50–60% ($P < 0.05$) in this 3D coculture system (Fig. S2), thus accurately recapitulating the proliferation-suppressing phenotype it produced in tumor-bearing mice (Table 1). To assess whether PECAM-1 regulates proliferation via soluble mediators, B16-F10 cells were grown in conditioned medium from anti–PECAM-1– or control mAb-treated 3D cocultures. Anti–PECAM-1 mAb conditioned medium inhibited tumor cell proliferation by >60% (Movies S1 and S2), indicating that anti–PECAM-1 mAb-regulated paracrine factors mediate its ability to suppress tumor cell proliferation. Anti–PECAM-1 mAb 390 therapy also inhibits the growth of primary tumors that do not express PECAM-1 (13), consistent with its ability to act, at least in part, through its regulation of paracrine factors.

Lack of PECAM-1–Dependent Cellular Infiltration in Anti–PECAM-1–Treated Tumors. Multiple H&E-stained sections from metastatic tumors and surrounding tissues were examined to identify any characteristics that might differentiate anti–PECAM-1 mAb-treated mice from control mice. None were detected. Tumors were examined specifically for accumulations of F4/80 antigen-positive macrophages using immunohistochemistry (25). The presence of macrophages within individual tumor nodules varied from rare to moderate. However, neither the pattern nor the extent of macrophage infiltration differed between anti–PECAM-1 mAb-treated and control specimens (Fig. S3). Thus, although tumor-infiltrating macrophages may play a role in mediating the antimetastatic effects produced by anti–PECAM-1 mAb, these results suggest that this role is limited. This hypothesis is supported by results obtained in the 3D coculture assay (in which no macrophages were present), where anti–PECAM-1 mAb exerted antitumor and antiproliferative effects comparable to those it produced in tumor-bearing mice.

Discussion

Although rarely studied in preclinical models, advanced metastatic progression causes death in the great majority of patients who die from cancer. Although the early stages of tumor metastasis result in the formation of clinically silent micrometastatic foci (2, 4, 6), its advanced stages primarily reflect the progressive, organ-destructive growth of already well-established metastases (5). The molecular determinants that control the end stages of metastatic progression remain largely uncharacterized. Mechanistically, our results support the hypothesis that VEC PECAM-1–regulated paracrine factors drive the lethal progression of advanced tumor metastases. Anti–PECAM-1 mAb blocks this progression by altering the release of soluble factors that drive proliferation within these advanced metastases. This model is supported by each of the following observations. Anti–PECAM-1 mAb, even at very high concentrations, does not directly inhibit tumor cell proliferation in culture. In contrast, conditioned medium (which contains PECAM-1–regulated secreted factors) from mAb 390-treated, but not from isotype control mAb-treated, cocultures strongly inhibits tumor cell proliferation in culture. Furthermore, anti–PECAM-1

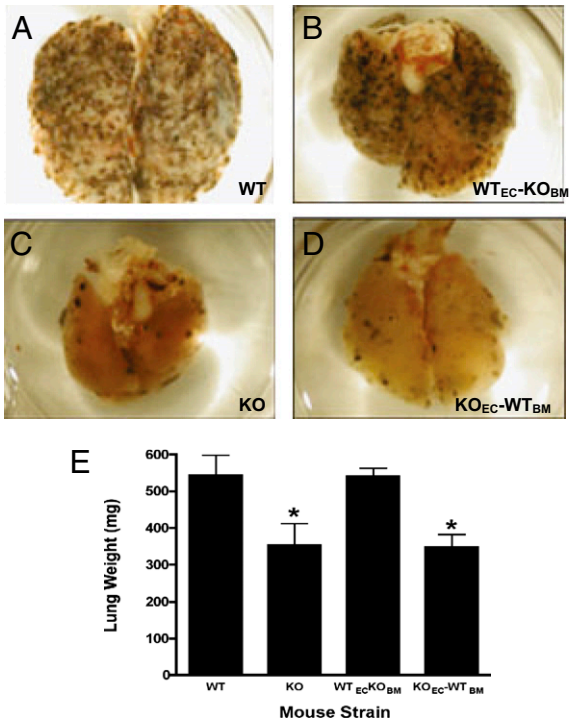

Fig. 4. Metastatic progression of B16-F10 melanoma tumors in reciprocal bone marrow chimeric mice reveals that VEC PECAM-1 mediates its prometastatic effects. Shown are lungs from animals injected with B16-F10 melanoma cells. The following animals were studied: (*A*) WT mice, (*B*) WT mice reconstituted with PECAM-1–KO marrow (WT$_{EC}$-KO$_{BM}$,), (*C*) PECAM-1–KO mice, and (*D*) PECAM-1–KO mice reconstituted with WT marrow (KO$_{EC}$-WT$_{BM}$). (*E*) Lung weights differed significantly among the four strains (*$P = 0.03$ by Kruskal–Wallis rank test). Lung weights were significantly decreased in the PECAM-1–KO mice and PECAM-1–KO mice reconstituted with WT marrow. Lung weights were significantly reduced in the KO mice and KO mice reconstituted with WT marrow vs. WT mice and WT mice reconstituted with KO marrow. Also, the pairs WT vs. KO and WT-KO vs. KO-WT differed significantly ($P = 0.0497$ and $P = 0.0463$, respectively, based on Mann–Whitney rank test). $n = 10$. Values are mean ± SEM.

mAb 390 does not bind to any of the tumor cell types whose metastasis it suppresses. Rather, the antimetastatic activity produced by anti–PECAM-1 mAb is mediated specifically by its binding to PECAM-1 expressed on VEC.

Intriguingly, we found that anti–PECAM-1 mAb suppressed tumor metastasis more effectively when administered at an advanced stage (Fig. 1*B*), a time when the explosive growth of macroscopic, already well-established metastases typically is seen (5). Conversely, administration of the antibody during the initial formation of micrometastatic tumor foci did not inhibit the emergence of clinically apparent metastases. In addition, late-stage tumor metastases were suppressed strongly, whereas early metastatic spread was unaffected in PECAM-1–KO versus WT mice. Chimeric mice revealed that the PECAM-1 metastasis-promoting effects are mediated by VEC-expressed, not by WBC-expressed, PECAM-1. Because its antimetastatic effects are mediated by binding to VEC rather than the tumor cells themselves, anti–PECAM-1 mAb appears to act independent of tumor type.

Single-agent anti–PECAM-1 mAb is highly effective against advanced, life-threatening tumor metastases but is ineffective against clinically silent micrometastases. Our results demonstrate that an anticancer treatment can effectively treat the preterminal stages of metastatic progression, but be ineffective when administered during its early, asymptomatic stages. In contrast, the currently used antitumor mAbs are being used increasingly to treat earlier-stage human cancers (6, 26). Furthermore, PECAM-1 acts through VEC to regulate metastasis in a novel way, by specifically controlling proliferation, not angiogenesis, in advanced tumor metastases. Targeted VEGF antagonists inhibit angiogenesis in both primary and metastatic tumors and play a major role in treating metastatic human cancers (27). Anti–PECAM-1 mAb inhibits angiogenesis in primary tumors (13) but does not affect angiogenesis within advanced tumor metastases, indicating that some molecularly targeted therapies can elicit different biologic responses within different tumor microenvironments. Thus, the vascular endothelium, acting through VEGF, as well as PECAM-1, can regulate metastatic progression through different mechanisms, further expanding its role in directing tumor metastasis.

Remarkably, dose-intensive, preterminal mAb administration effectively treated the treatment-refractory end stages of metastatic progression. Specifically, one additional (sixth) dose of anti–PECAM-1 mAb, administered to mice that were already preterminal, was itself strikingly effective, further reducing lung metastatic burden by an additional 50% against B16-F10 and an additional 35% against 4T1 tumors, when compared to the five anti-PECAM-1-mAb dose regimen lacking a pre-terminal dose. Although many anticancer treatments are significantly more toxic in hosts already debilitated from advanced tumor metastases, high doses of anti–PECAM-1 mAb administered during the preterminal phase not only appeared nontoxic but also significantly reduced tumor-induced cachexia. In addition, PECAM-1–KO mice grow and develop normally (22). Taken together, these results suggest anti-PECAM mAb therapy may be well tolerated, even in human patients already severely debilitated by advanced metastases.

Studies of metastasis often focus on the early stages of metastatic spread, and the study of preterminal metastatic progression generally has been avoided. In contrast, clinical trials of investigational anticancer agents, selected based on early-stage preclinical studies, often are conducted in patients bearing late-stage metastases, suggesting a mismatch between models studied and patients treated. The striking efficacy of anti–PECAM-1 mAb against preterminal metastases coupled with its inactivity against very early-stage metastatic spread suggests that the lethal growth of advanced tumor metastases is controlled, at least in part, by late-stage–specific, prometastatic drivers. Furthermore, these results indicate that late-stage–specific testing of novel antitumor agents will reveal some agents active only during this usually treatment-resistant phase of metastatic progression. Such agents may include agents previously determined to be ineffective when tested solely against early-stage metastatic spread.

This apparent anomaly may result in part from the largely proliferation-driven nature of advanced metastatic disease (5). Conversely, the successful establishment of micrometastatic foci depends upon the abilities of tumor cells to invade locally, intravasate home to distant organs, extravasate, and induce tumor neoangiogenesis (4). Recent studies have shown that i.v. injected nontumorigenic mammary gland cells can colonize and grow within the lung for prolonged periods (28), further supporting the concept that early metastatic spread occurs by a series of discrete stages. Taken together, our studies indicate that a complex interplay between elements of the TME, paracrine factors, and advanced tumor metastases controls the lethal progression of advanced tumor metastases. Selectively targeting PECAM-1 represents a TME-targeted therapeutic approach that suppresses even lethal, end-stage metastatic progression, until now a refractory clinical entity.

Materials and Methods

Monoclonal Antibodies. Anti–PECAM-1 mAb 390 is an IgG2A class anti-murine CD31 antibody that binds to a 14-aa epitope on domain II of the extracellular Ig domains of CD31 (6). An IgG2A rat isotype control mAb was purchased from Sigma. mAbs were cleared of LPS using the EndoTrap Red system (Lonza) to fewer than two units of endotoxin per milliliter as determined by a limulus amebocyte lysate assay (Pyrogent Plus; Lonza).

3D Coculture Assay. Six-well polystyrene plates (Corning) were coated with 300 μL of Matrigel (BD Biosciences). One hour later, 2×10^5 CD3 or H5V cells (VEC lines) were plated. Eight hours later, after VEC capillary-like structures had formed, 2×10^5 B16-F10 or 4T1 cells were added, together with 200 μg/mL of either anti–PECAM-1 or control mAb. mAbs were added again at 24 and 48 h, and all cells and culture supernatants for conditioned media were harvested at 72 h. All wells were trypsinized and counted using a hemocytometer.

In Vivo Monoclonal Antibody Treatments and Analysis of Antitumor Activity. B16-F10 murine melanoma cells, LOX human melanoma cells, and 4T1 breast carcinoma cells were freshly thawed and grown in 10% FBS in RPMI-1640 medium (Invitrogen) for 48 h. On day 0, groups of 6-wk-old female C57BL/6 (B16-F10), BALB/C (4T1), or BALB/C nude (LOX) mice (n = 10 mice per group) (Simonsen Laboratories) were injected i.v. with 25,000 B16-F10 cells, 50,000 4T1 cells, or 1,000,000 LOX cells, respectively, in 200 μL of culture medium. In groups receiving early-stage treatment, each mouse received one i.v. injection of 200 μg of anti–PECAM-1 mAb 390 or isotype control mAb on day 0 and one dose every other day through day 7. The groups receiving late-stage treatment received one i.v. injection of 200 μg of anti–PECAM-1 or isotype-control mAb on day 7 and then every other day through day 15. All mice were weighed on day 0, before tumor cell injection, and then were randomized so that treated and control groups had comparable weights. The mice were weighed again before they were killed. Differences in mean total body weight represent those occurring over the entire 21-d duration of the experiment. All mice were killed humanely when multiple tumor-bearing control mice required sacrifice. Although survival studies could not be performed (in accordance with institutional animal-care guidelines), the lack of early deaths in the six-dose mAb-treated group suggests their survival would be prolonged. Lungs dissected from each mouse were weighed immediately. For B16-F10–inoculated mice, lungs were infused transtracheally with 5% neutral buffered formalin/PBS. For 4T1- and LOX-inoculated mice, lungs were infused with 15% India ink in Fekete's solution. Black-brown B16-F10 metastatic tumors and counterstained 4T1 and LOX tumors (white) were counted under a dissecting microscope.

Analysis of Lung Surface Area Occupied by Metastatic Tumors. Images of all histologic sections in the anti–PECAM-1 mAb and control groups were captured using a Nikon Digital Sight D5-U1 camera and Nikon 80i microscope. The total lung surface area and the surface area occupied by individual tumor masses within the lung were outlined using the area function of NIS-Elements Software (Nikon Instruments), and the percentage of lung occupied by tumor was calculated.

Generation of Mice Chimeric for CD31 on VEC and WBC. Bone marrow chimeric mice were generated as previously described (23). Within 24 h after irradiation, 5×10^6 cells of donor marrow obtained from nonirradiated mice were injected i.v. into irradiated recipient mice. Tumor cells were injected 4–6 wk after transplantation. Flow cytometry analysis of leukocytes using an anti-mouse PECAM-1 antibody confirmed the chimeric phenotype.

Immunohistochemistry. Antibodies used include rat anti-murine K_i-67 antigen and rabbit anti-human von Willebrand factor antigen (both from Dako) and rat anti-murine CD-34 antigen (Abcam). Sections were pretreated with microwave antigen retrieval in 10 mM citrate buffer for 10 min. Endogenous antibodies were blocked with normal goat serum (1:10 dilution (Vector Laboratories) and then were incubated with the primary antibody localized using an avidin–biotin complex kit (Vector Laboratories) appropriate for the primary antibody. A red alkaline phosphatase substrate was used to avoid confusion with melanin granules.

Assessment of Angiogenesis Rates Within Metastatic Tumors. Intratumoral blood vessels were quantitated using anti-von Willebrand's factor staining, as previously described (17). Intratumoral blood vessels also were assessed by immunoreactivity to CD34, using criteria previously described (19).

Assessment of Apoptosis and Mitosis Rates Within Metastatic Tumors. Mitotic and apoptotic figures were counted on 4-μm H&E-stained slides with a conventional light microscope. Apoptotic bodies (21) were counted, and apoptotic rates were calculated as previously described. For determination of K_i-67 positivity, individual K_i-67 positively stained cells within grid spaces completely occupied by tumor were counted (≈40 grids per lung) and were expressed as the mean number of K_i-67–positive cells per 100 μm^2 of tumor tissue.

Statistical Methods. For continuous, normally distributed data, a one-way ANOVA was used to determine whether there were any differences among different treatments. If this test was significant ($P < 0.05$), pairwise two-sided Student's t tests were conducted to compare the different treatments. This method was used to avoid inflation of P values by multiple testing. When measurements were not normally distributed, a Kruskal–Wallis rank test was used first to test whether there were differences among different treatments (including no treatment). If the Kruskal–Wallis test was significant ($P < 0.05$), the Mann–Whitney rank test was used for comparisons between pairs of treatments. Statistical calculations were carried out using Stata version 11.1 (StataCorp).

ACKNOWLEDGMENTS. We thank R. Chu, Tri Lu, Wayne Liao, Charles Ma, and Kevin Chen for their experimental assistance and T. Heath, P. Billings, J. Patton, J. Muschler, J. Sabry, S. Mintz, and M. Kope for helpful comments on the manuscript. This work was supported by Department of Defense Grant PR043482 (to H.D.), National Institutes of Health Grants HL079090 (to H.D.), U54RR24379 (to D.L.), CA114337 and CA122947 (to M.K.-S.), and CA109174 (to R.D.), and Genomic Systems.

1. Chambers AF, Groom AC, MacDonald IC (2002) Dissemination and growth of cancer cells in metastatic sites. *Nat Rev Cancer* 2:563–572.
2. Gupta GP, Massagué J (2006) Cancer metastasis: Building a framework. *Cell* 127: 679–695.
3. Liotta LA, Kohn EC (2001) The microenvironment of the tumour-host interface. *Nature* 411:375–379.
4. Woodhouse EC, Chuaqui RF, Liotta LA (1997) General mechanisms of metastasis. *Cancer* 80(8, Suppl):1529–1537.
5. Cameron MD, et al. (2000) Temporal progression of metastasis in lung: Cell survival, dormancy, and location dependence of metastatic inefficiency. *Cancer Res* 60: 2541–2546.
6. Steeg PS (2006) Tumor metastasis: Mechanistic insights and clinical challenges. *Nat Med* 12:895–904.
7. O'Brien CD, Cao G, Makrigiannakis A, DeLisser HM (2004) Role of immunoreceptor tyrosine-based inhibitory motifs of PECAM-1 in PECAM-1-dependent cell migration. *Am J Physiol Cell Physiol* 287:C1103–C1113.
8. Yan HC, et al. (1995) Alternative splicing of a specific cytoplasmic exon alters the binding characteristics of murine platelet/endothelial cell adhesion molecule-1 (PECAM-1). *J Biol Chem* 270:23672–23680.
9. Muller WA (1995) The role of PECAM-1 (CD31) in leukocyte emigration: Studies in vitro and in vivo. *J Leukoc Biol* 57:523–528.
10. Newman PJ, Newman DK (2003) Signal transduction pathways mediated by PECAM-1: New roles for an old molecule in platelet and vascular cell biology. *Arterioscler Thromb Vasc Biol* 23:953–964.
11. Kashani-Sabet M, et al. (2002) Identification of gene function and functional pathways by systemic plasmid-based ribozyme targeting in adult mice. *Proc Natl Acad Sci USA* 99:3878–3883.
12. Vantyghem SA, Postenka CO, Chambers AF (2003) Estrous cycle influences organ-specific metastasis of B16F10 melanoma cells. *Cancer Res* 63:4763–4765.
13. Zhou Z, Christofidou-Solomidou M, Garlanda C, DeLisser HM (1999) Antibody against murine PECAM-1 inhibits tumor angiogenesis in mice. *Angiogenesis* 3:181–188.
14. Cao G, et al. (2009) Angiogenesis in platelet endothelial cell adhesion molecule-1-null mice. *Am J Pathol* 175:903–915.
15. DeLisser HM, et al. (1997) Involvement of endothelial PECAM-1/CD31 in angiogenesis. *Am J Pathol* 151:671–677.
16. Tasaka S, et al. (2003) Platelet endothelial cell adhesion molecule-1 in neutrophil emigration during acute bacterial pneumonia in mice and rats. *Am J Respir Crit Care Med* 167:164–170.
17. Liu Y, et al. (1999) Systemic gene delivery expands the repertoire of effective antiangiogenic agents. *J Biol Chem* 274:13338–13344.
18. Nico B, et al. (2008) Evaluation of microvascular density in tumors: Pro and contra. *Histol Histopathol* 23:601–607.
19. Weidner N, Carroll PR, Flax J, Blumenfeld W, Folkman J (1993) Tumor angiogenesis correlates with metastasis in invasive prostate carcinoma. *Am J Pathol* 143:401–409.
20. Werner N, et al. (2005) Circulating endothelial progenitor cells and cardiovascular outcomes. *N Engl J Med* 353:999–1007.
21. van Diest PJ, Brugal G, Baak JP (1998) Proliferation markers in tumours: Interpretation and clinical value. *J Clin Pathol* 51:716–724.
22. Duncan GS, et al. (1999) Genetic evidence for functional redundancy of platelet/endothelial cell adhesion molecule-1 (PECAM-1): CD31-deficient mice reveal PECAM-1-dependent and PECAM-1-independent functions. *J Immunol* 162:3022–3030.
23. Mahooti S, et al. (2000) PECAM-1 (CD31) expression modulates bleeding time in vivo. *Am J Pathol* 157:75–81.
24. Vailhé B, Vittet D, Feige JJ (2001) In vitro models of vasculogenesis and angiogenesis. *Lab Invest* 81:439–452.
25. Malorny U, Michels E, Sorg C (1986) A monoclonal antibody against an antigen present on mouse macrophages and absent from monocytes. *Cell Tissue Res* 243: 421–428.
26. Adams GP, Weiner LM (2005) Monoclonal antibody therapy of cancer. *Nat Biotechnol* 23:1147–1157.
27. Ferrara N (2005) VEGF as a therapeutic target in cancer. *Oncology* 69(Suppl 3):11–16.
28. Podsypanina K, et al. (2008) Seeding and propagation of untransformed mouse mammary cells in the lung. *Science* 321:1841–1844.